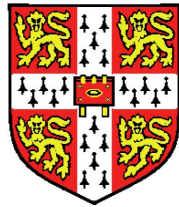# Transcriptional Functions of the Co-Repressor Sin3A in Skin

Claire Cox

Clare College

University of Cambridge

A dissertation submitted for the degree of

Doctor of Philosophy

September 2012

This dissertation is dedicated to my wonderful parents, sisters and Nanna. I would also like to dedicate this dissertation to my amazing Grandad, who may be gone, but will never be forgotten.

Declaration

This dissertation is the result of my own work and includes nothing which is the outcome of work done in collaboration except where specifically indicated in the text.

The work described was carried out at the Wellcome Trust Medical Research Council Stem Cell Institute, University of Cambridge, under the supervision of Dr. Michaela Frye and Dr. Brian Hendrich.

The length of this thesis does not exceed 60,000 words, not including figures, photographs, tables, appendices and bibliography, as specified by the Biology Degree Committee.

This dissertation is not substantially the same as any that I submitted for a degree or diploma or other qualification at any other University.

Furthermore, I state that no part of this dissertation has been, or is concurrently being, submitted for any degree, diploma, or other qualification.

Claire Cox
September 2012

Abstract

Upon activation in epidermal stem cells, the proto-oncogene c-Myc triggers their exit from the stem cell compartment resulting in an increase in progenitor cell proliferation and an induction in terminal differentiation. Whether c-Myc plays a direct transcriptional role in epidermal stem cell differentiation was unknown. The exploration of c-Myc's transcriptional roles at the epidermal differentiation complex (EDC), a locus essential for skin maturation demonstrated that binding of c-Myc to the EDC can simultaneously recruit and displace specific sets of differentiation-specific transcriptional regulators to EDC genes. Among these factors, Sin3A acts as a transcriptional co-repressor and was initially discovered via its direct interaction with Mxi1 and Mxd1, which are antagonists of the Myc family network. As such, I concentrated on the role of Sin3A as a potential opposing factor to c-Myc activity in the epidermis.

To analyse the role of Sin3A in regulating epidermal stem cell fate in vivo, I generated a number of trangenic mouse models. To determine whether Sin3A functions in hair follicle stem cells, I inducibly deleted Sin3A in the hair follicle bulge, where quiescent stem cells reside. However, lack of Sin3A in the hair bulge did not cause any aberrant phenotype and I concluded that Sin3A is dispensable for hair follicle homeostasis. I next analysed a mouse model in which Sin3A is inducibly deleted in the basal layer of the epidermis. Deletion of Sin3A resulted in a severe disruption of epidermal homeostasis-namely due to increases in proliferation and differentiation. Further investigation demonstrated that this phenotype is driven by enhanced genomic recruitment of c-Myc to the epidermal differentiation complex and reactivation of c-Myc target genes involved in cellular proliferation. I found that Sin3A causes de-acetylation of the c-Myc protein to directly repress c-Myc's transcriptional activity and is antagonistic to c-Myc in the interfollicular epidermis. I hypothesised that simultaneous deletion of Sin3A and c-Myc might return the skin to normality. Indeed, when Sin3A and Myc are concurrently deleted, proliferation and differentiation levels returned to normal. These results demonstrate how levels of Sin3A and c-Myc must be carefully balanced for epidermal homeostasis to be maintained.

Decreased expression of Sin3A has been linked to tumour susceptibility in other tissues for example in non-small cell lung carcinoma making Sin3A a candidate tumour suppressor gene. I therefore considered that loss of Sin3A may lead to increased susceptibility to skin cancer. To investigate this I performed pilot experiments using UVB irradiation of skin that has one copy of Sin3A deleted in the basal layer of the epidermis. Under normal conditions, these mice have no identifiable phenotype, but pilot experiments demonstrated that after short term and long term UVB irradiation, they exhibit increased epidermal thickness and proliferation relative to controls. This recapitulated the phenotype observed when Sin3A is inducibly deleted in the interfollicular epidermis and further demonstrates the role of SinA as an inhibitor of proliferation in this tissue. Overall, these results demonstrate that an interplay between the opposing functions of Sin3A and c-Myc are necessary to ensure that there is balanced homeostasis in the interfollicular epidermis.

Acknowledgements

I would like to thank Michaela Frye for allowing me to join her lab and for being an excellent and enthusiastic point of guidance and expertise during my PhD. Under her supervision I believe that I have matured as a scientist and an individual and I am now prepared to pursue a career in academic research. Thank you!!

Thank you to all Frye lab members, past and present, for helping me through my PhD experience. Thank you for constant support, scientific discussion, non-scientific discussion and for joining me in pursuit of lab singing and dancing as a pastime. Particular thanks to Iwona Driskell who has been with me every step of the way as a companion and science expert. Thanks also to Brian Hendrich and Austin Smith whose constructive criticism challenged me along the way and made me into a much better scientist than I ever anticipated.

Thank you to the Biofacility, Histology, Imaging, Transgenics, Flow Cytometry and Tissue Culture facilities, without your expertise, this work would never have come to fruition.

This dissertation was financially supported by an MRC studentship.

On a personal note, I would like to thank everyone who has made my Cambridge experience special and one of the most amazing periods of my life. There are too many people to name individually, but you all know who you are! Thanks for all the memories! A special thank you to Thomas Walpole, who helped me get through my thesisitis. Finally and perhaps most importantly I have to thank my family members for all their love and support. To my Dad, who has turned many a bad science day around with his amazing ability to write inspiring emails, my Mum, who is always on the end of the phone and to my two sisters, who provide me with constant laughs and inspiration. A special mention to my Nanna who never fails to look after me and to my Grandad, whose memory will always live on. I hope that I have made them all proud.

List of abbreviations

APS Ammonium Persulphate

BCS Bovine Calf Serum

BMP Bone Morphogenic Protein

Blimp1 B lymphocyte Induced Maturation Protein 1

bp base pair

BrdU Bromodeoxyuridine

Cbx4 Chromobox Homolog 4

cDNA Complementary Deoxyribonucleic Acid

Cebp CCAAT-enhancer Binding Protein

ChIP Chromatin Immunoprecipitation

D Day

DAPI 4',6-Diamidino-2-Phenylindole

DMBA 7,12-Dimethylbenz(a)anthracene

DMEM Dulbecco's Modified Eagle's Medium

DMSO Dimethyl Sulphoxide

DNA Deoxyribonucleic Acid

DNMT1 DNA Methlytransferase I

dNTP Deoxynucleotide Triphosphate

E Embryonic Day

ECL Electrochemiluminescence

EDC Epidermal Differentiation Complex

EDTA Ethylenediaminetetraacetic Acid

EGF Epidermal Growth Factor

EPU Epidermal Proliferative Unit

ER Oestrogen Receptor

GAPDH Glyceraldehyde 3-Phosphate Dehydrogenase

EV Empty Vector

EZH1/2 Enhancer of Zester Homologs 1/2

FAD F12 + Adenine + DMEM

FCS Foetal Calf Serum

FGF Fibroblast Growth Factor

Flg Filaggrin

Gata-3 GATA Binding Protein 3

H&E Haemotoxylin and eosin

HAT Histone acetyltransferase

HCR Highly conserved region

HDAC Histone deacetylase

HF Hair Follicle

HID HDAC interaction domain

Hr Hours

HRP Horseradish Peroxidase

IFE Interfollicular Epidermis

IMS Industrial Methylated Spirit

IP Immunoprecipitation

IRS Inner Root Sheath

IS Isthmus

ISH *In Situ* Hybridisation

Itgα6 Integrin α6

Ivl Involucrin

Jarid2 Jumonji, AT-Rich Domain 2

JZ Junctional Zone

K Keratin

Kb Kilobase

Klf4 Kruppel-Like Factor 4

LCE Late Cornified Envelope

Lgr5 Leucine-rich Repeat Containing G Protein-coupled Receptor 5

Lgr6 Leucine-rich Repeat Containing G Protein-coupled Receptor 6

Lhx2 LIM/Homeobox Protein 2

Lor Loricrin

Lrig1 Leucine-rich Repeat and Immunoglobulin-like Domain Protein 1

MAB Maleic Acid Buffer

Mb Megabase

Misu Myc-induced SUN-domain-containing Protein

mRNA Messenger Ribonucleic Acid

Myc c-Myc

NFATc1 Nuclear Factor of Activated T-cells, Cytoplasmic, Calcineurin-Dependent1

NuRD Mi-2/Nucleosome Remodeling and Deacetylase

4-OHT 4-hydroxy-tamoxifen

OCT Optimal Cutting Temperature solution

Ovol1 Ovo-like1

P Postnatal day

PAGE Polyacrylamide Gel Electrophoresis

PAH Paired amphipathic helix

PBS Phosphate-buffered Saline

PBST 0.2% (v/v) Tween 20 in PBS

PBT Phosphate-buffered Saline-Tween

PCR Polymerase Chain Reaction

PE Phycoerythrin

Per Period

PI Propidium Iodide

pRB Retinoblastoma 1

PRC Polycomb repressive complex

QPCR Quantitative Real Time Polymerase Chain Reaction

RIPA Radio-Immunoprecipitation Assay

RNA Ribonucleic Acid

RT Real Time

Runx1 Runt-related Transcription Factor 1

SATB1 Special AT-Rich Sequence Binding Protein1

SDS Sodium Dodecyl Sulphate

Setd8 SET Domain Containing (Lysine Methyltransferase) 8

SG Sebaceous Gland

SHH Sonic Hedgehog

SID Sin3-interaction Domain

Sin3A SIN3 Transcription Regulator Homolog A

Sin3A SIN3 Transcription Regulator Homolog B

SPRR Small Proline Rich

STAT Signal Transducer and Activator of Transcription

SSC Saline-Sodium Citrate

TA Transit Amplifying

TAE Tris-acetic Acid-EDTA

TBS Tris-buffered Saline

TBST Tris-buffered Saline-Tween

TEMED Tetramethylethylenediamine

Tgm1 Transglutaminase1

TPA Phorbol 12-myristate 13-acetate

tRNA Transfer RNA

UV UltraViolet

UVB UltraViolet B

WCL Whole cell lysate

WT Wild-type

X-Gal 5-bromo-4-chloro-indolyl- β-D-galactoside

Mouse Lines

f/f floxed alleles

Δ/Δ deleted alleles

Contents

List of Figures

List of Tables

Chapter 1

Introduction

1.1 Structure of mammalian skin

Mammalian skin is a remarkable organ in terms of its numerous functions, structural complexity and high turnover of cells, thus requiring tightly regulated homeostasis. Skin consists of the epidermis, separated from the dermis via a basement membrane (Figure 1.1). The epidermis, a stratified epithelium, comprises the outer layer of the skin and functions primarily as a barrier providing protection against harmful external effects such as ultraviolet radiation and microbial invasion as well as acting to prevent dehydration [Fuchs and Horsley, 2008]. A single layer of proliferative cells forms the basal layer of the interfollicular epidermis (IFE), which are tethered to the basement membrane. Cells from the basal layer migrate upwards to generate the terminally differentiating stratified suprabasal layers allowing replenishment of cells that are lost from the cornified layers [Pincelli and Marconi, 2010] (Figure 1.1). The IFE has a number of appendages that are specified via epithelial-mesenchymal interactions throughout development. These appendages include nails and sweat glands as well as the hair follicle (HF) and sebaceous gland (SG), which are key components of the pilosebaceous unit [Mikkola, 2007].

To give rise to, repair and maintain the IFE and its appendages, (Figure 1.1), there is a reliance on epidermal stem cells. Stem cells have been identified and

characterized in the epidermis and its appendages for example stem cells reside in the bulge region of the HF, the SG and the basal layer of the IFE [Fuchs, 2008]. Understanding how these cells give rise to and maintain balanced epidermal homeostasis and allow response to injury such as wounding is subject to intense investigation. Firstly, I will discuss how skin is specified during embryogenesis and then will progress to the discussion of maintenance of adult skin.
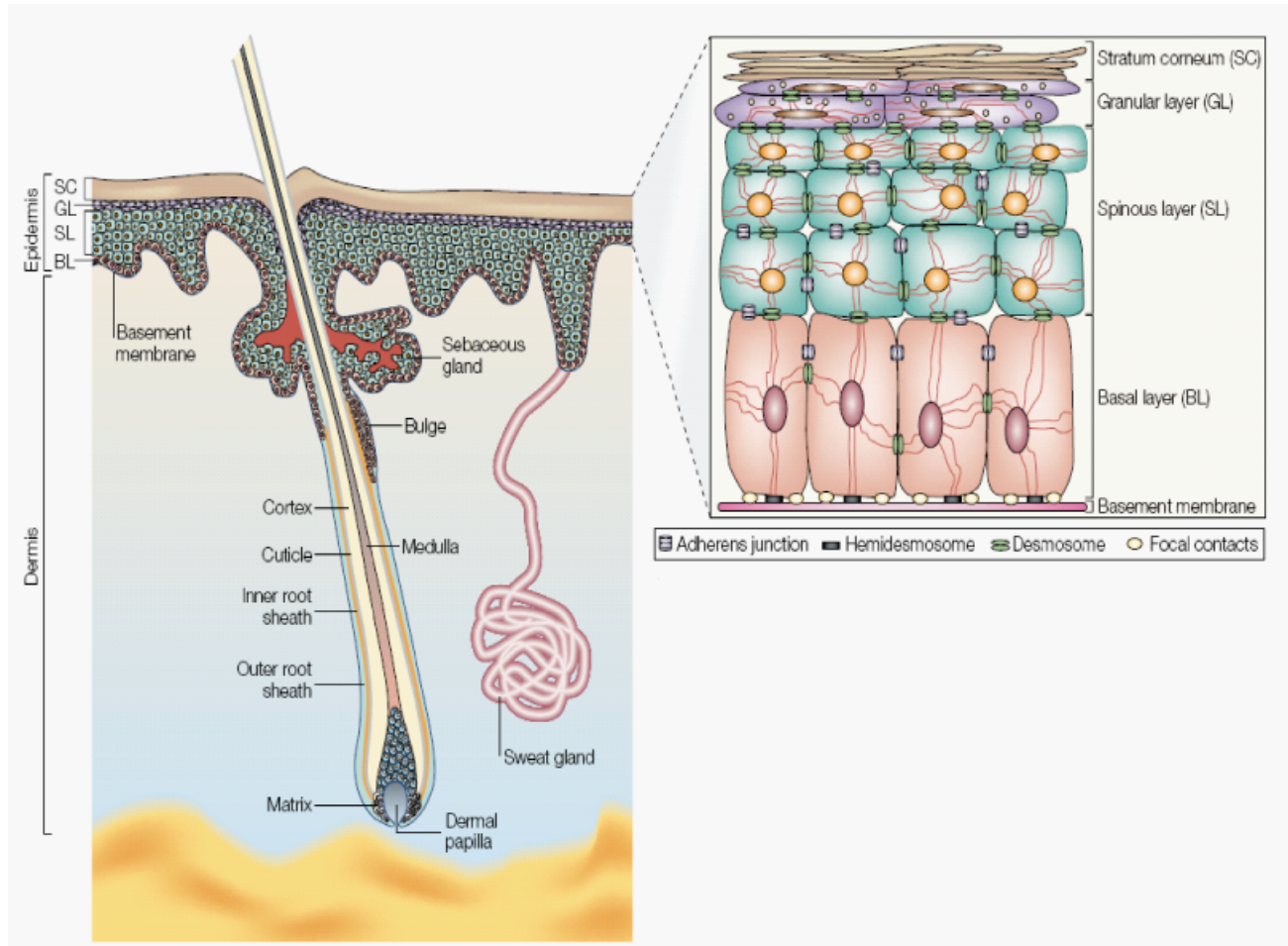
Figure 1.1: Schematic structure of mammalian skin. The outer layer of skin, the epidermis, is separated from the inner layer, the dermis, via a basement membrane. The epidermis can be considered as the interfollicular epidermis and its appendages the hair follicle and sebaceous gland. Proliferative cells in the basal layer of the interfollicular epidermis give rise to the cells of the differentiated spinous and granular layers. This generates a system in which cells from the basal layer divide to replace those that are lost from the surface, the cornified layer. The interfollicular epidermis, hair follicle and sebaceous glands are maintained by numerous stem cell populations. Taken from [Fuchs and Raghavan, 2002].

1.2 Epidermal origins

Development of the skin throughout embryogenesis is a highly complex process that relies on tightly controlled mechanisms to ensure that specification of the layers of the skin is correct. I will concentrate on the development of the epidermis as this is the skin layer around which my PhD project is centred. During embryogenesis in mammals, the epidermis develops from a single layer of multipotent cells from the surface ectoderm, while the dermis originates from cells in the mesoderm and neural crest [Mack et al., 2005; Viallet and Thelu, 2004].

1.2.1 Development of the interfollicular epidermis

At mouse embryonic day 8.5 (E8.5), the single layer of multipotent epithelial cells is specified as a consequence of Wnt signalling, which blocks the ability of ectodermal progenitors to respond to signalling from fibroblast growth factors (FGFs) [Fuchs, 2007]. This allows the ectodermal progenitors to respond to bone morphogenic protein (BMP) signalling resulting in the adoption of an epidermal cell fate [Fuchs, 2007]. The IFE develops from this single layer of epithelial cells as a consequence of a number of developmental cues, which induce expansion and stratification ultimately leading to the generation of a fully stratified epithelium by E18.5 [Mack et al., 2005]. This stratified epithelium is composed of the basal layer, the terminally differentiated spinous and granular layers of the IFE, and the cornified envelope [Mack et al., 2005] (Figure 1.2).

The commitment to stratification is evident at the single layer stage as signified by the expression of Keratin 5 (K5) and K14 at E9.5 [Byrne et al., 1994] (Figure 1.2). A possible factor that acts as the cue for the initiation of stratification is the transcription factor p63, which is first expressed at E8.5 [Koster and Roop, 2004] (Figure 1.2). Initial evidence suggesting that p63 has this role came from two papers published in the same year, which describe mouse models in which p63 is deleted [Mills et al., 1999; Yang et al., 1999]. P63-null mice lack stratified epithelia and have abnormal skin consisting of just a single cell layer [Mills et al., 1999; Yang et al., 1999]. One of the key means by which p63 is thought to mediate stratification is via the activation of Special AT-rich Sequence Binding

Protein1 (SATB1), which remodels chromatin leading to transcriptional activation of genes involved in epidermal differentiation [Fessing et al., 2011].

At E10.5, the periderm, which is a temporary protective covering of the the epidermis is formed and the onset of stratification begins [Fuchs, 2007; Mack et al., 2005; MBoneko and Merker, 1988] (Figure 1.2). The function of the periderm is thought to be to protect the embryo from amniotic fluid during embryogenesis until barrier formation is complete [Koster and Roop, 2004]. The emergence of suprabasal layers marked by K1 and K10 occurs at E15.5 [Byrne et al., 1994], followed by a Loricrin-expressing layer by E16.5 and Filaggrin begins to be expressed at E17.5 [Mack et al., 2005] (Figure 1.2). The presence of the "living" layers of the IFE : the basal layer, the spinous and granular layers as well as the "dead" cornified layer are therefore specified and barrier function is formed by E18.5.

This layout of the IFE, as can be seen in Figure 1.3, is maintained throughout the life of adult skin. The maintenance of the structure of the IFE is dependent on a stem cell population that is unique to the IFE under normal homeostatic conditions [Benitah and Frye, 2012]. This stem cell population will be discussed in further detail in Section 1.3.1. In order for homeostasis to be maintained, there must be a careful balance between stem cell self-renewal and differentiation.
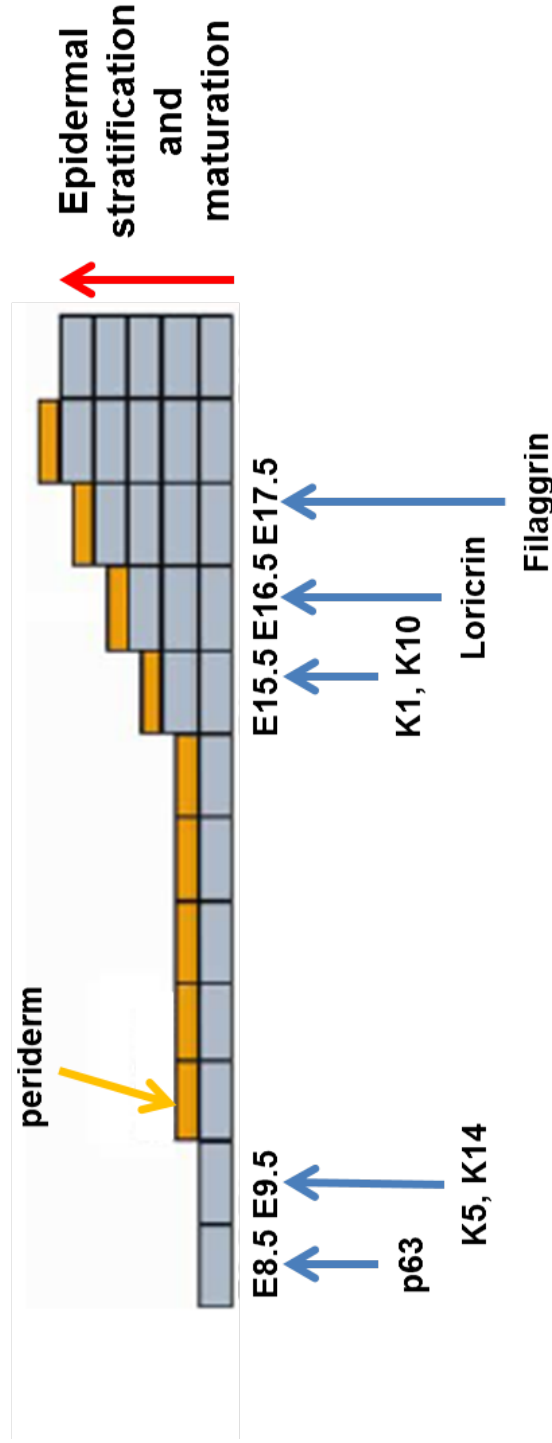
Figure 1.2: Schematic representation of stages in IFE development. The epidermis develops from a single layer of ectodermal cells, which are specified towards an epidermal fate at E8.5. Commitment to stratification is evident at E9.5 with the onset of expression of K5 and K14. The initiation of the stratification process is indicated by the formation of the periderm. Maturation of the epidermis continues throughout embryonic development as indicated by the expression of differentation markers K1, K10, Loricrin and Filaggrin. By E18.5 the spinous, granular and cornified layers are specified and there is the loss of the periderm. Modified from [Koster and Roop, 2004].
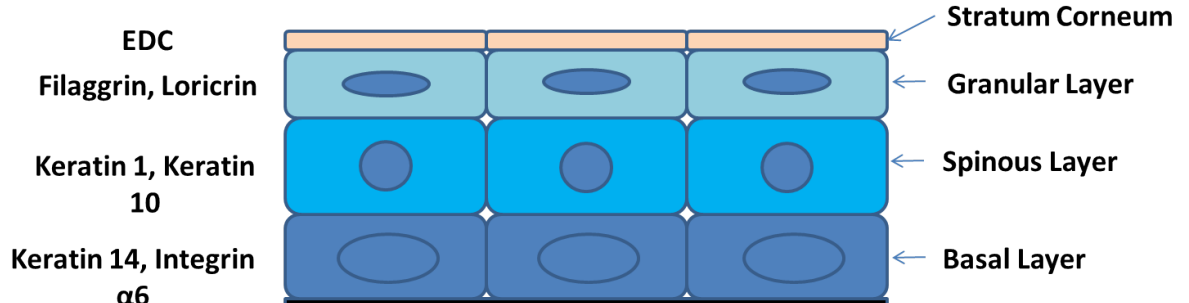
Figure 1.3: Schematic representation of the established interfollicular epidermis (IFE) The layers of the IFE are specified during embryonic development. The basal layer, containing undifferentiated cells, is marked by expression of K14 and integrin α6. The next layer is the spinous layer, which expresses K1 and K10. The granular layer is marked by expression of Filaggrin and Loricrin. Proteins encoded by the epidermal differentiation complex (EDC) are cross-linked to form the stratum corneum (cornified envelope), which is essential for barrier function. See [Fuchs, 2008].

1.2.2 Differentiation processes in the interfollicular epidermis

The majority of the genes responsible for differentiation in the IFE are clustered in a genomic region spanning 2.2 megabases (Mb) in mouse and 1.6Mb in human, called the Epidermal Differentiation Complex (EDC) [Brown et al., 2007; Nascimento et al., 2011]. The EDC is located on chromosome 3f2.1 in the mouse and chromosome 1q21 in humans [Brown et al., 2007; Nascimento et al., 2011]. The EDC encodes four clustered gene families: the Filaggrin-Like (Flg), Late Cornified Envelope (LCE), Small Proline Rich Region (SPRR) and S100 gene families and is schematically represented in Figure 1.4.

Members of the Flg-like, LCE and SPRR families encode structural proteins that are cross-linked by transglutaminases to form the cornified envelope (Figure 1.3), which is essential for the establishment of normal barrier function in the IFE [de Guzman Strong et al., 2010; McGrath and Uitto, 2008]. The S100 gene family encodes calcium sensor proteins that are involved in signal transduction and act as chemoattractants [Broome et al., 2003]. It has also been proposed that
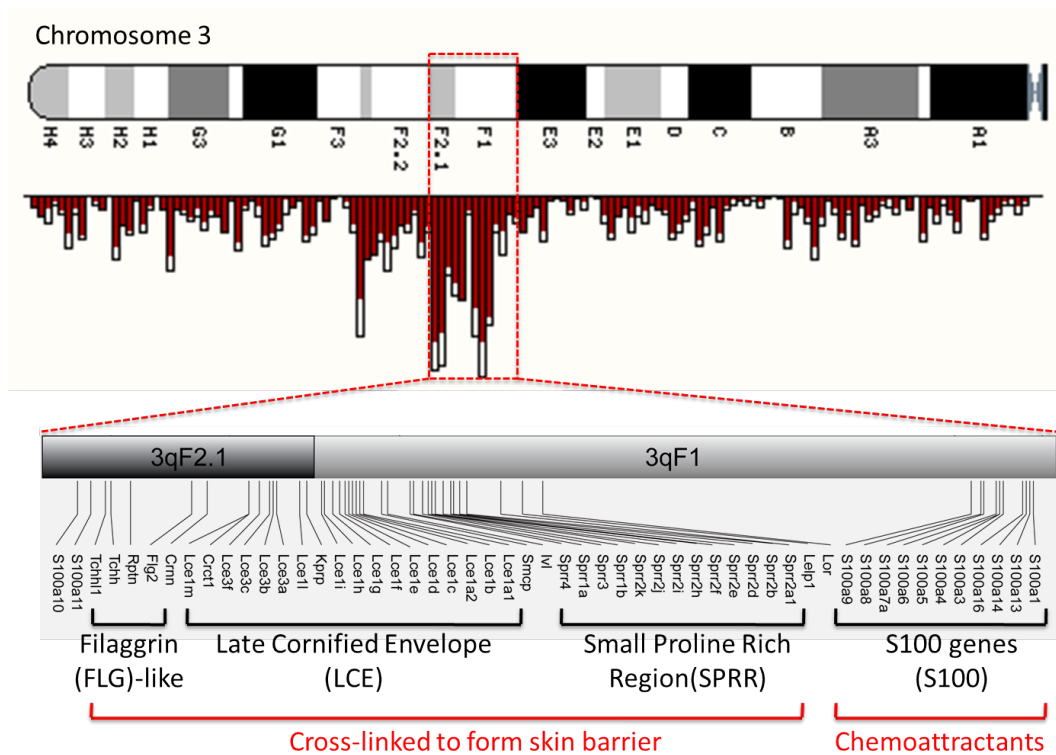
Figure 1.4: Schematic representation of the mouse epidermal differentiation complex. The EDC encodes four clustered gene families. The Filaggrin-Like (Flg), Late Cornified Envelope (LCE) and Small Proline Rich Region (SPRR) encode proteins that are cross-linked to form the skin barrier while the S100 gene family encodes calcium sensor proteins that are chemoattractants.

S100 proteins encoded for by the EDC are involved in membrane remodelling and there is evidence that the gene products are involved in inflammatory processes [Eckert et al., 2003]. The importance of proper expression of EDC genes is indicated by the fact that disruption of their expression leads to skin disease. For example, a number of members of the S100 gene family have been observed to be up-regulated in psoriasis and skin cancer [Hoffjan and Stemmler, 2007]. Disruption of the expression of genes in the Flg-like, LCE and SPRR families has been linked with the development of atopic dermatitis and psoriasis as well as ichthyosis vulgaris [de Guzman Strong et al., 2010].

A number of transcription factors have been implicated in the control of epidermal differentiation and the expression of genes in the EDC. One of these transcription factors is Kruppel-like Factor 4 (Klf4), which is expressed in the suprabasal layers of the IFE [Segre et al., 1999]. Klf4 has been demonstrated to be essential for correct barrier formation and there is misexpression of a number of EDC genes encoding structural components of the IFE when Klf4 is mutated [Dai and Segre, 2004]. The zinc finger protein Ovo-like1 (Ovol1) is also a regulator of differentiation and Ovol1-depleted epidermis has defective terminal differentiation and increased proliferation [Nair et al., 2006]. The basic region leucine zipper transcription factors CCAAT-enhancer Binding Protein α (Cebpα) and Cebpβ are expressed in basal keratinocytes and are important in differentiation commitment [Lopez et al., 2009]. When these transcription factors are deleted, basal keratinocytes fail to exit the cell cycle leading to increased proliferation and an impairment in commitment to differentiation [Lopez et al., 2009]. c-Myc is also an important transcription factor in the process of epidermal differentiation. The functions of c-Myc will be discussed in Section 1.5.

1.2.3 Hair follicle morphogenesis

HFs can be considered to function as factories for the production of hair shafts, as a sensory organ for the skin, are important immunologically, provide thermal protection and HF cells can repopulate the IFE after injury [Paus et al., 1999]. The process of HF development begins with the formation of a hair placode at

E14.5, whose formation is induced by signals from mesenchymal cells underlying the epidermis [Benitah and Frye, 2012]. One of the first and predominant factors in hair placode induction is the Wnt signalling pathway, which is active from E13.5 followed by Edar activities at E14.5 [Wang et al., 2012]. Sonic Hedgehog is expressed in the placode and is responsible for the formation of the dermal papilla at E16.5 [Fuchs, 2007; Wang et al., 2012]. Between E16.5 and E17.5 there is directional downgrowth leading to the formation of hair pegs, which is mediated by microRNAs as well as cell matrix interactions [Benitah and Frye, 2012]. At E18.5 the inner root sheath (IRS) develops, providing a channel for hair emergence and the outer root sheath contacts the basement membrane, which is followed by hair emergence at birth [Fuchs, 2008]. Hair maturation continues postnatally and the first entry into the hair cycle occurs at postnatal day 17 (P17). The steps of morphogenesis and subsequent entry into the hair cycle are schematically represented in Figure 1.5.

1.2.4 Hair beyond morphogenesis:- the hair cycle

The first two hair cycles are synchronised in mouse back skin [Müller-Röver et al., 2001]. The hair cycle consists of 3 different stages:- anagen, catagen and telogen (Figure 1.5). The hair follicle is quite remarkable in that this cycling through the hair cycle stages is maintained throughout the life of the animal. Anagen represents the growth phase of the hair cycle and recapitulates hair follicle development. The process is reliant on proliferation and differentiation of HF matrix cells and ultimately leads to the regeneration of the cycling portion of the HF with daughter cells differentiating into one of the six IRS or hair shaft lineages [Alonso and Fuchs, 2006]. Following anagen, the hair follicles progress into the catagen stage, which is termed the destructive phase as the non-permanent portions of the hair follicle undergo apoptosis and regression occurs [Müller-Röver et al., 2001]. A number of factors have been implicated in this transition, such as FGF5 and Epidermal Growth Factor (EGF), but the transitional process is not yet fully understood [Alonso and Fuchs, 2006]. Catagen leads to the dermal papilla being located just below the bulge region of the hair follicle, a situation which is maintained during the transition to the third hair cycle stage, telogen
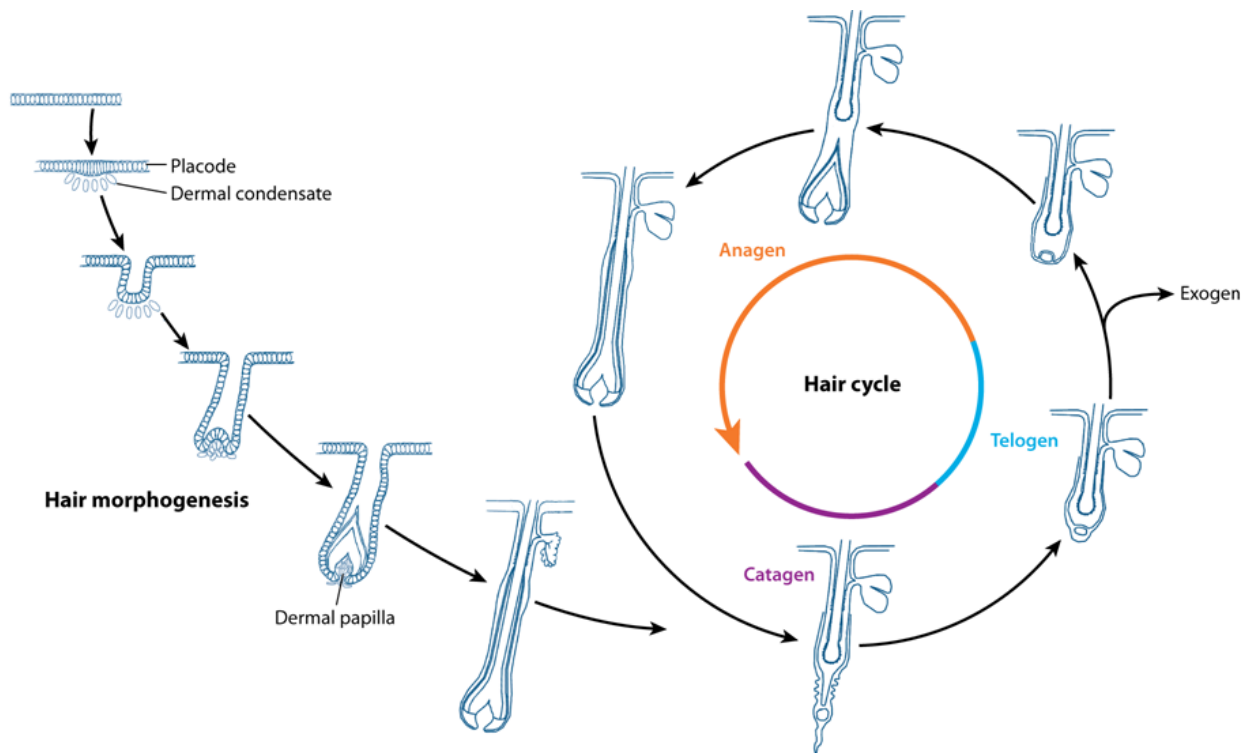
Figure 1.5: Schematic representation of hair follicle morphogenesis and the hair cycle. Hair follicle morphogenesis begins in embryonic development and continues postnatally. Following the completion of hair follicle morphogenesis, the hair follicles progress into the hair cycle, which is synchronised for the first two cycles in mice. Following anagen (the growth phase), the hair follicles synchronously enter catagen (the destructive phase) and then enter telogen (the resting phase). Taken from [Shimomura and Christiano, 2010].

(the resting phase). During the resting phase, the hair shaft undergoes maturation into a club hair, which is then shed from the hair follicle [Paus et al., 1999]. There is some debate as to whether the loss of this club hair, which has been termed as a fourth stage of the hair cycle "exogen", is an active process controlled by signalling mechanisms for example, or a passive process caused by force from the growing hair fiber [Higgins et al., 2009]. When each new cycle is initiated, the lower portion of the hair follicle is regenerated as a consequence of interactions between cells of the dermal papilla and the secondary germ cells in the bulge region of the hair follicle [Paus et al., 1999]. There is a reliance on HF stem cells for the process of HF cycling to be continued, a role which will be discussed in more detail below.

1.2.5   Sebaceous gland development

SGs are an appendage of the IFE are located above the bulge region of the HF and secrete sebum and lipids [Stewart and Downing, 1991]. These secretions from the SGs provide lubrication to the hair shaft and prevent microbial infection [Stewart and Downing, 1991]. The SG starts to develop at a late point in embryogenesis and how this process occurs is much less defined than that of the HF [Fuchs, 2007]. Two models as to how SGs come into existence have been postulated. The first is that bulge stem cells produce multipotent progenitors that differentiate to develop the SG while the second considers that SG-specific progenitor cells are responsible for the production of SGs [Horsley et al., 2006]. Weight was leant to this second model by the finding that B lymphocyte Induced Maturation Protein 1 (Blimp1)-positive progenitor cells generated late in embryogenesis appear to establish and form the sebaceous gland [Horsley et al., 2006]. In the case of Blimp1 mutation or wounding, bulge stem cells can be induced to produce sebaceous gland cells [Fuchs, 2007].

1.3 Epidermal stem cells and their markers

Epidermal homeostasis involves a careful balancing act between cell loss and cell replacement in order to avoid excess proliferation, which could lead to disorders such as psoriasis and cancer or hypoproliferation and thinning of the skin. In order for the epidermis to be maintained there is the reliance on stem cell populations whose behaviour must also be controlled. Stem cells are defined by two key properties. Firstly these cells have the ability to self-renew and secondly the ability to produce daughter cells that can differentiate into more specialised cell types [Smith, 2006]. The epidermis is a remarkable system in which to study stem cell behaviour and regulation as it is known to harbour a number of stem cell populations. Epidermal stem cells have been identified in the IFE, HF and SG and are responsible for tissue maintenance. I will now discuss the information that is known about these stem cell populations.

1.3.1 Stem cells in the interfollicular epidermis

An independent population of stem cells to the HF is responsible for the maintenance of the IFE under normal homeostatic conditions and is located in the basal layer of the IFE [Benitah and Frye, 2012]. These stem cells express K5 and K14 (Figure 1.6). It has been postulated that these stem cell populations are found in epidermal proliferation units (EPUs), which consist of a central stem cell with surrounding transit amplifying (TA) cells and that one in ten basal cells are stem cells [Strachan and Ghadially, 2008]. This model linked into the pre-existing stem cell/ TA cell model, in which the epidermis is considered to be maintained by long-lived, self-renewing stem cells that give rise to short-lived TA cells, which give rise to the differentiated progeny of the IFE [Doupé and Jones, 2012]. In this model, long-lived stem cells can undergo asymmetric division to produce a TA daughter cell and a stem cell daughter cell or potentially can undergo symmetrical divisions to produce either two TA daughter cells or two stem cells in order to maintain the IFE.

More recently, this model has been challenged as a consequence of results obtained from lineage tracing experiments in mouse epidermis, leading to the postulation
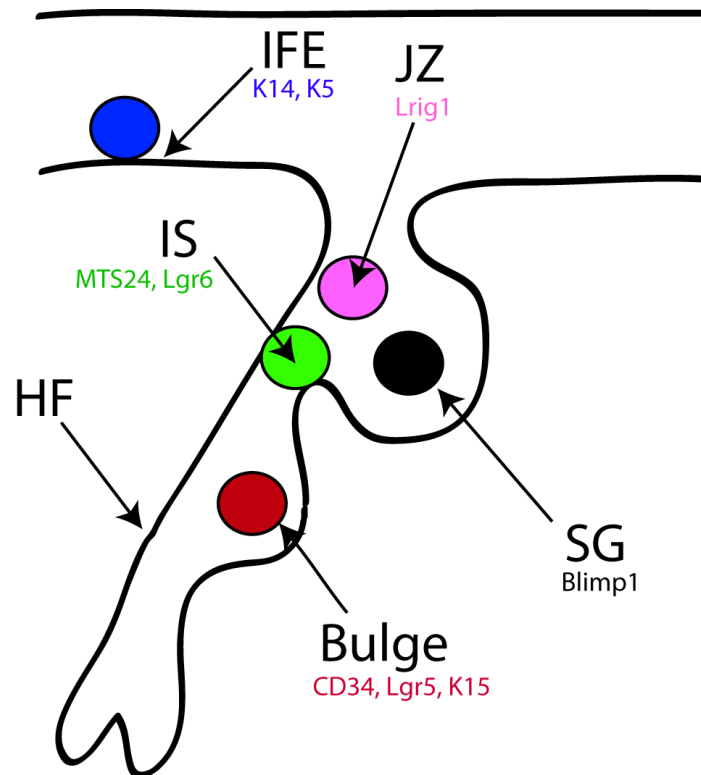
Figure 1.6: Schematic representation of the different epidermal stem cell populations. The different epidermal stem cell populations that have been identified are represented in this figure. IFE stem cells and markers are shown in blue. Stem cells in the junctional zone (JZ) and markers are shown in pink. Stem cells in the isthmus (IS) and corresponding markers are represented in green. Finally, the stem cells located in the bulge region of the HF and their markers are shown in red. Based on [Beck and Blanpain, 2012].

of the commited progenitor model [Clayton et al., 2007]. This model argues that the results from lineage tracing experiments exclude the EPU and stem cell/TA cell model. Instead, there is the proposal that the IFE is maintained by a single population of equivalent progenitors that choose one of 3 potential fates stochastically. In order for epidermal homeostasis to be maintained, the probability of the three different outcomes, the production of two stem cells, two differentiated cells or a stem cell and a differentiated cell, is equal [Doupé and Jones, 2012].

A recent publication has reconciled these apparently contradictory theories [Mascré et al., 2012]. Using transgenic mouse models and quantitative analysis of lineage tracing, the authors demonstrated that in the IFE there is a slow-cycling stem cell population and a population of TA cells that cycle more rapidly and that both of these populations exhibit stochastic choice in cell fate [Mascré et al., 2012]. Furthermore, under conditions of wounding, the stem cell population is activated to effect repair while the contribution of TA cells is limited [Mascré et al., 2012]. Potentially, under normal homeostatic conditions, the TA population are mainly responsible for maintenance of the IFE while activation of normally quiescent stem cells are activated to mediate repair in response to injury [Mascré et al., 2012].

1.3.2 Stem cells of the hair follicle and the sebaceous gland

The HF is home to numerous stem cell populations (Figure 1.6). The best characterised of these stem cell populations is the relatively quiescent population that resides in the bulge region of HF. Bulge stem cells are label-retaining cells and are slow-cycling under adult homestatic conditions [Cotsarelis et al., 1990; Tumbar et al., 2004]. One of the first markers identified for the bulge stem cell population in the mouse was CD34 [Cotsarelis, 2006; Trempus et al., 2003]. A number of different lineage-tracing studies using reporter genes under the control of HF-specific promoters including K15 [Morris et al., 2004] and K19 [Youssef et al., 2010] have revealed that under normal homeostatic conditions the stem cells of

the bulge are involved in the regeneration of the HF in the adult [Sotiropoulou and Blanpain, 2012]. Furthermore, all hair lineages can be generated upon the transplantation of the progeny of a single bulge stem cell [Blanpain et al., 2004]. An actively cycling, multipotent stem cell population that expresses Leucine-rich Repeat-Containing G-protein Coupled Receptor 5 (Lgr5) and can give rise to new HFs is also found in the bulge region [Jaks et al., 2008].

In the past few years, lineage tracing has become established as a gold standard technique to study stem cell behaviour thus helping to characterise stem cell populations in the hair follicle, as well as other tissues. Lineage tracing is advantageous as it allows the analysis of progeny from a single cell under homeostatic conditions although drawbacks are that stem cells can exhibit different properties during homeostasis and after wounding for example and that different techniques used for lineage tracing can yield different results [Kretzschmar and Watt, 2012]. Despite these caveats, results from such studies have provided new information about stem cell populations in the hair follicle. A number of stem cell populations have been identified that are responsible for the maintenance of the SG and the upper portion of the HF [Sotiropoulou and Blanpain, 2012].

A Leucine-rich Repeat and Immunoglobulin-like Domain Protein 1 (Lrig1) positive stem cell population has been identified in the junctional zone in the upper region of the HF (Figure 1.6). Under normal homeostatic conditions this population is bipotent and gives rise to cells of the SG and the IFE, but this population has been shown to be able to contribute to all epidermal lineages in epidermal reconstitution assays [Jensen et al., 2009]. An Lgr6-expressing stem cell population has been identified in the isthmus portion of the hair follicle [Beck and Blanpain, 2012; Snippert et al., 2010]. Lineage-tracing experiments have demonstrated that Lgr6-positive cells in this region can contribute to the SG, IFE and HF postnatally (although the HF contribution declines with age) [Snippert et al., 2010]. An additional stem cell population, which is distinguished by the expression of MTS24 also resides in the isthmus [Jaks et al., 2010; Nijhof et al., 2006]. These cells can reconstitute the HF and IFE and thus can be considered to have the properties of multipotent stem cells [Nijhof et al., 2006]. It is noteworthy that a

subset of Lgr6-positive stem cells also express MTS24 [Beck and Blanpain, 2012; Snippert et al., 2010]. In the SG, a resident unipotent stem cell population that expresses Blimp1 has been identified, which under physiological conditions can give rise to sebocytes [Horsley et al., 2006; Schneider and Paus, 2010] (Figure 1.6).

1.4 Key transcriptional regulators of epidermal stem cells

The maintenance of stem cell populations in the epidermis and lineage commitment involves dynamic regulation via regulators of transcription. I will discuss some of the key transcription factors that have been demonstrated to be of importance in governing epidermal stem cell fate and maintenance. As I have previously explained (see Section 1.2.1), p63 is thought to be of key importance in the epidermal stratification process. In addition to this role, p63 has been demonstrated to be expressed in epidermal stem cells [Pellegrini et al., 2001] and is required for the maintenance of the proliferative ability of this cell type [Senoo et al., 2007; Truong et al., 2006]. There is some debate as to whether p63 also has a role in lineage commitment [Sotiropoulou and Blanpain, 2012]. It appears that the TA isoforms of p63 are dispensable for differentiation while the ΔN isoforms of p63 are involved in lineage specification [Vanbokhoven et al., 2011]. It is clear that p63 has an essential role in epidermal stem cells, however, further examination is needed to elucidate the exact functions mediated by p63 in these cells. This is a process that is high in complexity due to the number of different p63 isoforms and their potentially differing roles. The canonical Notch signalling pathway also has a role to play in in regulating cell fate in the epidermis, including the transcription factors RBP-Jk and Hes1 [Sotiropoulou and Blanpain, 2012; Watt et al., 2008b]. Deletion of RBP-Jk or Hes1 in mouse models results in defective differentiation and a disruption to skin barrier formation [Blanpain et al., 2006; Moriyama et al., 2008]. The proto-oncogene c-Myc has also been demonstrated to be of key importance in the regulation of epidermal stem cells and will be discussed in Section 1.5.

A number of transcription factors have been demonstrated to have a key role in regulating stem cell fate in the hair follicle. One of these important factors is NFATc1 (nuclear factor of activated T-cells, cytoplasmic, calcineurin-dependent 1), which is expressed in bulge stem cells and is involved in the maintenance of bulge quiescence [Horsley et al., 2008]. During the active phase of the hair cycle (anagen), expression of NFATc1 is down-regulated and bulge stem cells are activated to produce progenitors [Horsley et al., 2008]. The importance of NFATc1

is highlighted by the phenotype of premature activation of the bulge stem cell compartment when NFATc1 is depleted in this region [Horsley et al., 2008]. Another factor that is important in HF stem cells is Sox9, which has a role in HF stem cell specification [Nowak et al., 2008]. In the absence of Sox9, there are hair cycle defects, adult bulge stem cells fail to be specified correctly and expression of the bulge stem cell marker CD34 is lost [Vidal et al., 2005].

The circadian molecular clock has also been demonstrated to have a key role in the regulation of epidermal stem cells [Janich et al., 2011; Lin et al., 2009]. In the absence of the core clock components Clock and Bmal1 there is a delay in anagen indicating a functional role of clock genes in cell cycle progression [Lin et al., 2009]. Further studies have demonstrated that deletion of Bmal1 or Per (Period) 1/2 leads to a disruption of the maintenance of stem cells in the epidermis and leads to defective homeostasis [Janich et al., 2011]. These results imply that the circadian molecular clock is necessary in the balance of stem cell activation and quiescence in the epidermis.

A further transcription factor that is important in HF development and maintenance is LIM/Homeobox Protein 2 (Lhx2),which has been demonstrated to maintain "stemness" of bulge stem cells [Rhee et al., 2006]. Evidence has shown that Runt-related Transcription Factor 1 (Runx1) is another important factor in both HF development and maintenance of HF stem cells [Osorio et al., 2008, 2011; Raveh et al., 2006]. Skin transplantation experiments and the use of a conditional knockout model in which GATA Binding Protein 3 (Gata-3) is deleted in the epidermis have demonstrated the importance of Gata-3 in development and maintenance of the HF and for lineage determination in the skin [Kaufman et al., 2003; Kurek et al., 2007]. In the absence of Gata-3 there is aberrant proliferation in the IFE leading to hyperplasia as well as the HF leading to defects in hair maintenance and development [Kaufman et al., 2003; Kurek et al., 2007].

The canonical Wnt/β catenin signalling pathway is of key importance in the development of the HF and in the maintenance of the HF postnatally [Reya and Clevers, 2005; Sotiropoulou and Blanpain, 2012]. Transcription factors of the

Tcf/Lef (Lymphoid Enhancer Binding Factor) family are key mediators of Wnt signalling:- when Wnt signalling is active Tcf/Lef1 are bound by β catenin and become transcriptional activators while in the absence of Wnt, Tcf1/Lef1 transcription factors repress their target genes [Reya and Clevers, 2005]. Lef1-null mice have a loss of hair formation while over-expression of Lef1 in the bulge and IFE leads to increased formation of HFs [van Genderen et al., 1994; Zhou et al., 1995]. Furthermore, transgenic expression of a dominant-negative form of Lef1 in K14-positive cells led to a push towards a SG fate and reduced hair differentiation implicating Lef1 in fate determination in the HF [Merrill et al., 2001]. Tcf3, which is expressed in bulge stem cells, has been proposed to have a role in bulge stem cell maintenance as expressing Tcf3 in epidermis leads to promotion of bulge cell characteristics [DasGupta and Fuchs, 1999]. Finally, Tcf3/4 have been demonstrated to be involved in lineage-determination in HFs as well as being required for the maintenance of epidermal homeostasis [Nguyen et al., 2009].

1.4.1 Chromatin regulators and epidermal stem cell fate

The governing of epidermal stem cell fate via transcriptional regulation involves a complex interplay between transcription factors and chromatin-modifying factors. Here I will discuss some the roles of known regulators of chromatin that have been implicated in the regulation of epidermal stem cell populations. The histone deacetylases (HDACs) HDAC1/2 have been demonstrated to have an important role in the epidermis and are critical for the development of the epidermis. When both HDAC1 and HDAC2 are deleted, there is a recapitulation of the phenotype observed in p63 knockout mice, namely the failure of HF specification, a lack of proliferation and failure of the IFE to stratify [LeBoeuf et al., 2010]. Consequently, it has been proposed that HDAC1/2 redundantly mediate the repressive functions of p63 and as such play a key role in epidermal stem cell regulation [LeBoeuf et al., 2010]. Another chromatin regulator linked to the transcriptional roles of p63 in epidermal stem cell fate is the histone methyltransferase Setd8 (SET Domain Containing (Lysine Methyltransferase) 8). When Setd8 is conditionally deleted in mouse epidermis, there is a loss of epidermal progenitors due

to the loss of p63 expression and an increase in p53 activity leading to apoptosis [Driskell et al., 2011]. At this stage whether Setd8 directly modifies p63 is unclear. Another key chromatin regulator implicated in p63-mediated control of epidermal stem cell fate is SATB1 [Botchkarev et al., 2012]. It is proposed that p63 regulates SATB1 to establish tissue-specific chromatin organisation in the epidermis [Fessing et al., 2011].

Another chromatin regulator linked to epidermal stem cell fate is Mi-2β, which is a component of the NuRD (Mi-2/Nucleosome Remodeling and Deacetylase) chromatin remodelling complex [McDonel et al., 2009]. Upon conditional deletion of Mi-2β in keratinocytes during development, the ability of basal epidermal cells to proliferate is compromised, there are defects in terminal differentiation in the IFE and impaired specification of HFs [Kashiwagi et al., 2007]. Additionally, DNA Methyltransferase I (DNMT1) expression is enriched in IFE progenitor cells and has been implicated in the maintenance of these cells [Sen et al., 2010]. In the absence of DNMT1 epidermal progenitors lose their ability to self-renew, exhibit defects in proliferation and there is an abnormal induction of cell cycle arrest genes [Sen et al., 2010], demonstrating the importance of DNA methylation patterns in epidermal stem cell fate.

In mammals, Polycomb Repressive Complexes (PRCs) 1 and 2 consist of polycomb group proteins and are known to mediate the compaction of chromatin and promote silencing of transcription [Botchkarev et al., 2012]. A number of components of these chromatin-modifying complexes have been implicated in epidermal stem cell behaviour. Chromobox Homolog 4 (Cbx4) is a member of PRC1 and has been implicated in control of human epidermal stem cells in two key ways [Luis et al., 2012]. Firstly, Cbx4 protects human epidermal stem cells from undergoing senescence in a process linked to its chromodomain and secondly prevents excessive proliferation and differentiation via a SUMO-lygase-dependent pathway [Luis et al., 2011]. Bmi1, another PRC1 member, has also been implicated in the control of senescence and proliferation in human epidermal stem cells [Botchkarev et al., 2012]. The PRC2 complex component Jumonji, AT-Rich Domain 2 (Jarid2) is a key player in epidermal stem and progenitor cells as Jarid2-depleted mouse

keratinocytes exhibit decreased proliferation and increased differention both *in vitro* and in conditional knockout mice [Mejetta et al., 2011]. Additionally, Jarid2 conditional knockout mouse HFs have delayed entry into anagen, meaning that Jarid2 potentially also has a role in regulation of HF stem cells [Mejetta et al., 2011]. Furthermore, Enhancer of Zester Homologs 1/2 (EZH1/2), which are also components of the PRC2 complex, have functionally redundant roles in epidermal stem cells [Botchkarev et al., 2012; Ezhkova et al., 2011; Zhang et al., 2012]. Evidence for the importance of these factors comes from mouse models in which EZH1/2 are both depleted in mouse epidermis, which demonstrate that epidermal development is disrupted and there is progressive degeneration of the HF and SG [Ezhkova et al., 2009, 2011].

1.5   c-Myc as a regulator of epidermal stem cell fate

As explained in the previous section, there are a number of factors involved in the transcriptional regulation of epidermal stem cells and I will now focus on a major player in epidermal homeostasis:- c-Myc. The Myc-family of genes encodes basic region helix- loop- helix leucine zipper transcription factors that are known to bind to E box sequences in target genes [Hooker and Hurlin, 2006]. Of these, c-Myc (which will now be referred to as Myc) has been a subject of intense study since its identification just over 25 years ago, mainly due to its oncogenic properties, contribution to tumorigenesis and its involvement in many other fundamental processes such as the cell cycle and apoptosis [Meyer and Penn, 2008]. Interestingly, prior studies have shown that Myc is a player in the regulation of epidermal stem cell homeostasis. Upon activation in epidermal stem cells, Myc triggers their exit from the stem cell compartment, increases progenitor cell proliferation and induces terminal differentiation [Arnold and Watt, 2001; Frye et al., 2003; Waikel et al., 2001] (Figure 1.7 A).

As part of the differentiation process, Myc mediates the up-regulation of genes involved in growth and proliferation, for example, Myc-induced SUN-domain-containing Protein (Misu) [Gebhardt et al., 2006; Nascimento et al., 2011; Watt et al., 2008a] (Figure 1.7 C). Direct down-regulation of genes involved in cell adhesion via binding of Myc to Miz-1 is important for the exit of the stem cell niche [Gebhardt et al., 2006; Nascimento et al., 2011; Watt et al., 2008a] (Figure 1.7 B). Myc/Miz-1-mediated gene repression is dependent on HDAC activity in promoter regions [Zhang et al., 2008]. Myc-induced epidermal stem cell differentiation is accompanied by a global increase of histone modifications that are largely associated with gene repression, a process dependent on the HDAC complex [Frye et al., 2007]. It has also recently been demonstrated that Myc acts in conjunction with Setd8 to maintain epidermal homeostasis and that this interplay is important for epidermal stem cell survival and behaviour to be maintained [Driskell et al., 2011].

Transgenic mouse models in which activation of Myc is sustained in the epidermis

have revealed that erroneous activation of Myc in the basal layer of the IFE leads to excessive proliferation and differentation into IFE and SGs [Arnold and Watt, 2001; Frye et al., 2003; Waikel et al., 2001]. Analysis of Myc's role at the EDC has revealed further information about Myc's role in the epidermis. When Myc is recruited to this locus, Myc can simultaneously recruit and displace specific sets of differentiation-specific transcriptional regulators to EDC genes [Nascimento et al., 2011]. More specifically, Myc binds to the EDC in conjuction with Klf4 and Ovol1, leading to activation of EDC targets whereas SIN3 Transcription Regulator Homolog A (Sin3A) and Cebpα are displaced [Nascimento et al., 2011]. The activation of Myc and thus the expression of the target genes it controls must therefore be tightly regulated for epidermal homeostasis to be maintained. Opposing transciptional regulators to prevent Myc becoming over-active is necessary and given that Sin3A can bind to the EDC and is displaced when Myc is over-expressed, Sin3A is a likely candidate for this role.
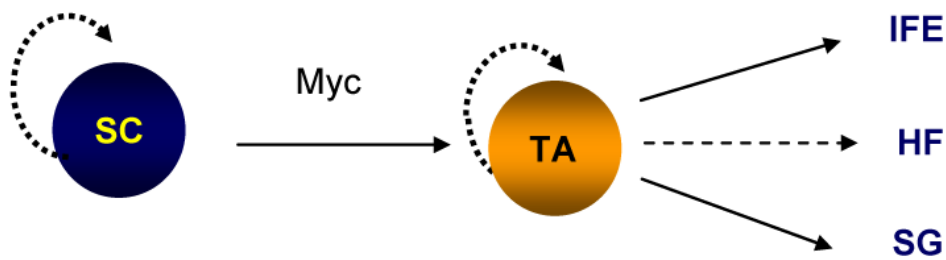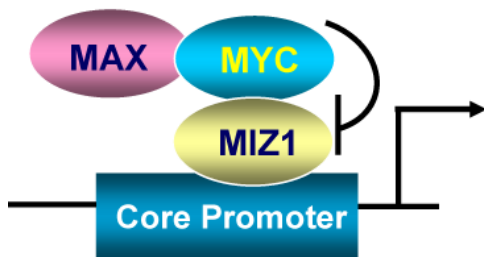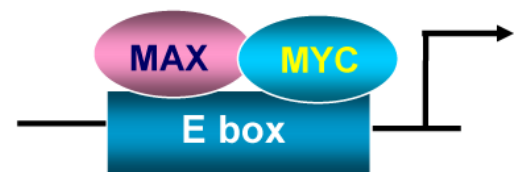
Figure 1.7: Activation of Myc in epidermal stem cells leads to terminal differentiation. A) Stem cells have the capacity to self-renew and give rise to Transit-Amplifying (TA) cells. TA cells undergo terminal differentiation to produce cells from the epidermal lineages. Myc activation drives terminal differentiation in the epidermis. B) Differentiation by Myc is mediated by down-regulation of genes involved in cell adhesion and the cytoskeleton. C) Myc up-regulates genes involved in growth and proliferation promoting epidermal differentiation. Modified from [Watt et al., 2008a].

1.6 The Sin3A transcriptional co-repressor complex

Sin3A, one of the two mammalian homologues of the yeast repressor Sin3, is a core component of a large, multi-protein repressor complex [Grzenda et al., 2009]. Sin3 proteins have been conserved throughout metazoan evolution with homologues found in yeast, mice and humans, amongst others, indicating their functional importance [McDonel et al., 2009]. Sin3A was initially discovered along with its paralog Sin3B, via its direct interaction with transcriptional repressors of the Myc family network, Mad1 and Mxi1 and has been shown to supress epidermal proliferation [Ayer et al., 1995; Hassig et al., 1997; Laherty et al., 1997; Rao et al., 1996; Schreiber-Agus et al., 1995]. Sin3A complexes are known to harbour a number of core components and these transcriptional co-repressor complexes are recruited to DNA via an array of transcription factors, for example, p53 [Murphy et al., 1999] and pRB (Retinoblastoma 1) [Brehm et al., 1998], leading to repression of their target genes. In fact, it has been demonstrated that Sin3A is recruited by the amino-terminal repression domain of Mxi1 to mediate anti-Myc activity [Rao et al., 1996].

1.6.1 Sin3A structure, complex components and key interactions

The role of Sin3A, which itself has no intrinsic DNA binding capacity, is to act as a scaffold protein that mediates interactions between factors that lead to gene repression and sequence-specific transcription factors [McDonel et al., 2009] (Figure 1.8). The key domains of the Sin3A protein that are required for these interactions to occur are the four paired amphipathic helix (PAH) domains, which are highly conserved domains and the regions that share the highest homology between Sin3A and Sin3B. Another important region that is required for protein-protein interactions is the HDAC interaction domain (HID), which is a a highly conserved region located between PAH3 and PAH4 [Laherty et al., 1997]. Although Sin3A and Sin3B share extensive structural homology in terms of their
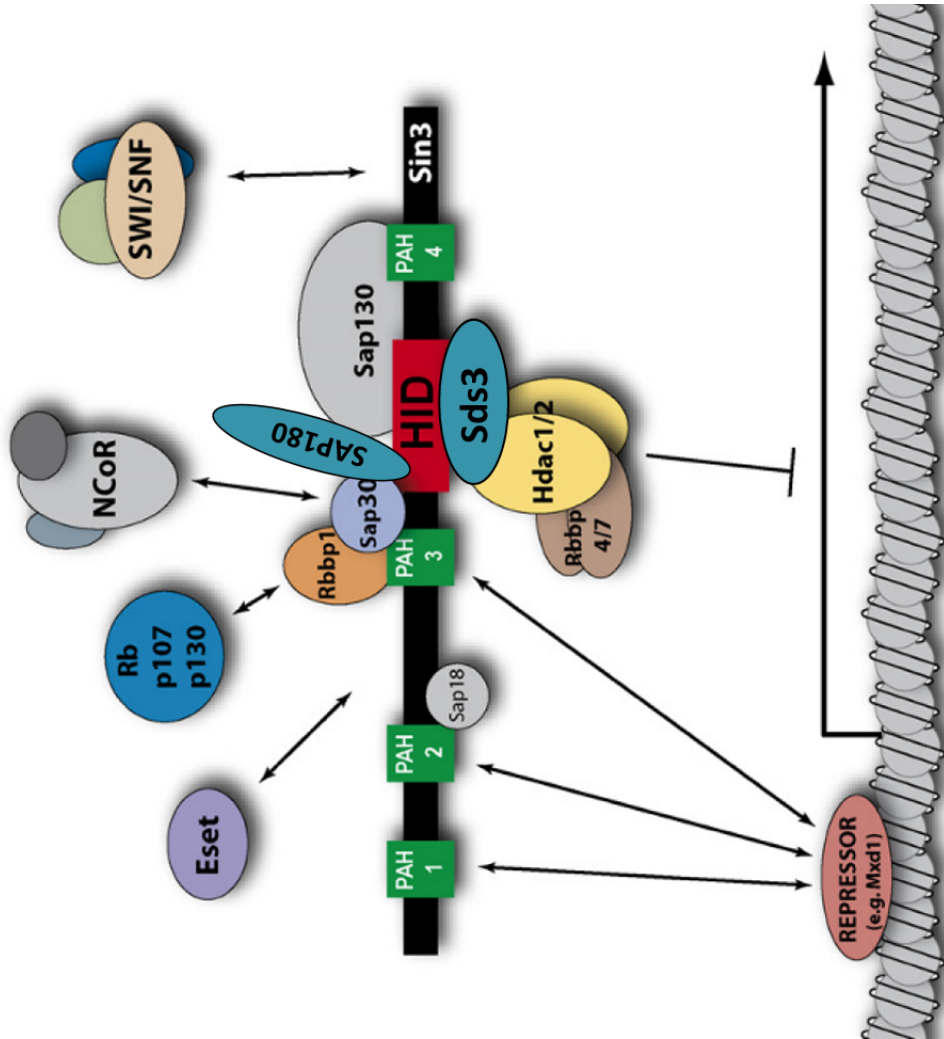
Figure 1.8: The Sin3A transcriptional co-repressor complex. Sin3A acts as a scaffold that mediates protein-protein interactions to bring together transcriptional repressors and transcription factors to mediate transcriptional repression. Adapted from [McDonel et al., 2009].

HID and PAH domains and have some overlap in terms of transcription factor binding partners and target genes [Le Guezennec et al., 2006], the two proteins are not completely functionally redundant. Evidence for this lack of complete functional redundancy comes from studies demonstrating that Sin3A and Sin3B are independently required for mouse embryonic development as embryonic lethality occurs at different stages in Sin3A or Sin3B null embryos [Cowley et al., 2005; Dannenberg et al., 2005; David et al., 2008].

It is known that the PAH domains of Sin3A, each consisting of about 100 residues [Pang et al., 2003], are of the utmost importance in allowing physical interactions of Sin3A with key transcriptional repressors, which form the co-repressor complex, and sequence-specific transcription factors, which bind to DNA. In particular, the PAH1 and PAH2 domains are known to interact with DNA-binding transcription factors [Le Guezennec et al., 2006]. For example, it is known that members of the Mad family repressors interact with Sin3A's PAH2 domain via a motif termed the Sin3-interaction domain (SID) [Ayer et al., 1995; Brubaker et al., 2000; Swanson et al., 2004].

In contrast to the PAH1 and PAH2 domains, which as described above interact with DNA-binding proteins, the function of the PAH3 domain appears to be to interact with core subunits of the Sin3A complex [Grzenda et al., 2009]. Sin3A-associated Protein 30 (SAP30), one of the first core components of the Sin3A co-repressor complex to be determined, is known to interact with Sin3A's PAH3 domain via its SID [Xie et al., 2011; Zhang et al., 1998]. As SAP30 contacts many other core components of the Sin3A complex, including HDAC1, it is thought that the function of this protein is to act to stabilise the complex [Xie et al., 2011]. It is also thought that SAP30 acts as a bridging protein between Sin3A and co-repressors such as RBP1, N-CoR, transcription factors such as YY1 [Lai et al., 2001; Viiri et al., 2009] and core complex components ING1/2 [Grzenda et al., 2009; Kuzmichev et al., 2002] . In mammals, a paralog of SAP30, SAP30-like (SAP30L), shares 70% sequence identity with SAP30 [Korkeamäki et al., 2008; Viiri et al., 2006]. SAP30L also interacts with the Sin3A complex via the PAH3 domain to mediate transcriptional repression [Korkeamäki et al., 2008; Viiri et al.,

2006]. Another SAP, SAP18 binds to PAH2 and mediates interactions with members of the Hedgehog signalling pathway [McDonel et al., 2009].

The key enzymatic activity by which Sin3A complexes mediate modifications of chromatin is via the recruitment of class I HDACs HDAC1 and HDAC2 [Alland et al., 1997; Ayer, 1999; Hassig et al., 1997]. The acetylation of histones is a dynamic process with histone acetyltransferases (HATs) mediating acetylation at lysine residues while HDACs act to reverse this process [Yang and Seto, 2007]. Histone acetylation is associated with active gene expression while HDAC activity is predominantly associated with transcriptional silencing [Grozinger et al., 2002]. In similarity to the NuRD co-repressor complex, the HDACs form a complex with the histone-interacting proteins, Retinoblastoma Binding Proteins 4 and 7 (Rbbp4/7) that is necessary for HDAC activity and is also thought to stabilise the interaction between the complex and nucleosomes [Fleischer et al., 2003; Grzenda et al., 2009; McDonel et al., 2009].

Acetylation of non-histone proteins has also emerged as a critical modification for a number of cellular processes and protein stability [Kouzarides, 2000]. For example, Myc is known to be stabilised by acetylation at specific lysine residues by HATs [Patel et al., 2004]. HDACs have been demonstrated to have a role in the reversal of the acetylation modification of non-histone proteins, for example p53 and E2F1 [Marks et al., 2003; Ozaki et al., 2009]. Interestingly, the Sin3A complex has recently been shown to be responsible for the deacetylation of the oncogenic transcription factor STAT3 leading to the repression of STAT3 activity [Icardi et al., 2012].

Another core component of the Sin3A complex, Sds3, is a key mediator of the relationship between Sin3A and HDACs. Sds3 appears to act as a 'bridge' between the interaction of Sin3A with HDACs via the HID [Alland et al., 2002]. It has also been shown that Sds3 has an essential role in the formation of pericentric heterochromatin and chromosome segregation [David et al., 2003]. Additionally, two further SAP proteins, SAP180 and SAP130 have been identified, which bind to Sin3A's HID and are thought to be involved in complex stability [Fleischer

et al., 2003].

The interactions that occur via the PAH4 domain and the C-terminus highly conserved region (HCR) are quite poorly characterised [Grzenda et al., 2009]. One interaction that occurs via the PAH4 domain that has been identified is the interaction with O-GlcNAc transferase and it is thought that this mediates O-GlcNAc modifications that aid transcriptional repression in conjuction with histone deacetylation [Yang et al., 2002]. It is interesting to note that the HCR of Sin3A, which shares over 80% identity with the corresponding region in Sin3B and is located within the HID has been identified as the domain by which Sin3A interacts with the co-repressor Alien [Moehren et al., 2004].

1.6.2 Functional roles of the Sin3A co-repressor complex

In the mouse, Sin3A has been linked to the regulation of key biological processes including peri-implantation development, T-cell differentiation, cellular proliferation, embryonic stem cell pluripotency and cell cycle progression. A number of studies providing these insights into Sin3A function have made use of transgenic mice harbouring Sin3A floxed alleles in which Sin3A is deleted after exon 3 upon recombination, which corresponds to a region prior to any known functional domains in the Sin3A protein [Dannenberg et al., 2005; McDonel et al., 2011; Pellegrino et al., 2012]. Sin3A was shown to have an essential function during early embryogenesis in two key papers published in 2005, which indicated that embryonic lethality occurs at E6.5 upon Sin3A deletion [Cowley et al., 2005; Dannenberg et al., 2005]. Sin3A has subsequently been shown to play a key role in maintaining genomic integrity in embryonic stem cells and is a key regulator in maintaining the cell cycle embryonic stem cells, which differs from the cell cycle in somatic cells as embryonic stem cells drive from mitosis through to S phase [McDonel et al., 2011].

Analysis of the loss of Sin3A in mouse embryonic fibroblasts revealed a phenotype of apoptosis and cell cycle arrest at G2/M phases. Perhaps the most interest-

ing aspect of the analysis of Sin3A deletion in this cell type was the revelation that known targets of Myc, such as Cyclin D2 and Nucleolin are up-regulated, implicating that Sin3A has a role in repressing Myc target genes [Dannenberg et al., 2005]. Additionally, Myc has been found in co-repressor complexes that include HDACs and Sin3A [Satou et al., 2001] and Sin3A has been found to have a role in the transcriptional repression of the Myc target gene Cad [Pal et al., 2003]. These studies all implicate Sin3A in the modification of Myc activity and regulation of Myc target genes. Interestingly, Sin3A has a role in T-cell differentiation and loss of a single allele of Sin3A has been shown to induce splenomegaly, indicating that Sin3A is not required for proliferation to occur in this cell type [Cowley et al., 2005]. Although the predominant activity of Sin3A complexes appears to be transcriptional repression via HDAC activity, Sin3A can mediate HDAC-independent transcriptional repression and has even been shown to have a role in promoting transcriptional activation via the promotion of Nanog expression in embryonic stem cells [Baltus et al., 2009]. This variability highlights the importance and complexity of Sin3A function and it is possible that Sin3A and the transcriptional networks it controls have tissue-specific roles.

The knowledge of the function of Sin3A in tissue-specific transcriptional networks in adult tissues to date is quite limited. However, Sin3A has been established as an important regulator in the testis and muscle. A study in which Sin3A was conditionally deleted in sertoli cells showed that loss of Sin3A in this cell type led to loss of differentiated spermatogonia followed by degeneration of germ cells leading to the conclusion by the authors that Sin3A is required in establishment of the niche for male germline stem cells by sertoli cells and thus has a key role in ensuring that this tissue is maintained normally [Payne et al., 2010]. Further investigations have demonstrated that Sin3A is essential for male fertility and confirmed that loss of Sin3A leads to loss of viable germ cells [Pellegrino et al., 2012]. Sin3A has been linked with the maintenance of differentiated muscle cells as Sin3A-mediated repression is utilised in differentiated muscle cells and myotube-specific deletion of Sin3A leads to massive disruption in muscle maintenance, with a loss of differentiated cells [van Oevelen et al., 2008; VanOevelen et al., 2010]. Additionally, Sin3A can regulate myogenic progenitors via an inter-

action with Foxk1, which interacts with Sin3A's PAH2 domain via its SID [Shi and Garry, 2012; Xiaozhong et al., 2012].

Taking into account these different lines of data, there is the indication that Sin3A potentially has an important role in Myc-mediated transcriptional repression. Due to the role of Myc in the epidermis and its impact on epidermal stem cell homeostasis, it is possible that Sin3A also has a role in governing epidermal stem cell behaviour. Therefore the main goal of my PhD was to uncover a role for Sin3A's transcriptional functions in skin.

1.7 Research aims

Given that the exploration of Myc's transcriptional roles at the EDC has revealed that binding of Myc to this region leads to displacement of specific sets of differentiation-specific transcriptional regulators from EDC genes, which includes Sin3A, whose function as a transcriptional co-repressor is well established, I speculated that Sin3A can function in the epidermis as an antagonist to Myc activity. As such the aim of my PhD project was to determine whether Sin3A does indeed have a function in the epidermis, in particular as an opposing factor to Myc function and to examine whether Sin3A is necessary for balanced homeostasis to be maintained. I set out to examine the role of Sin3A and the transcriptional networks it governs by using mouse models in which Sin3A was conditionally deleted. Analysis of the phenotypes of these mouse models and also the relationship of Sin3A with Myc and their shared targets produced important revelations as to the transcriptional functions of Sin3A in the epidermis.

Chapter 2

Material and Methods

2.1 Mouse lines

2.1.1 Ethical statement

During the course of this work all mouse breeding and experimental protocols used were subjected to ethical approval and performed under the terms of United Kingdom Government Home Office Project and Personal Licenses.

2.1.2 Generation of mouse lines

All mouse lines were bred to a mixed genetic background of CBA x C57BL/6J. Mice carrying floxed alleles for *Sin3A* (Sin3A$^{F/F}$) [Dannenberg et al., 2005; McDonel et al., 2011] and *Sin3B* (Sin3B$^{F/F}$) were kindly provided by Brian Hendrich, Cambridge. In these transgenic mice, Sin3A is deleted after exon 3 upon recombination leading to a truncated protein that does not contain any known conserved functional domains. Sin3A$^{F/F}$ mice were crossed with the (Krt14-Cre)1Amc/J line (The Jackson Laboratory, originally generated by [Dassule et al., 2000]) to generate the K14Sin3A line. Rosa26RLacZ-Cre mice [Soriano, 1999] (kindly provided by Jennifer Nichols, Cambridge), Sin3A$^{F/F}$ and Sin3B$^{F/F}$ lines were crossed with the Krt14-cre/Esr1 line (The Jackson Laboratory) to generate the R26K14ERLacZ reporter line, K14ERSin3A$^{F/F}$ and K14ERSin3B$^{F/F}$ lines respectively. The K14ERSin3A$^{F/F}$ line was crossed with mice carrying floxed alleles for

Myc (kindly provided by Alan Clarke, Cardiff) to generate the
K14ERSin3A$^{F/F}$Myc$^{F/F}$ mouse line. Sin3A$^{F/F}$ mice were crossed with the
K19CreERT line [Means et al., 2008] (kindly provided by Guoqiang Gu, Nashville)
to generate the K19ERSin3A$^{F/F}$ mouse line.

2.1.3 Genotyping

2.1.3.1 Dexoxyribonucelic acid (DNA) extraction

A buffer composed of 25mM NaOH and 0.2mM EDTA was used for DNA extrac-
tion. 25μl of this buffer was added to each ear snip and incubated for 15 minutes
at 95°C. Following this incubation period 25μl of 40mM Tris-HCl pH 5 was added
to neutralise the solution. The samples were then stored at -20°C until ready for
use in Polymerase Chain Reaction (PCR) analysis.

2.1.3.2 Genotyping primers

All genotyping primers were purchased from Sigma Aldrich.

Sin3A:- To distinguish between the Wild-type, floxed and null Sin3A alleles the
following primers:- 5'-TAC AAA GCC AGC CCT GAG AC-3', 5-'CAA GAT
GGC TTG AAC TTT TGG-3' and 5'- GCA TCC TTC CCA GCC TTC ATC-
3'. PCR amplification using these primers results in the amplification of 3 bands,
the first being the floxed allele (340 base pairs (bp)), the second being the Wild-
type (290bp) and finally the null allele (270bp).

K14CreER:- PCR amplification was also used to distinguish between K14CreER
positive and Wild-type using the following primers:- 5'-CTA GGC CAC AGA
ATT GAA AGA TCT-3' and 5-'GTA GGT GGA AAT TCT AGC ATC ATC
C-3', which amplifies a 324bp fragment from the Wild-type allele. An 440bp
fragment from the Cre/Esr1 construct is amplified by 2 primers:- 5'-AGG TGG
ACC TGA TCA TGG AG-3' and 5'-ATA CCG GAG ATC ATG CAA GC-3'.

K14Cre:- The presence of the K14Cre allele was determined using the follow-
ing primers:- 5'-TTC CTC AGG AGT GTC TTC GC-3' and 5'-GTC CAT GTC

CTT CCT GAA GC-3', which amplifies a 494bp product from the human growth hormone fragment of the transgenic. Two further primers:- 5'-CAA ATG TTG CTT GTC TGG TG-3' and 5'-GTC AGT CGA GTG CAC AGT TT-3' amplify a 200bp fragment from the Wild-type allele.

Myc Flox:- Primers used to detect floxed Myc alleles were as follows:- 5'-GCC CCT GAA TTG CTA GGA AGA CTG-3' and 5'-CCG ACC GGG TCC GAG TCC CTA TT-3', which give a 450bp fragment for the Wild-type allele or a 500bp fragment for the floxed allele when amplified using PCR.

Sin3B:- To identify the Sin3B floxed allele, the following primers were used:- 5'-TGG CTG GCA CTG CTA CCC TCT GG-3' and 5'-GCT CTT GGT CCT ACC CGC AGG C-3', which amplifies a Wild-type product of 283bp and floxed product of 350bp.

K19CreER:- The presence of K19CreER was determined using two primers:- 5'-GTT CTT GCG AAC CTC ATC ACT C-3' and 5'-GCA GAA TCG CCA GGA ATT GAC C-3', which give a 300bp product if the K19CreER allele is present.

2.1.3.3   PCR amplification

PCR was performed using the above primers for specific mouse lines using a C100 Thermal Cycler (Bio-Rad). Each reaction contained 0.1μM of each primer, 2μl of DNA (extracted as described above), 2X PCR Master Mix (Promega) and Milli-Q water (Millipore) to achieve a total reaction volume of 25μl. Cycling conditions for Sin3A, Sin3B and K14Cre were as follows:- 94°C for 5 minutes followed by 35 cycles of denaturing (94°C for 30 seconds), annealing (61°C for 30 seconds) and extension (72°C for 30 seconds). After the 35 cycles, there was another extension step (72°C for 2 minutes) and the reactions were then held at 4°C until the samples were processed using gel electrophoresis. The cycling conditions for MycFlox, K14CreER and K19CreER were the same except for the annealing temperature, which was 60°C for these reactions.

2.1.3.4 Gel electrophoresis

PCR products were resolved using a 2% (w/v) agarose gel (composed of 2% agarose powder (Sigma Aldrich) in Tris-acetate-EDTA (TAE) buffer) containing $0.5\mu g/ml$ Ethidium Bromide (Sigma Aldrich). To determine product size, all gels were ran with $10\mu l$ of 1Kb DNA ladder (Invitrogen) in the first well. Gels were ran in TAE buffer at 100 volts for 45 minutes using the Mupid-One electophoresis system. Products were then visualised and images taken using the G:Box system (Syngene).

2.1.4 Treatment with 4-hydroxy-tamoxifen (4-OHT)

Mice were treated with 1.5mg of 4-OHT (Sigma Aldrich) diluted in acetone. 4-OHT was topically applied to either a shaved area of the dorsal skin or to the tail skin as indicated. Unless otherwise stated, K14ERSin3A$^{F/F}$ mice were treated every second day for 14 days, K14ERSin3A$^{F/F}$Myc$^{F/F}$ mice were treated every second day for 21 days and K14ERSin3B$^{F/F}$ and K19ERSin3A$^{F/F}$ mice were treated every second day for 28 days. R26K14ERLacZ mice were treated every second day for the time period stated. Mice were sacrificed a day after the last 4-OHT treatment for collection of dorsal and/or tail skin. All mouse lines were compared to either 4-OHT treated Wild-type mice or vehicle (acetone) treated transgenic littermates. For all experiments, a minimum of 3 biological replicates were used per mouse line or condition unless otherwise stated.

2.1.5 Treatment with phorbol 12-myristate 13-acetate (TPA)

Mice were treated every second day with 4-OHT or vehicle (acetone) as described above for 9 days. On days 7, 8 and 9 of treatment, $3.1\mu g$ of TPA (Sigma Aldrich) or acetone was topically applied onto the dorsal skin or tail skin of all animals to induce proliferation. Mice were sacrificed one day after the last TPA treatment for collection of dorsal and/or tail skin.

2.1.6 Treatment with ultraviolet (UV) irradation

To subject mice to UVB irradation (310nm emission) a UV-Dosimeter system was used (Tyler Research Corporation). Dorsal and tail skin was exposed to $2500j/m^2$ of UVB radiation in one treatment. To calculate the exposure time in seconds, the exposure desired ($2500j/m^2$) was divided by the flux ($j/m^2/second$) which was detected using a photonic dosimeter, using the 310nm attachment, (Tyler Research Corporation). Once exposure time was calculated, mice were restrained in custom-made polycarbonate restraints (Department of Pathology, University of Cambridge) and exposed to UVB radiation for the calculated time. The irradiated area of dorsal skin was marked using a permanent marker while the mice were still in the restraint. For short term UVB experiments, mice were subjected to one treatment with UVB irradiation and sacrificed either 24 hours or 48 hours post-treatment for tissue collection. For long term UVB experiments, mice were treated 3 times a week over a 25 week period unless advised otherwise by a veterinarian. The mice were sacrificed 24 hours after their last treatment for tissue collection. For all experiments, a minimum of 3 biological replicates were used per mouse line or condition unless otherwise stated.

2.1.7 Bromodeoxyuridine (BrdU) tissue labelling

For BrdU labelling, mice were injected via the intraperitoneal route with 50 mg of BrdU (Sigma Aldrich) per kg body weight. The mice were then sacrificed 2 hours post-injection for tissue collection.

2.2 Isolation of primary keratinocytes from mouse skin

Primary mouse keratinocytes were isolated from shaved dorsal skin of transgenic and non-transgenic mice. The dorsal skin was removed and washed in 10% (v/v) betadine solution (20ml in 180ml sterile water), followed by one wash in 70% (v/v) ethanol and two washes in 1X Phosphate Buffer Saline (PBS) (PAA Laboratories). The dermal side of the skin was thoroughly scraped with a scalpel to remove excess fat. In order to separate the dermis from the epidermis, the tissue was trypsinized for 2 hours at 37°C floating epidermal side up in 0.25% (v/v) trypsin without EDTA (Invitrogen). The epidermis was subsequently scraped from the dermis, cut into small pieces and re-suspended in 30 ml of FAD(-Ca) medium [1 part Ham's F12 medium, 3 parts Dulbecco's modified Eagle's medium (DMEM), 1.8×10^{-4}M adenine] (custom made by PAA Laboratories) supplemented with 10% fetal calf serum (FCS) (Sigma Aldrich) and a cocktail of 0.5μg/ml hydrocortisone (Fisher Scientific), 5μg/ml insulin (Sigma Aldrich), 10^{-10}M cholera toxin (Enzo Life Sciences) and 10ng/ml epidermal growth factor, EGF (Peprotech), as previously described [Jensen et al., 2010]. The cell suspensions were filtered through a 70μm cell strainer (BD Biosciences) and centrifuged for 5 minutes at 1200 rpm (Eppendorf, Centrifuge 5702). Cell pellets were resuspended in 3ml of complete FAD(-Ca) media and kept on ice until further processing.

2.3 *In Situ* Hybridisation (ISH)

2.3.1 ISH solutions

1) Maleic Acid Buffer (MAB), pH 7.5

11.6g Maleic Acid (Sigma Aldrich)

8.7g NaCl

MilliQ Water to 1 Litre

2) 10% Blocking Buffer

10% (w/v) Blocking reagent (Roche) in MAB pH 7.5

3) 1.5% Blocking Buffer

15% (v/v) 10% Blocking Buffer

85% MAB

4) Dot Blot Reaction Buffer pH 9.5

5.84g NaCl

10.02g $MgCl_2$ $6H_2O$

0.83g Tris HCl

11.58g Tris Base

MilliQ Water to 1 litre

5) PBS-Tween (PBT)

0.1% Tween 20 in 1X PBS

6) ISH Fixative

5ml 37% (v/v) Formaldehyde

$200\mu l$ 0.5M EGTA (Sigma Aldrich)

45ml 1X PBS pH 7.4

7) ISH Post-Fixative
4% (v/v) Formaldehyde
0.1% Glutaraldehyde
95.9% PBT

8) 20X Saline-Sodium Citrate (SSC)
0.3M NaCl
0.3M Sodium Citrate

9) ISH Hybridisation Mix
50% Formamide
1.3X SSC
5.0mM EDTA pH 8
50μg/ml tRNA (Sigma Aldrich)
0.2% Tween 20
0.1% Sodium Dodecyl Sulphate (SDS)
100μg/ml Heparin (Sigma Aldrich)

10) 10X ISH Tris-buffered-Saline (TBS) pH 7.4
80g NaCl
2g KCl
30g Tris Base

11) ISH TBS-Tween (TBST)
0.1 % (v/v) Tween 20 in 1X PBS

12) ISH Blocking Solution
2% Blocking Buffer
20% Goat Serum (previously decomplemented for 30 minutes at 56 °C)
Diluted in TBST

13) NTMT

0.1M NaCl

0.1M Tris-HCl pH 9.5

1% Tween 20

0.05M MgCl$_2$

2.3.2 Generation of DNA templates

The 1Kb target region of mSin3A was amplified from Wild-type mouse cDNA using the following primers (Sigma Aldrich):-

mSin3A-ISH forward:- 5'-ATG AAG CGA CGT TTG GAT GAC-3'

mSin3A-ISH reverse:- 3'-CTT TGT AGA TGT CTG GTT GGC-3'

PCR was performed using the above primers using a C100 Thermal Cycler (Bio-Rad). Each reaction contained 0.1μM of each primer, 2μl of cDNA (generated as described below), 2X PCR Master Mix (Promega) and Milli-Q water (Millipore) to achieve a total reaction volume of 25μl. Cycling conditions were as follows:- 94°C for 3 minutes followed by 40 cycles of denaturing (94°C for 30 seconds), annealing (60°C for 120 seconds) and extension (72°C for 60 seconds). After the 40 cycles, there was another extension step (72°C for 10 minutes) and the reactions were then held at 4°C until the samples were processed using gel electrophoresis as described above. The PCR product was extracted using a Qiaquick Gel Extraction Kit (Qiagen). The purified PCR products were then ligated into the Strataclone PCR cloning vector (pSc-A-amp/kan) using the Strataclone PCR Cloning Kit (Agilent Technologies) according to manufacturer's guidelines. Colonies containing the Sin3A insert were picked and cultured overnight in LB Broth Media, prepared from LB Broth Powder according to manufacturer's guidelines (Sigma Aldrich). The plasmids were purified using the Qiaprep Spin Miniprep Kit (Qiagen) according to manufacture's instructions. In order to amplify the quantity of plasmid DNA, DH5α competent cells (Invitrogen) were transformed with the plasmids containing the Sin3A probe sequence according to manufacturer's guidelines and the plasmids were purified using a Plasmid Maxi Kit (Qiagen).

2.3.3 Ribonucleic (RNA) probe generation

5 μg of plasmid containing the mSin3A probe sequence was linearised using either EcoRV or SmaI restriction enzymes according to manufacturer's guidelines (New England Biolabs). Linearised plasmids were sequenced to ensure they contained the correct target sequence. To generate DIG-labelled RNA probes, 1μg of linearised template was transferred to an RNase-fee eppendorf tube and mixed with 4μl of 5x RNA polymerase Transcription buffer (Promega), 1μl of 0.75M DTT, 2μl of 10-X DIG-RNA labelling mix (Roche), 1μl of RNAsin (Promega) and 2μl (20 units) of T7 or T3 RNA polymerase (Promega) and nuclease-free water to give a final reaction volume of 20μl. Transcription of SmaI digested plasmids using T3 RNA polymerase generated the sense probe and T7 RNA polymerase generated the antisense probe. Transcription of EcoRV-digested plasmids with T3 RNA polymerase generated the sense probe while T7 RNA polymerase generated the antisense probe. The samples were incubated at 37°C for three hours and then put on ice. While on ice, 2μl of Dnase I (Promega) and 1μl of RNasin was added to each sample followed by a 1 hour incubation at 37 °C. The probe was then purified using an RNeasy kit (Qiagen) and left at -20°C overnight. Samples were then centrifuged for 30 minutes at 13,000 rpm and the pellet was washed with 70% (v/v) EtOH. After the wash step, the samples were centrifuged for an additional minute at 13,000 rpm and any remaining EtOH was removed using a pipette. The resulting pellet was resuspended in 100μl of 10mM EDTA and the probe was stored at -20°C.

2.3.4 Dot blot analysis

To check that the RNA probes were DIG-labelled a dot blot assay was performed for each probe. 0.5μl of each probe was dotted onto a nitrocellulose membrane (GE Healthcare) followed by cross-linking at 80°C for 15-20 minutes. Membrane equilibration was then performed by incubating the membrane in nuclease-free water for 5 minutes followed by a 5 minute incubation in MAB pH 7.5. The membrane was then blocked in 1.5% blocking buffer for 30 minutes and then incubated for 45 minutes in an alkaline phosphatase-coupled anti-DIG (DIG-AP) antibody (1:2000 dilution in 1.5% blocking buffer) (Roche). The membrane was

then subjected to 3 x 10 minute washes in MAB and then incubated with Dot Blot Reaction Buffer for 10 minutes. To develop, the membrane was then incubated with NBT-BCIP (Roche) (1:1500 dilution in Dot Blot Reaction buffer) for 3 hours and was then washed for 15 minutes in nuclease-free water to remove non-specific staining.

2.3.5 Tissue preparation

Whole mounts of mouse tail epidermis were prepared as described in section 2.9.5 except for the fixation step. For ISH, the whole mounts were fixed overnight at 4°C in ISH fixative. The whole mounts were then dehydrated by incubating for 5 minutes in 25% (v/v) MeOH in PBT, 5 minutes in 50% (v/v) in PBT, 5 minutes in 75% (v/v) in PBT and finally 5 x 10 minute incubations in 100% MeOH. The dehydrated tissues were then stored in 100% MeOH at -20°C until ready for ISH.

2.3.6 Tissue rehydration, protein digestion and post-fixation

Epidermal whole mounts prepared as described in section 2.3.5 were rehydrated by incubation for 5 minutes in 75% (v/v) MeOH in PBT, 5 minutes in 50% (v/v) MeOH in PBT, 5 minutes in 25% MeOH in PBT and 2 x 5 minute washes PBT. Following rehydration, the samples were incubated in PBT containing 10μg/ml proteinase K for 50 minutes. Post-fixation was then performed by incubating the samples in ISH Post-Fixative for 20 minutes. The samples were then washed twice with PBT and once with a 1:1 (v/v) mixture of PBT and ISH Hybridisation mix. The whole mounts were then transferred to ISH Hybridisation Mix. Once the whole mounts sank, the ISH hybridisation was replaced with fresh ISH hybridisation mix and the samples were stored at -20°C overnight.

2.3.7 Hybridisation

The epidermal whole mounts were then incubated at 58°C for a minimum of 3 hours after which, the ISH hybridisation mix was replaced with 1ml of fresh hybridisation mix containing 50μl of DIG-labelled RNA probe. The samples were incubtated with the probe overnight at 58°C. The next day, the whole mounts

were briefly washed twice with ISH hybridisation mix prewarmed to 58°C followed by 2 x 30 minute washes at 58°C with ISH hybridisation mix pre-warmed to 58°C. Whole mounts were then washed in a 1:1 (v/v) solution of ISH Hybridisation Mix and ISH TBST (pre-warmed to 58 °C) for 15 minutes at 58°C.

2.3.8   Immuno-revelation

Samples were then briefly washed twice at room temperature in TBST followed by a 15 minute wash in TBST with gentle agitation at room temperature. The tissues were then blocked for 2 hours at room temperature using ISH Blocking Solution followed by overnight incubation in DIG-AP antibody (1:2000 dilution in ISH Blocking Solution). The antibody-labelled whole mounts were then briefly washed 3 times with TBST and then washed 3 x 1 hour in TBST with gentle agitation at room temperature. The next step was to wash the samples 2 x 10 minutes in freshly made NTMT on a roller followed by incubation in NBT-BCIP solution (0.5mg/ml diluted in NTMT) at 37 °C until staining developed. Once the staining had sufficiently developed, the samples were rinsed 3 times in PBT and then post-fixed in ISH post-fixation buffer for 20 minutes with gentle agitation. Whole mounts were then mounted using Mowiol prepared as described in Section 2.9.6.

2.4 Flow cytometry

2.4.1 Cell cycle analysis

For cell cycle analysis, mouse epidermal keratinocytes isolated following the protocol described above. Ice cold 70% (v/v) ethanol was added dropwise to the resulting cell pellet while vortexing. The cells were incubated at 4°C for at least 30 minutes to allow fixation to occur. The cells were then washed twice with 1X PBS and the resulting cell pellet was resuspended with 200μl of 50μg/ml propidium iodide (PI) (Sigma Aldrich). 50μl of 100μg/ml RNase stock solution (Sigma Aldrich) was added and the cells were incubated at room temperature for 30 minutes. Following this incubation period, analysis was carried out on a CyAN ADP analyzer (Beckman Coulter) with the help of Rachael Walker[1]. The cell cycle profile was then analysed using FlowJo software (http://www.flowjo.com).

2.4.2 Sorting cells based on Integrin α6 expression

Mouse epidermal keratinocytes were isolated following the protocol described in Section 2.2. Cell pellets were resuspended in PE-conjugated integrin α6 antibody (1:500,Clone GoH3, eBiosciences) diluted in 0.2% (v/v) Bovine Calf Serum (BCS) (Invitrogen) in 1X PBS. The cells were incubated for 45 minutes at 4°C and then washed twice in PBS (PAA Laboratories). The cells were resuspended in 0.2% (v/v) BCS (Invitrogen) in PBS containing 1μg/ml DAPI (4',6-diamidino-2-phenylindole, dihydrochloride) nucleic acid staining reagent (Sigma Aldrich). Cell sorting was performed using a MoFlo high-speed sorter (Beckman Coulter). DAPI was excited using a UV laser and PE was excited by a 488nm laser. Cells were then gated using forward versus side scatter to eliminate debris. Cell doublet discrimination was carried out using pulse width. The non-viable cells, stained with DAPI, were then gated for their exclusion using a 450/50 nm filter. After gating out dead cells, the cells were then sorted based on Integrin α6 PE levels (fluorescence detected using a 580/30 nm filter) into Integrin α6 ^{High}, Integrin α6 ^{Mid} and Integrin α6 ^{Low} populations. The cells were sorted into 0.2% (v/v) BCS

---

[1]Flow Cytometry Facility, Wellcome Trust Centre for Stem Cell Research - University of Cambridge

in PBS. This work was performed in collaboration with Rachael Walker.

2.4.3   RNA isolation from sorted cells

Following sorting, the cells were transferred to RNase-free Eppendorf tubes and centrifuged for 5 minutes at 2000 x g at 4°C. After discarding the supernatant, being careful not to lose the pellet, RNA was isolated using the Purelink-RNA micro kit (Invitrogen) following manufacturer's guidelines. Conversion of the RNA to cDNA and quantitative PCR was carried out as described in Section 2.8.

2.5   Cell culture

All mammalian cell culture was performed using aseptic technique under a laminar flow hood. Cells were maintained at 37°C in a humidified incubator with a 5% CO_2 atmosphere. Cells were grown on plastic dishes or flasks of tissue culture grade (Falcon). Medium renewal was performed every two to three days and, when necessary cells were frozen in 1ml aliquots containing 10^6 cells per mililiter in freezing medium (FCS and 10% (v/v) DMSO). Cell were first subjected to freezing in a *Mr. Frosty* freezing container (Nalgene) and kept one day at -80°C following transfer to a liquid nitrogen container used as a cell bank.

2.5.1   Cell lines

COS-7 cells were obtained from ATCC and maintained in DMEM (Invitrogen) supplemented with 10% FCS (Sigma-Aldrich), 100U/ml penicillium (PAA laboratories), 100μg /ml streptomycin (PAA laboratories) and were split 1:5 once a week according to ATCC guidelines.

3T3 J2 cells were generated from the J2 clone of random-bred Swiss mouse 3T3 cells which was selected to provide optimal feeder support of keratinocytes [Rheinwald and Green, 1975]. These cells were maintained in DMEM (Invitrogen) supplemented with 10% (v/v) BCS (Invitrogen), 100U/ml penicillin (PAA Laboratories), 100 μg/ml streptomycin (PAA Laboratories). Cells were passaged when they reached near-confluency and re-seeded at a density of approximately 3,000/cm^2. Cells were maintained for up to 12 passages after thawing, after which a new stock of low passage number feeder cells was thawed to replace the old stock. Feeder cells were mitotically inactivated by incubation with 4μg/ml mitomycin C (Sigma Aldrich) for 2 hours at 37°C to inhibit mitosis. The feeder cells were then washed twice with PBS to remove the mitomycin C and incubated in fresh FAD medium before used as feeders for keratinocytes. Cells were split 1:5 once a week.

Primary mouse keratinocytes

Mouse keratinocytes were isolated as described above and were maintained on J2-3T3 mouse feeder cells. These cells were maintained in complete FAD(-Ca) medium (FAD-Ca + FCS + HICE) which included one part Ham's F12 medium and three parts Dulbecco's modified Eagle's medium (DMEM), supplemented with 1.8 x 10^{-4}M adenine (FAD); 10% (v/v) FCS (Sigma-Aldrich); 0.5μg/ml hydrocortisone (Fisher Scientific), 5μg/ml insulin (Sigma Aldrich), 10^{-10}M cholera toxin (Sigma Aldrich), 10ng/ml EGF (Peprotech) (HICE). FAD(-Ca) media without phenol red was used to avoid erroneous activation of the ER domain. Before passaging the keratinocytes, the J2-3T3 feeder cells were removed by incubation in versene (Gibco) for 5 minutes. Keratinocytes were dissociated by incubation in a 1:4 dilution of 0.25% v/v trypsin solution with no EDTA (Invitrogen) in PBS (PAA Laboratories) for 5 minutes. Complete FAD medium was added and the cells were recovered by centrifugation at 1000 x g for 5 minutes. Keratinocytes were resuspended in complete FAD(-Ca) medium and replated at a density of 4,000/cm^2 on inactivated J2-3T3 feeder cells. After a number of weeks the keratinocytes underwent spontaneous immortalisation and no longer needed to be maintained on J2-3T3 mouse feeder cells.

2.6 Transient transfection of Cos-7 cells for acetylation analysis

For Myc co-immunoprecipitation and acetylation assays the following constructs were cloned into eukaryotic expression vectors: estrogen receptor domain fused to a Flag-tag (ER-Flag), human Myc fused to ER and Flag-tag (MycER-Flag) (kindly provided by S. Aznar Benitah), and full length cDNA for *SIN3A* (kindly provided by P. McDonel [McDonel et al., 2011]). The cytomegalovirus-driven expression vector containing *TIP60* was a kind gift from S. Khochbin [Legube et al., 2002], *GCN5* was kindly provided by S. Dent. Constructs were transfected using Cos-7 cells which were grown in 150mm^2 dishes and transfected at 50%

confluence with the empty vector, or *MYC*, *TIP60*, *GCN5* and *SIN3A* constructs with Lipofectamine LTX and Plus Reagent (Invitrogen) and harvested after 24 hours.

2.7 Treatment of primary mouse keratinocytes with tamoxifen

In order to activate Cre-recombinase activity in Sin3A$^{F/F}$ keratinocytes, cells at 70% confluency were treated with 200nM tamoxifen (Sigma-Aldrich) and then 24hrs after the intial treatment. To provide a control, Sin3A$^{F/F}$ keratinocytes were treated with the equivalent volume of EtOH. Keratinocytes were harvested 48 hours after intitial treatment with tamoxifen or EtOH.

2.8 mRNA expression analysis

2.8.1 Extraction of total RNA from dorsal tissue

Samples from dorsal skin of transgenic and non-transgenic mice treated with 4-OHT or acetone as described in Section 2.1.4 were taken and flash-frozen in liquid nitrogen. Samples were stored in a liquid nitrogen dewar until further processing. Frozen tissues were added to nalgene centrifuge 50ml tubes, previously rinsed with *RNAaseZap* solution (Ambion) and containing 3ml of Trizol reagent (Invitrogen). Tissues were macerated using a homogeneizer (this step, and all involving Trizol usage were performed under a chemical hood) and the resulting suspensions were incubated for 5 minutes at room temperature. Following this incubation period, 0.6ml of chloroform was added to each sample, the samples were then vortexed for 15 seconds and subsequently incubated for 15 minutes at room temperature. The samples were then subjected to centrifugation at 12000 x *g* for 30 minutes at 4°C. The aqueous supernatant was removed and RNA was kept for 30 minutes on ice while precipitating in 1.5 ml of isopropanol. RNA pellets were collected by centrifugation at 12000 x *g* for 30 minutes at 4°C. The RNA pellets were then washed with 500μl of 70% (v/v) ethanol by centrifugation at 12000 x *g* for 5

minutes at 4°C . RNA samples were air-dried and diluted in 50μl of Milli-Q water and the concentration content was assessed using a Nanodrop spectrophotometer (ND-1000, Nanodrop Technologies).

2.8.2 Reverse transcriptase PCR and quantitative real time PCR (qPCR)

Total RNA samples were extracted as described in section 2.8.1. Double stranded cDNA was generated from 1μg of RNA using 250ng random primers (Promega) and Superscript III reverse transcriptase (Invitrogen) enzyme following manufacturer's instructions. QPCR and analysis was conducted using the 7900HT Real-Time PCR System (Applied Biosystems). The standard amplification protocol was used with pre-designed probe sets and TaqMan Fast Universal PCR Master Mix (2) (Applied Biosystems) according to manufacturer's instructions. A list of the pre-designed probes used is shown in Table 2.1. A *Gapdh* probe (4352932E) was used to normalize samples using the ΔCt method. The significance of quantitative data was tested using the unpaired, two-tailed Student's T test. The standard deviation of the mean of quantitative data was also calculated and is graphically represented by error bars.

Gene	Taqman Probe ID
Filaggrin	Mm0176522_m1
Integrin $\alpha 6$	Mm01333831_m1
Involucrin	Mm00515219_s1
Loricrin	Mm01219285_m1
Myc	Mm00487803_m1
Sin3a	Mm00488255_m1
Transglutaminase1	Mm00505602_m1

Table 2.1: List of probes used for qPCR.

2.8.3 Microarrays

Microarray experiments and analysis were performed in collaboration with Elisabete Nascimento[1]. Experimental procedures and analysis were performed as described in [Nascimento et al., 2011].

---

[1]Frye Lab, Wellcome Trust Centre for Stem Cell Research - University of Cambridge

2.9 Histology and immunostaining

2.9.1 Histology

Skin tissue samples from back and tail-skin was fixed overnight with 4% (w/v) formaldehyde and then transferred to 70% (v/v) ethanol. Samples were paraffin embedded and 5 to $10\mu m$ sections cut at the CSCR Histology facility with the help of Margaret McLeish[1]. Sections were stained using standard haemotoxylin and eosin (H&E) staining.

2.9.2 Immunohistochemistry

Paraffin sections prepared as described above were de-waxed and re-hydrated using standard protocols. Antigen retrieval was performed by covering the slides with Vector antigen unmasking solution pH 6.0 (Vector Laboratories) and heating for 14 minutes in a microwave at full power. The slides were cooled for 5 minutes and then washed for 10 minutes with running tap water. Endogenous peroxidase was blocked by incubating the slides in a hydrogen peroxide-methanol solution for 10 minutes. Slides were then washed in 0.2% (v/v) Tween 20 in PBS (PBST) twice with each wash lasting 3 minutes and then incubated in 2.5% horse serum (ImmPressKit, Vector) for 20 minutes. Slides were then incubated in primary antibody (Ki67; 1:100; SP6; Vector Laboratories) diluted in PBS for 60 minutes and then rinsed twice in PBST for 3 minutes. The sections were then incubated in rabbit Immpress-labelled polymer Horseradish Peroxidase (HRP) (Vector Laboratories) for 30 minutes and then 3 x 3 minute washes with PBST were performed. Following a 5 minute incubation in chromagen (Vector DAB), the slides were washed in running tap water for 1 minute, counterstained in Haematoxylin for 30 seconds and then washed in running tap water for 2 minutes. The next step was to differentiate in 1% (v/v) acid alcohol for 5-10 seconds and wash in water for 5 minutes. Slides were then immersed in 95% Industrial Methylated Spirit (IMS) for 1 minute, 99% IMS for 2 x 3 minutes and immersed in xylene for 2 x 3 minutes and then mounted using Mowiol.

---

[1]Histology Facility, Wellcome Trust Centre for Stem Cell Research - University of Cambridge

2.9.3   Immunohistochemistry using Ventana Discovery

Automated immunohistochemistry was performed using the Ventana Discovery (Ventana Medical Systems, Inc) on paraffin embedded tissues, following manufacturer's guidelines. Antigen retrieval was performed using Ventana Cell Conditioning 1 solution (Roche) for 40 minutes at 99°C. Primary antibody incubation was performed for 54 minutes at 37°C. Secondary antibody incubation (Donkey anti-rabbit or anti-goat Ig biotinylated, Jackson) was performed for 30 minutes at 37°C. Antibody detection was performed using the DAB Map detection kit (Ventana) and sections were counterstained using hematoxylin and bluing reagent (Roche).The primary antibodies used were Sin3A (1:100; sc-767, Santa Cruz), c-Myc (1:100; sc-769, Santa Cruz), Ki67 (1:100; SP6, Vector Laboratories), Cyclin B1 (1:100; LS-C95967, Lifespan Biosciences), p53 (1:100; CM5, Vector Laboratories) and Uhrf1 (1:100; ab100810, Abcam).

2.9.4   Immuno-labelling of cryosections

Dorsal or tail skin samples were embedded in Optimal Cutting Temperature (OCT) solution (Raymond A Lamb) and stored at -80°C. 5-10μm cryosections of mouse skin, cut with the help of Margaret McLeish, were fixed in 4% (w/v) paraformaldehyde for 10 minutes at room temperature and then permeabilised for 5 minutes with a 0.2% (v/v) solution of Triton X-100 at room temperature. The sections were then blocked for 1 hour with blocking buffer containing 10% (v/v) FCS, 0.05% (w/v) Na-azide in 1X PBS and incubated overnight at 4°C with the primary antibody (diluted in blocking buffer). After washing 3 times for 10 minutes with 1X PBS to remove excess antibody, the sections were incubated for 60 minutes with the secondary antibody. Following the incubation period, sections were washed 3 times for 10 minutes with PBS and then incubated with DAPI DNA staining reagent (Sigma Aldrich) (1:1000 dilution) for 5 minutes. Following 3 x 5 minute washes with 1X PBS, the sections were mounted using Mowiol mounting media (Calbiochem) and stored at 4°C.

The primary antibodies used were Sin3A (1:100; sc-767, Santa Cruz), Keratin14 (1:2000; PRB-155P Covance), Keratin10 (1:250; PRB-159P, Covance), Integrin

α6 (1:250; GoH3 clone, Serotec), Involucrin (1:250; ERLI-3; a kind gift from Li [Li et al., 2000]), Filaggrin (1:250; PRB-417-P, Covance), Cleaved Caspase 3 Asp175 (1:100; 9661, Cell Signaling Technology) and Mcm2 (1:100; LS B391, Lifespan Biosciences). Secondary antibodies used were Rabbit IgG whole molecule Alexa 594 and 488 or Rat IgG whole molecule Alexa 594 and 488 (1:1000, Molecular Probes).

2.9.5 Preparation and immuno-labelling of epidermal whole mounts

Whole mounts of mouse tail epidermis were prepared and labelled as previously described [Braun et al., 2003]. In brief, tail skin was slit lengthways using a scalpel, peeled from the tail bone and incubated in 0.005M EDTA in 1X PBS at 37°C for 4 hours. The epidermis was then peeled from the dermis using forceps and the dermis discarded. The epidermis then fixed in 4% (w/v) paraformaldehyde for 2 hours and subsequently washed 3 times with 1X PBS. The fixed epidermal sheets were stored at 4°C in 0.2% (w/v) Sodium Azide in PBS until further processing.

For labelling, the fixed epidermal sheets were blocked and permeabilised by incubation in PB buffer (0.5% skim milk powder, 0.25% fish skin gelatin (Sigma Aldrich), 0.5% (v/v) Triton X-100 in TBS (0.9% (w/v) NaCl, 20mM HEPES, pH 7.2) for 30 minutes. The tissue was then incubated with primary antibody (diluted in PB buffer) overnight at room temperature with gentle agitation. The epidermal whole mounts were then washed with PBST over a period of at least four hours changing the buffer several times to remove excess antibody and unspecific binding. The whole mounts were then incubated with secondary antibodies using the same conditions and washed in the same way. The epidermal sheets were then incubated with DAPI for 5 minutes followed by 3 x 5 minute washes with PBS. The epidermal sheets were mounted using Mowiol mounting media (Calbiochem) and stored at 4°C. When detecting BrdU-positive cells, the epidermal sheets were incubated in 2N HCl at 37°C for 20 minutes prior to incubation with the primary (anti-BrdU) antibody.

The primary antibodies used were Sin3A (1:100; sc-767, Santa Cruz), Ki67 (1:100; SP6, Vector Labs), Keratin14 (1:250; PRB-155P Covance), BrdU (1:100; Abcam), Cleaved Caspase 3 Asp175 (1:100; 9661, Cell Signaling Technology) and Integrin α6 (1:250; GoH3 clone, Serotec). The secondary antibodies used were the same as described in Section 2.9.4.

2.9.6   Preparation of Mowiol mounting media

Mowiol was prepared by using 24g analytical grade glycerol (Sigma Aldrich), 9.6g Mowiol 4-88 (Sigma-Aldrich), 24ml distilled water and 48ml 0.2M Tris buffer, pH 8.5 were combined and homogeneized with a stir bar on a hot plate on 60°C for at least 4-5 hours until dilution of the Mowiol powder in the solution. The solution was centrifuged at 5000 x g for 15 minutes and the supernatant was stored in aliquots at -20°C for a maximum of 12 months. Mowiol was used at 21-25°C.

2.10 β-Galactosidase analysis

To determine the pattern of recombination in the R26K14ERLacZ reporter line, a 5-bromo-4-chloro-indolyl- β-D-galactoside (X-Gal) protocol to detect β-galactosidase activity was used. β-galactosidase analysis was performed in 20μm cryosections from OCT-embedded skin. Testes and salivary glands obtained from the R26K14ERLacZ reporter line were embedded in OCT and 20μm cryosections cut for this analysis.

2.10.1   Reagents

1) 0.1M phosphate buffer (pH 7.3)

2) Fix buffer:- 0.1M phosphate buffer (pH 7.3) supplemented with 5mM EGTA (Sigma Aldrich), pH 7.3, 2mM $MgCl_2$ and 0.2% (v/v) glutareldahyde (Sigma Aldrich). Stored at 4°C for up to 4 months.

3) Wash buffer:- 0.1M phosphate buffer (pH 7.3) supplemented with 2mM $MgCl_2$. Stored at 4° indefinitely.

4) X-gal staining buffer:- 0.1M phosphate buffer (pH 7.3) supplemented with 2mM $MgCl_2$, 5mM potassium ferrocyanide ($K_4Fe(CN)_6$-$3H_2$0 SigmaAldrich) and 5mM potassium ferricyanide ($K_3Fe(CN)_6$ Sigma Aldrich). Stored at 4°C covered in foil as it is light sensitive. Before use, X-gal was added to a final concentration of 1mg/ml and filter sterilized to minimize the formation of crystals in the staining reaction.

5) X-gal stock solution (50mg/ml):- 500mg of X-Gal (Sigma Aldrich) was resuspended using 10ml dimethylformamide (BDH) to generate the stock solution and was stored at 20°C.

2.10.2 Experimental procedure

Sections from skin, testes or salivary glands were thawed in 1X PBS for 30 minutes at room temperature. Slides were then incubated in Fix buffer for 15 minutes followed by 2 x 5 minute washes in Wash buffer. X-Gal staining buffer containing 1mg/ml X-Gal was added to the slides, ensuring that the sections were fully covered, in a humidified chamber. After covering the slides, the sections were incubated overnight at 37°C followed by 2 x 5 minute washes in Wash buffer. Subsequently the sections were incubated in Fix buffer for 15 minutes at room temperature and then mounted using Mowiol.

2.11 Biochemistry

2.11.1 Protein extraction from mouse skin tissue

Samples of frozen tissue were added to 1.5ml of RIPA lysis buffer: 0.05% (w/v) SDS (Sigma-Aldrich), 0.1% (w/v) Na-deoxycholate (Sigma-Aldrich), 0.5% NP-40 (v/v) (Sigma-Aldrich) in PBS containing tablets of complete Mini EDTA-free Protease Inhibitor Cocktail (Roche) and mixed using a homogeneizer. The cell lysate was transfered to 1.5ml microcentrifuge tubes and incubated on ice for 30 minutes. Samples were centrifuged at 4600rpm (Eppendorf 5424R) for 10 minutes at 4°C.The supernatant was kept, but when still cloudy, due to skin fat, it was centrifuged several times until it became completely clear. Protein sample from the cell lysates was diluted in SDS sample buffer [40% (v/v) of glycerol, 0.8% (v/v) of SDS and 40mM of DTT] after protein concentration was quantified using the Pierce bicinchoninic (BCA) Protein Assay Kit, according to the manufacturer's instructions. Protein concentration was measured using a Spectrophotometer and the Softmax program for protein quantification. Samples were aliquoted and kept at -80°C with no more than two cycles of freezing and thawing.

2.11.2 Protein extraction from cell lines

Transfected cells lines or cells treated with cycloheximide (50μg/μl) (Sigma-Aldrich) were lysed in RIPA buffer, (see section 2.11.1) and the protein content was quantified using Pierce bicinchoninic (BCA) Protein Assay Kit, according to the manufacturer's instructions. Samples were aliquoted and kept at -80°C with no more than two cycles of freezing and thawing.

2.11.3 Western-blotting

Cell protein lysates were homogeneized in SDS sample buffer [40% (v/v) of glycerol, 0.8% (v/v) of SDS and 40mM of DTT], containing bromophenol blue and heated between 60-90 °C for 5 minutes before loading onto a stacker gel on top of a 10% polyacrylamide (PAA) gel. The components of stacker gels and 10% PAA

gels are as follows:-

10% PAA gel
40% PAA (Bio-Rad) 7.5ml
1.5M Tris pH 8.8 7.5ml
10% (w/v) SDS 0.3ml
10% (w/v) Ammonium Persulphate (APS) 300μl
Tetramethylethylenediamine (TEMED) 30μl
Autoclaved water 14.7ml

Stacker gel
40% PAA (Bio-Rad) 1.125ml
0.5M Tris pH 6.8 2.5ml
10% (w/v) SDS 0.1ml
10% (w/v) APS 100μl
TEMED 10μl
Autoclaved water 6.28ml

To determine band size, a protein ladder (Spectra Multicolor High Range Protein Ladder, Thermo Fisher Scientific) was loaded into the first well of each gel. Gels were run in SDS Running buffer [14g Glycine, 3g Tris base, 1g SDS diluted to 100ml in ultrapure water] at 200V for 40 minutes, after which the proteins were transferred onto a nitrocellulose membrane (GE Healthcare) in Transfer buffer [14g glycine, 3g of Tris-base diluted in 100ml of ultrapure water containing 10% (v/v) methanol] for 2 hours at 4°C. Membranes were blocked in 5% (w/v) non-fat milk in TBST (0.05% (v/v) Tween-20 in TBS) for 1 hour at 21-25°C and incubated with primary antibody in blocking solution overnight at 4°C. Primary antibodies used detected either Myc (1:500 sc-764, N-262, Santa Cruz), Sin3A (1:500 sc-994, K-20, Santa Cruz), mouse monoclonal anti-acetyl-lysine (1:1000 Cell Signalling Technology) or rabbit polyclonal tubulin (1:2000 T3526, Sigma Aldrich). The membranes were then washed 5 times in TBST and then incubated with HRP-labeled secondary antibodies (1:5000 GE Healthcare) in blocking solution for 1 hour at room temperature on a rocker. The membranes were then washed

three times with TBST and the HRP was detected using the Amersham ECL detection system (GE Healthcare). Luminescence was detected by exposing the membrane to photographic film (Kodak) and the film was then processed using an X-Ray film processer (Photon).

2.11.4 Co-immunoprecipitation assays

Cells, treated with tamoxifen or EtOH as described in Section 2.7, were lysed, on ice, in lysis buffer consisting of 1X PBS without Ca^{2+} and Mg^{2+} (PAA Laboratories), 0.5% (v/v) NP-40, 0.1% (w/v) sodium deoxycholate, 0.05% (w/v) SDS, and protease inhibitor tablets following the lysis step, lysates were centrifuged at 13,000rpm (Eppendorf 5424R) for 10 minutes at 4 °C and the supernatant was then added to Protein G Dynabeads (Invitrogen) which had been pre-incubated with 50 μg of rabbit polyclonal anti-Myc antibody (N-262,; Santa Cruz) for 2 hours at 4°C. Following 2 hours incubation at 4°C, the beads were washed five times with lysis buffer and the immunoprecipitated protein was then eluted with SDS sample buffer (Section 2.11.3) at 80°C. The protein supernatant was collected and ran in a polyacrylamide gel as described in Section 2.11.3.

2.11.5 Chromatin Immunoprecipitation (ChIP)

ChIP experiments and analysis were performed in collaboration with Elisabete Nascimento[1]. Experimental procedures and analysis were performed as described in [Nascimento et al., 2011].

---

[1]Frye Lab, Wellcome Trust Centre for Stem Cell Research - University of Cambridge

2.12 Image acquisition

White field images were acquired using an Olympus IX80 microscope and a DP50 camera. Confocal images were acquired on a Leica TCS SP5 confocal microscope. Z-stacks were acquired at 100 Hz with an optimal stack distance and 1024 x 1024 dpi resolutions. Z-stack projections were generated using the LAS AF software package (Leica Microsystems). All the images were processed with Adobe Photoshop CS4 software.

2.13 Quantification

The number of Ki67 or p53 positive cells were counted in randomly selected fields of the same sized area from images of skin sections acquired as described above. 5 biological replicates of transgenic mice and appropriate controls were used unless otherwise stated. The average number of Ki67/p53 positive cells in interfollicular epidermis, sebaceous glands and hair follicles in transgenic mice and appropriate controls was then calculated. The significance of quantitative data was tested using the unpaired, two-tailed Student's T test. The standard deviation of the mean of quantitative data was also calculated and is graphically represented by error bars.

2.14 List of suppliers and distributors

Abcam, Cambridge, UK.

Ambion, Applied Biosystems, Foster City, CA, USA.

Applied Biosystems, Foster City, CA, USA.

BD Biosciences, Franklin Lakes, NJ, USA.

BDH, Hull, UK.

Beckman Coulter Instruments, Palo Alto, CA, USA.

Bio-Rad, Hercules, CA, USA.

Calbiochem, Darmstadt, Germany.

Cell Signaling Technology Inc, Danvers, MA, USA.

Covance Research Products, Cambridge Bioscience, Cambridge, UK.

Eppendorf, Histon, Cambridge, UK.

Enzo Life Sciences, Exeter, UK.

Falcon, part of Nunc A/S, Roskilde, Denmark.

Fisher Scientific, Loughborough, Leicestershire, UK.

GE Healthcare, Buckinghamshire, UK.

Invitrogen, Paisley, UK.

Jackson ImmunoResearch Laboratories, Inc, Newmarket, UK.

Leica Microsystems, Milton Keynes, UK.

Lifespan Biosciences, Stratech, Newmarket, UK.

Kodak, Hemel Hempstead, UK.

Millipore, Harrow, Middlesex, UK.

Molecular Probes, Leiden, Netherlands.

Nalgene, Thermo Fisher Scientific, Waltham, MA, USA.

Nanodrop Technologies, Thermo Fisher Scientific, Waltham, MA, USA.

New England BioLabs, Ispwich, UK.

PAA Laboratories GmbH, Pasching, Austria.

Peprotech EC Ltd, London, UK.

Photon, Swindon, UK.

Pierce, Thermo Fisher Scientific, Waltham, MA, USA.

Promega UK Ltd, Southampton, UK.

Qiagen Ltd, Crawley, UK.

Roche, Lewes, East Sussex, UK.

Santa Cruz Biotechnology, Heidelberg, Germany.

Serotec, Oxford, UK.

Sigma-Aldrich, St. Louis, MO, USA.

Stratagene, Agilent Technologies, Santa Clara, CA, USA.

Syngene UK, Cambridge, UK.

Thermo Fisher Scientific, Waltham, MA, USA.

Tyler Reseach Corporation, Edmonton, Canada.

Vector Laboratories, Peterborough, UK.

Ventana Medical Systems, Inc, Roche, Lewes, East Sussex, UK.

Chapter 3

In vivo analysis of Sin3A function in the epidermis

3.1 Endogenous expression of Sin3A in the epidermis

The aims of my project were to determine whether Sin3A has a role to play in epidermal homeostasis. However, the epidermal compartments in which Sin3A is expressed was unknown. To assess endogenous expression of Sin3A at the mRNA level in epidermis, I generated DIG-labelled RNA probes and performed *in situ* hybridisation in whole mounts of Wild-type tail epidermis. Importantly, staining was not detected using the sense (control) Sin3A probe (Figure 3.1A). Performing *in situ* hybridisation using the anti-sense Sin3A probe, thus targeting Sin3A mRNA, revealed that Sin3A expression occurs in all epidermal compartments-the interfollicular epidermis, sebaceous gland and the hair follicle (Figure 3.1B).

To determine Sin3A localisation at the protein level, immunofluorescence was performed in back and tail skin (Figure 3.2). Sin3A protein expression was observed throughout the interfollicular epidermis, the hair follicle and the sebaceous gland in the back skin (Figure 3.2A). To more closely determine in which layers of the interfollicular epidermis the Sin3A protein is expressed I performed immunostaining in tail epidermis as the basal and suprabasal layers can be more clearly

Figure 3.1: Endogenous expression of Sin3A mRNA. Whole mounts of tail epidermis were prepared from Wild-type tail skin and *in situ* hybridisation was performed using DIG-Labelled RNA probes. A) *in situ* hybridisation in Wild-type whole mounts of tail epidermis using control (sense) Sin3A probe. Yellow dashed lines outline the hair follicles and sebaceous glands. B) *in situ* hybridisation in Wild-type whole mounts of tail epidermis using anti-sense Sin3A probe. HF=hair follicle SG=sebaceous gland IFE=interfollicular epidermis. Scale Bar, 100 μm.
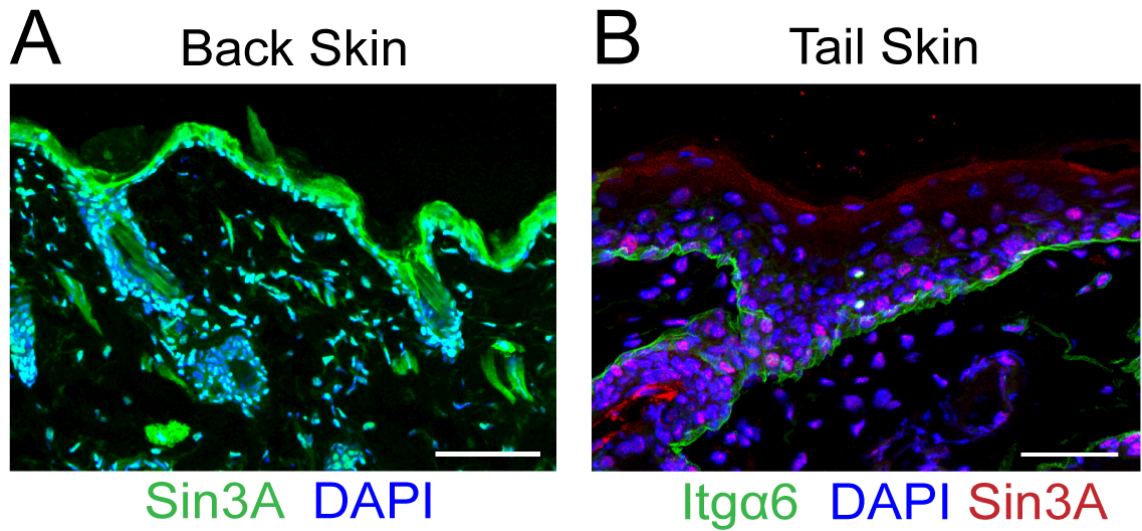
Figure 3.2: Endogenous expression of Sin3A protein. Sin3A expression was detected in sections of back or tail skin from Wild-type mice using immunofluorescence. A) Sin3A expression (green) in Wild-type back skin, counter-stained with DAPI (blue). B) Sin3A expression (red) in Wild-type tail skin counter-stained with DAPI (blue). The basal layer of the interfollicular epidermis was visualised by detecting the expression of the marker Integrin α6 (Itgα6) (green). Scale Bars, A) 75 μm B) 50 μm.
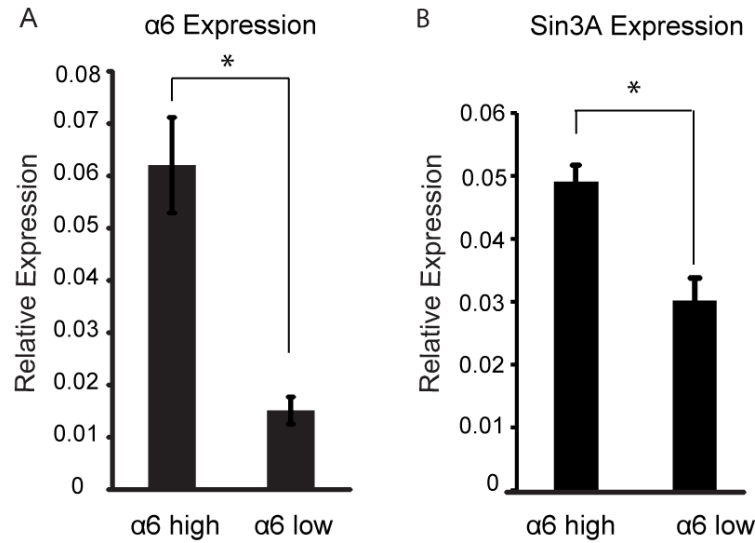
Figure 3.3: mRNA expression levels of Sin3A in undifferentiated and differentiated compartments of the interfollicular epidermis. Wild-type keratinocytes were isolated from back skin and then stained for the surface marker Integrin $\alpha6$. The cells were then sorted into Integrin $\alpha6$ high and low populations via flow cytometry. (A) qPCR confirmation of Integrin $\alpha6$ expression (Itg$\alpha6$) in Integrin $\alpha6$ high and Integrin $\alpha6$ low populations. (B) qPCR analysis of Sin3A expression in Integrin $\alpha6$ high and Integrin $\alpha6$ low populations. Higher expression of Sin3A is observed in the Integrin $\alpha6$ high population, which corresponds to undifferentiated cells of the IFE. Integrin $\alpha6$ is predominantly expressed in the basal cells of the IFE, however, as lower levels of this Integrin are expressed in the outer root sheath of the HF [Watt, 2002], samples analysed could potentially include HF cells. Error bars indicate standard deviation (n=3 biological replicates averaged over 3 technical replicates of each flow sorted population). * P<0.05.

visualised in this tissue. Sin3A is expressed in the basal layer and throughout the suprabasal layers, with Sin3A-positive nuclei being enriched towards the basal layer of the interfollicular epidermis (Figure 3.2B). To determine if this was true at the mRNA level, I stained keratinocytes isolated from Wild-type skin for Integrin $\alpha 6$ and then sorted the cells into Integrin $\alpha 6$ high (basal, undifferentiated) populations and Integrin $\alpha 6$ low (differentiated) populations and then determined Sin3A expression levels in these populations. Analysis of Sin3A RNA expression in undifferentiated cells (Integrin $\alpha 6$ high) and differentiated cells (Integrin $\alpha 6$ low) confirmed higher expression levels of Sin3A in undifferentiated cells (Figure 3.3).

Taken together, these results demonstrate that Sin3A is expressed throughout the different epidermal compartments at the mRNA and protein level. Sin3A is expressed throughout hair follicles, including the bulge region, and sebaceous glands. It appears that in the interfollicular epidermis, Sin3A expression is at its highest in the undifferentiated cells, located in the basal layer of the epidermis. Sin3A's widespread expression in the epidermis further indicated that Sin3A could have a key role to play in skin. To analyse the functional roles of Sin3A in the epidermis I generated conditional knockout mouse models for Sin3A in skin.

3.2 Targeting Sin3A deletion to bulge stem cells *in vivo*

Sin3A had been demonstrated to be a key factor in development and other cellular processes such as apoptosis and proliferation, but nothing was known about the role of Sin3A in skin stem cell homeostasis. To determine whether Sin3A has a function in this process, I first decided to focus on stem cells in the bulge region of the the hair follicle, which is the best characterised stem cell population in the skin to date. To pursue this aim I decided to conditionally delete Sin3A in bulge stem cells. As K19 is known to be a marker of bulge stem cells [Beck and Blanpain, 2012] (Figure 3.4), I targeted Sin3A deletion to K19-expressing cells in the skin.

In order to inducibly and conditionally delete Sin3A in bulge stem cells, I crossed mice harbouring Sin3A floxed alleles (Figure 3.5) with mice expressing CreER under the control of the K19 promoter, ultimately resulting in the generation of the K19ERSin3A$^{F/F}$ line. By using this strategy, I now had the appropriate mouse model to delete Sin3A specifically in K19-expressing cells upon topical application of 4-OHT to the skin. As such, my aim was to characterise the impact of loss of Sin3A in hair follicle stem cells by analysing the phenotype in K19ERSin3A$^{\Delta/\Delta}$ skin.

At the initiation of 4-OHT/ acetone application the mice used were 6 weeks old and were culled at 10 weeks old. At this stage, the hair cycle in the back skin is synchronised and HFs in this region should be in the telogen phase of the hair cycle [Müller-Röver et al., 2001]. Following the four weeks of treatment with 4-OHT, K19ERSin3A$^{\Delta/\Delta}$ mice were phenotypically indistinguishable from acetone-treated littermates (K19ERSin3A$^{F/F}$). To examine the impact of Sin3A deletion on hair follicle homeostasis, I initially analysed skin structure in K19ERSin3A$^{F/F}$ and K19ERSin3A$^{\Delta/\Delta}$ mice using H&E staining. Histological analysis of skin sections demonstrated no difference between hair follicles in K19ERSin3A$^{\Delta/\Delta}$ back skin (Figure 3.6B) in comparison to controls (Figure 3.6A). Likewise, hair follicles in K19ERSin3A$^{\Delta/\Delta}$ tail skin (Figure 3.7B) were indistinguishable from those
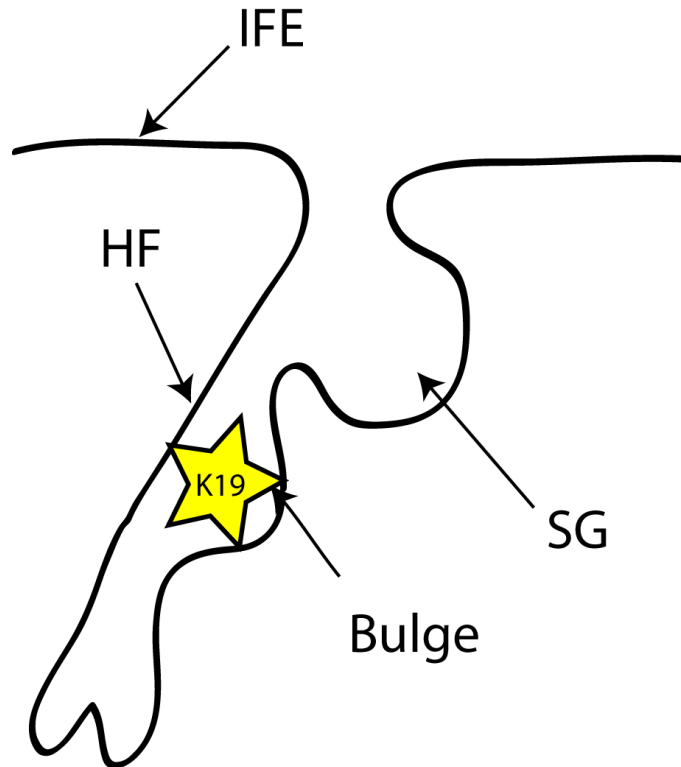
Figure 3.4: Schematic representation of K19 expression in the bulge region of the hair follicle. The region of the hair follicle in which K19 is expressed is highlighted.

Figure 3.5: Schematic overview of Sin3A floxed alleles. Red triangles represent LoxP sites. Black bars represent exons. In the Sin3A floxed allele, exon 4 is flanked by LoxP sites. Upon recombination, this leads to a deletion after exon 3, which corresponds to a region in the protein prior to all known functional domains.

observed in control tails (Figure 3.7A).

These results indicated that in the time-frame of treatment used, there was not an obvious phenotype when Sin3A was deleted from the hair follicle. Despite this, I believed that Sin3A deletion could still impact the bulge stem cell compartment, therefore I further characterised the K19ERSin3A$^{\Delta/\Delta}$ phenotype.
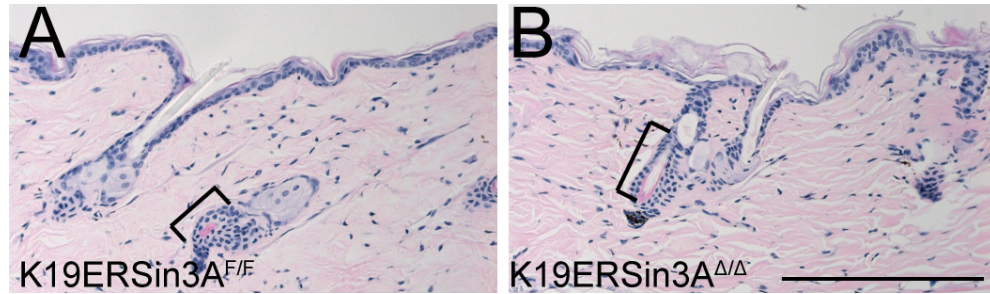
Figure 3.6: K19ERSin3A$^{\Delta/\Delta}$ back skin hair follicles are phenotypically normal. Sections of back skin treated with either A) acetone (K19ERSin3A$^{F/F}$) or B) 4-OHT (K19ERSin3A$^{\Delta/\Delta}$) were stained using H&E. Black lines highlight the bulge region. Scale Bar, 100 μm.
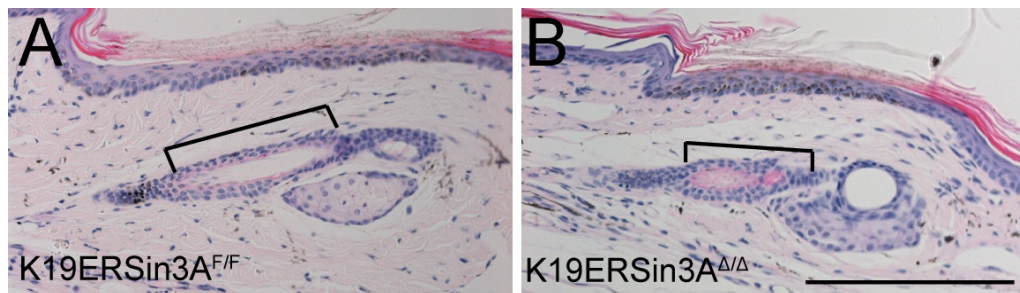
Figure 3.7: K19ERSin3A$^{\Delta/\Delta}$ tail skin hair follicles are phenotypically normal. Sections of tail skin treated with either A) acetone (K19ERSin3A$^{F/F}$) or B) 4-OHT (K19ERSin3A$^{\Delta/\Delta}$) were stained using H&E. Black lines highlight the bulge region. Scale Bar, 100 μm.

3.2.1 Sin3A is dispensable for bulge stem cell homeostasis

As Sin3A deletion has been shown to induce apoptosis in other cell types [Mc-Donel et al., 2011; Payne et al., 2010], I wanted to determine if deletion of Sin3A in bulge stem cells results in an induction of apoptosis. However, initial experiments indicate that this does not appear to be the case when Sin3A is deleted in the bulge stem cell population. As demonstrated by staining to detect cleaved Caspase 3, apoptosis does not appear to be erroneously induced in K19ERSin3A$^{\Delta/\Delta}$ hair follicles (Figure 3.8B), with levels of active Caspase 3 being indistinguishable from those observed in control hair follicles (Figure 3.8A). However, Caspase 3 is not a definitive apoptosis marker and further experiments are necessary to fully determine that apoptosis is not induced upon loss of Sin3A.
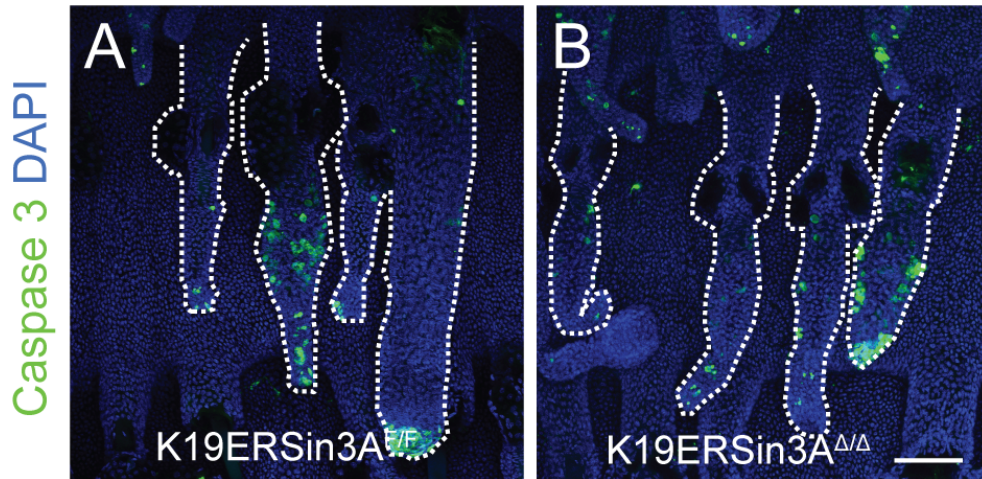
Figure 3.8: Loss of Sin3A in bulge stem cells does not induce apoptosis. Whole mounts of tail epidermis were prepared from K19ERSin3A$^{F/F}$ skin treated with either A) acetone (K19ERSin3A$^{F/F}$) or B) 4-OHT (K19ERSin3A$^{\Delta/\Delta}$) and were stained for cleaved Caspase 3 (green), which as a marker of apoptosis, and counter-stained using DAPI (blue). Dashed white lines outline hair follicles and sebaceous glands. Scale Bar, 100 μm.

In a parallel experiment in which I deleted Sin3A in the basal layer of the inter-follicular epidermis, which will be discussed in Section 3.4.3, I found that Sin3A deletion leads to increased proliferation. Due to these observations I next de-

cided to determine whether Sin3A-depletion in bulge stem cells had an impact on proliferation in this region. I first examined proliferation in back skin hair follicles by labelling sections of back skin from either K19ERSin3A$^{F/F}$ (Figure 3.9A) or K19ERSin3A$^{\Delta/\Delta}$ mice (Figure 3.9B) for the proliferation marker Ki67. Quantification of the number of Ki67 cells in hair follicles (Figure 3.10) revealed that there was no significant difference in the number of proliferating cells when comparing samples from K19ERSin3A$^{F/F}$ and K19ERSin3A$^{\Delta/\Delta}$ skin. Labelling for Ki67 in whole mounts of tail epidermis prepared from either K19ERSin3A$^{F/F}$ (Figure 3.11A) or K19ERSin3A$^{\Delta/\Delta}$ skin (Figure 3.11B) also demonstrated no difference in bulge stem cell proliferation when Sin3A is deleted.
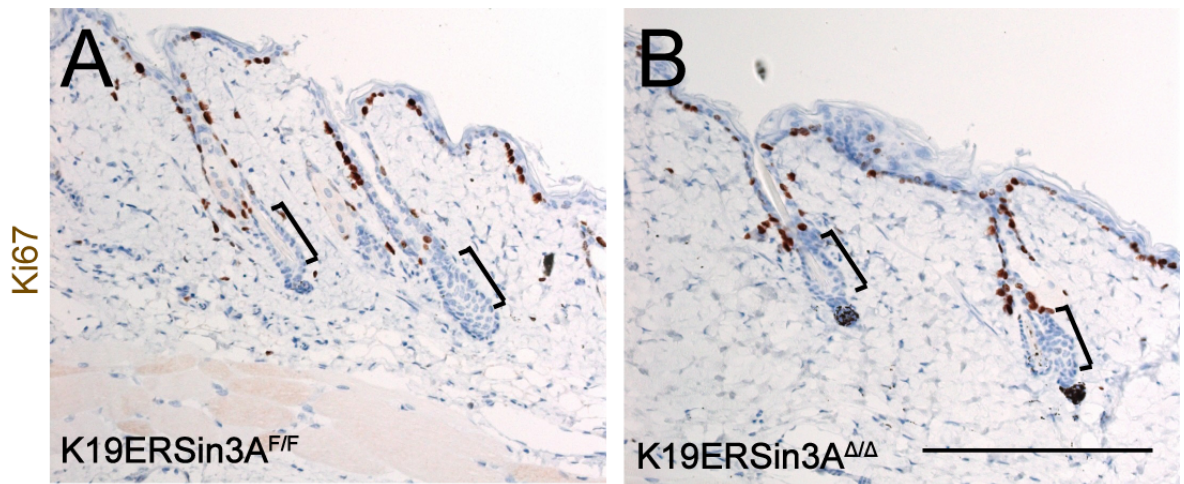
Figure 3.9: Loss of Sin3A in bulge stem cells does not induce proliferation in back skin hair follicles. Sections of back skin were prepared from K19ERSin3A$^{F/F}$ mice treated with either A) acetone (K19ERSin3A$^{F/F}$) or B) 4-OHT (K19ERSin3A$^{\Delta/\Delta}$) and were stained for the proliferation marker Ki67 (brown). Black lines highlight the bulge region. Scale Bar, 100 μm.
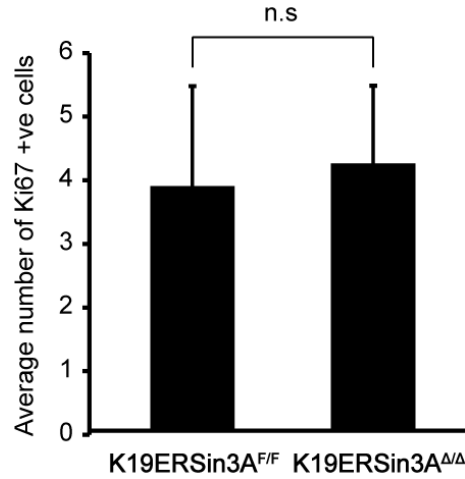
Figure 3.10: **Levels of Ki67 postive cells in K19ERSin3A$^{\Delta/\Delta}$ hair follicles are normal.** The average number of Ki67-positive cells in hair folllicles from K19ERSin3A$^{F/F}$ and K19ERSin3A$^{\Delta/\Delta}$ mice was calculated and is represented graphically. There was no significant difference between the two values (n.s, P>0.05). Error bars indicate standard deviation (n=3 biological replicates averaged over 3 hair follicles of each condition).
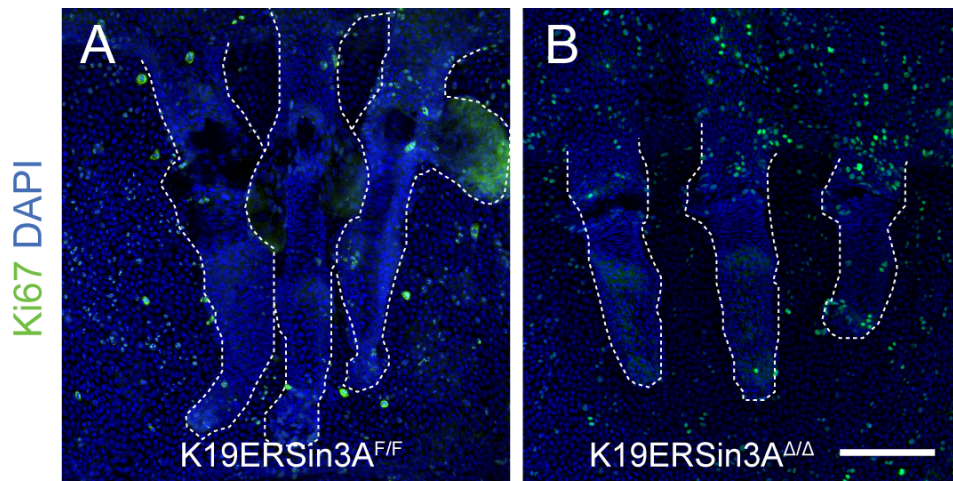
Figure 3.11: Loss of Sin3A in bulge stem cells does not induce proliferation in tail skin hair follicles. Whole mounts of tail epidermis were prepared from K19ERSin3A$^{F/F}$ skin treated with either A) acetone (K19ERSin3A$^{F/F}$) or B) 4-OHT (K19ERSin3A$^{\Delta/\Delta}$) and were stained for the proliferation marker Ki67 (green) and counter-stained using DAPI (blue). Dashed white lines outline hair follicles and sebaceous glands. Scale Bar, 100 μm.

These findings demonstrate that upon the loss of Sin3A, neither proliferation or apoptosis is induced in the bulge stem cell population. Thus it could be considered that Sin3A is dispensable for bulge stem cell homeostasis. At this point, I decided to switch focus to examine the possibility that Sin3A has a role in maintaining homeostasis in the interfollicular epidermis.

3.3 Conditional deletion of Sin3A in the basal layer of the epidermis

3.3.1 Conditional deletion of Sin3A in undifferentiated cells during development leads to embryonic lethality

In Section 3.1, I determined that Sin3A is expressed throughout the epidermal compartments and in the interfollicular epidermis, Sin3A expression is enriched in basal, undifferentiated cells. In order to address the role of Sin3A in regulating epidermal homeostasis, I generated a transgenic mouse model in which I conditionally deleted Sin3A in undifferentiated cells of the epidermis (K14Sin3A line). This was accomplished by crossing transgenic mice expressing Cre-recombinase under the control of the human K14 promoter with mice harbouring Sin3A floxed alleles (Figure 3.5). The aim of the K14Sin3A line was to generate K14Cre positive mice that were homozygous for the Sin3A floxed allele. However, from a total of 95 mice born, no mice of this genotype were detected (Table 3.1). This data strongly suggests that the phenotype caused by deletion of both Sin3A alleles in K14 positive cells is embryonic lethal.

Genotype	Sin3A$^{\mathbf{WT/WT}}$	Sin3A$^{\mathbf{WT/F}}$	Sin3A$^{\mathbf{F/F}}$
K14Cre Positive	18	62	**0**
K14Cre Negative	7	5	3

Table 3.1: Quantification of K14Sin3A genotypes.

3.3.2 Conditional loss of a single allele of Sin3A in the basal layer of the epidermis does not lead to an epidermal phenotype

I wanted to determine the impact of the loss of a single allele of Sin3A in the epidermis as there was the possibility that this could cause a disruption to epidermal homeostasis. As such I performed histological analysis of back and tail skin obtained from K14Sin3A$^{WT/\Delta}$ mice using samples from control littermates as a comparison. Back and tail skin obtained from K14Sin3A$^{WT/\Delta}$ mice was phenotypically indistinguishable from back and tail skin obtained from the control littermates (Figure 3.12). I contemplated that this lack of phenotype could be due to the short time-frame of Sin3A deletion and that a phenotype could potentially be observed in older mice. Consequently I analysed skin obtained from mice that were over 12 months of age (Figure 3.13, 3.14). However, even after this extended time period, K14Sin3A$^{WT/\Delta}$ back (Figure 3.13) and tail skin (Figure 3.14) was phenotypically indistinct from control skin. These results indicated that epidermal homeostasis was not disrupted by the loss of a single allele of Sin3A from undifferentiated epidermal cells.
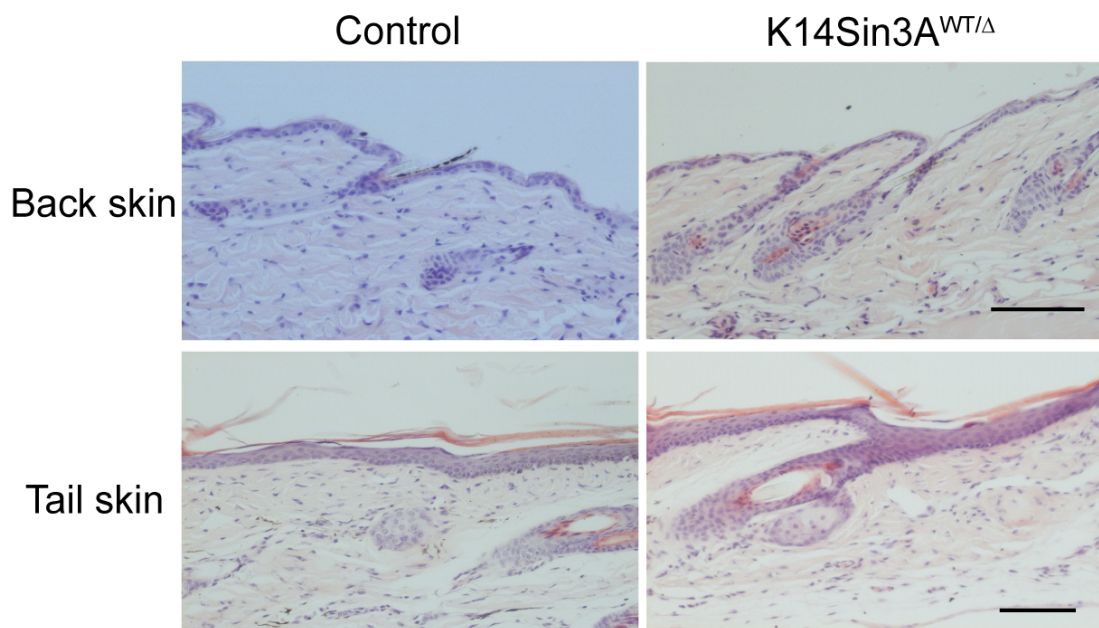
Figure 3.12: Conditional loss of a single allele of Sin3A does not lead to an epidermal phenotype. Histological analysis using H&E staining in sections of back skin (top panels) and tail skin (bottom panels) obtained from control mice (left panels) or K14Sin3A$^{WT/\Delta}$ (right panels). These images demonstrate that K14Sin3A$^{WT/\Delta}$ skin is phenotypically indistinct from control skin. Scale Bars, 100 μm.
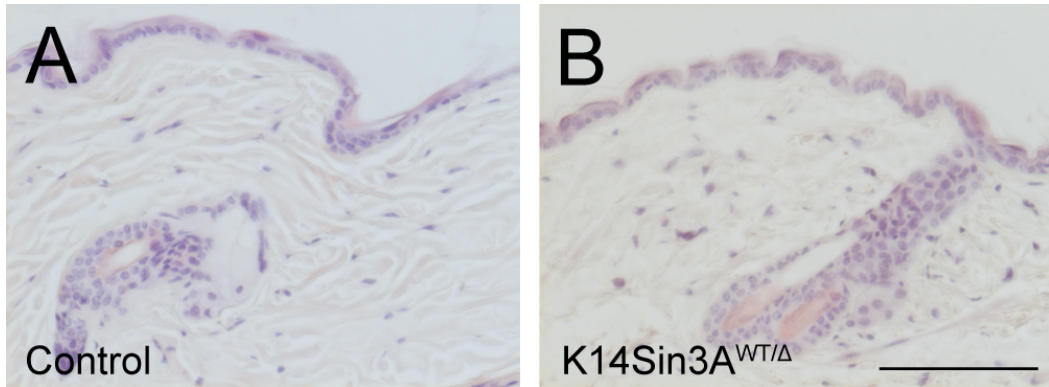
Figure 3.13: Loss of a single allele of Sin3A in dorsal skin for more than 12 months does not lead to an epidermal phenotype. Histological analysis using H&E staining in sections of A) control back skin and B) K14Sin3A$^{\text{WT}/\Delta}$ back skin obtained from mice that were over 12 months of age. These images demonstrate that K14Sin3A$^{\text{WT}/\Delta}$ back skin is phenotypically indistinct from control skin after an extended time period. Scale Bar, 100 μm.
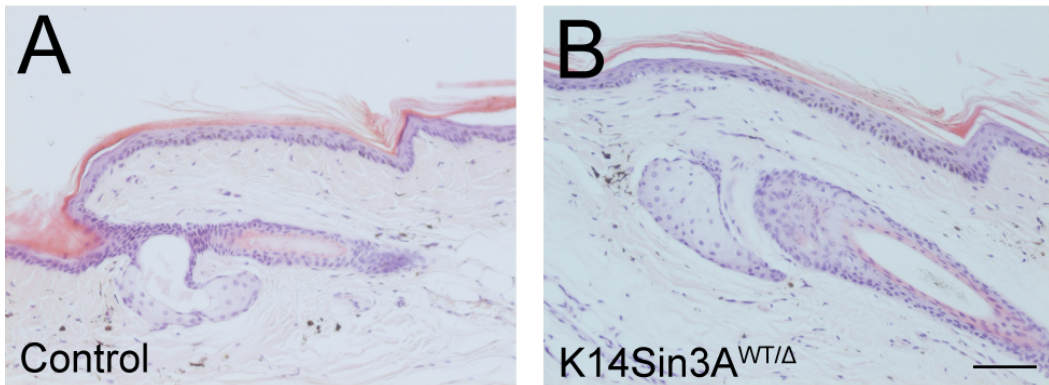
Figure 3.14: Loss of a single allele of Sin3A in tail skin for more than 12 months does not lead to an epidermal phenotype. Histological analysis using H&E staining in sections of A) control tail skin and B) K14Sin3A$^{\text{WT}/\Delta}$ tail skin obtained from mice that were over 12 months of age. These images demonstrate that K14Sin3A$^{\text{WT}/\Delta}$ tail skin is phenotypically indistinct from control skin after an extended time period. Scale Bar, 200 μm.

3.4 Sin3A is essential for the maintenance of epidermal homeostasis

3.4.1 Inducible, conditional deletion of Sin3A from the basal layer of the epidermis leads to a severe phenotype

As K14Sin3A$^{\Delta/\Delta}$ mice were not born and K14Sin3A$^{WT/\Delta}$ are phenotypically normal, this mouse model was not useful for analysing Sin3A function in adult skin. Consequently, a new breeding strategy was undertaken in which mice with floxed Sin3A alleles were crossed with K14CreER mice to generate the K14ERSin3A$^{F/F}$ mouse line thus allowing temporal control over Sin3A deletion. Upon topical application of 4-OHT to the skin of K14ERSin3A$^{F/F}$ mice, Sin3A can be deleted in all undifferentiated epidermal cells. This approach meant that loss of Sin3A could be analysed in the adult epidermis in order to gain insights into Sin3A function in epidermal homeostasis.

To confirm loss of Sin3A in K14-positive cells, expression of Sin3A was analysed at the RNA and protein level. Analysis of RNA expression levels via qPCR confirmed a reduction in Sin3A expression of treated K14ERSin3A$^{\Delta/\Delta}$ mice relative to controls (Figure 3.15). As Sin3A was deleted only in K14-positive cells, and RNA was isolated from a whole skin preparation, residual Sin3A expression is detected. Sin3A expression was also observed to be lost from the nuclei of K14 positive cells in the interfollicular epidermis of both back and tail skin of K14ERSin3A$^{\Delta/\Delta}$ mice (Figure 3.16).
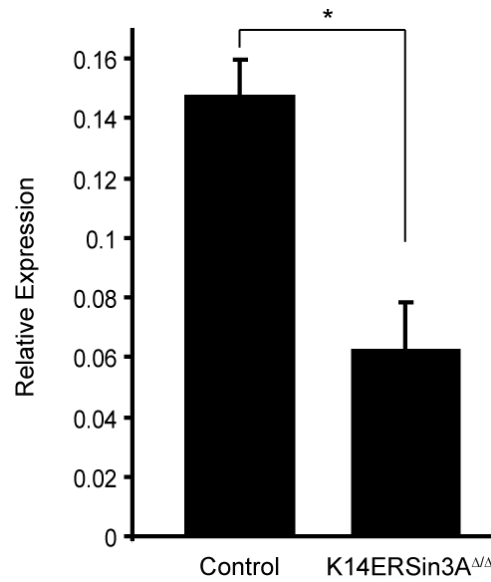
Figure 3.15: Confirmation of depletion of Sin3A RNA in K14ERSin3A$^{\Delta/\Delta}$ skin. RNA was isolated from back skin of control and K14ERSin3A$^{\Delta/\Delta}$ mice and converted to cDNA. Sin3A expression was analysed via qPCR confirming a reduction of Sin3A RNA expression in K14ERSin3A$^{\Delta/\Delta}$ skin. Error bars indicate standard deviation (n=3 biological replicates averaged over 3 technical replicates). * P<0.0005.
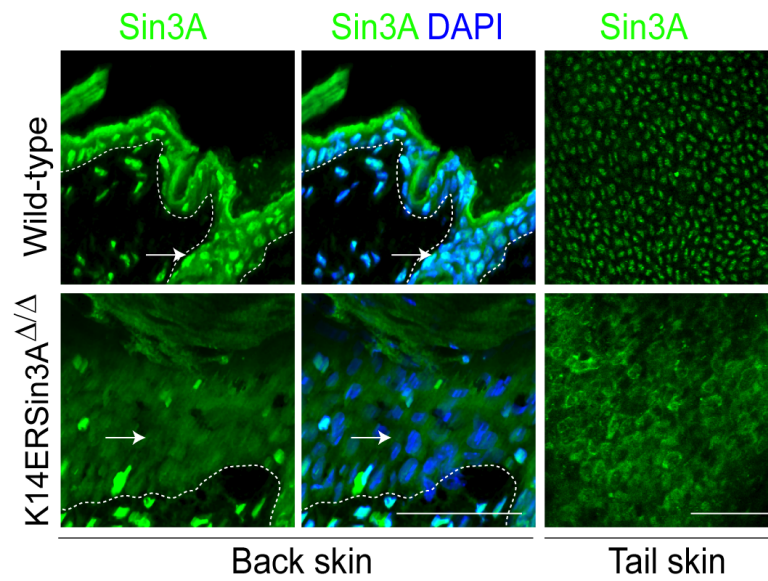
Figure 3.16: Confirmation of depletion of Sin3A protein in K14ERSin3A$^{\Delta/\Delta}$ skin. Sin3A protein was visualised via immunofluorescence in control back skin sections (upper left and middle panels) and tail whole mounts (upper right panel). Sin3A protein is deleted efficiently from the nuclei in K14ERSin3A$^{\Delta/\Delta}$ back skin (lower left and middle panels) and tail whole mounts (lower right panel). Sin3A-expressing nuclei are depicted by white arrows in upper panels and non-expressing nuclei by white arrows in lower panels. Scale Bars, 50 μm.

After topical application of 4-OHT to a shaved region of the back skin of K14ERSin3A$^{F/F}$ mice, a severe phenotype was observed. K14ERSin3A$^{\Delta/\Delta}$ mice can be distinguished from control littermates due to a number of features (Figure 3.17). Perhaps most importantly, areas of treated back skin were visibly much thicker, thicker to the touch and had lost elasticity in K14ERSin3A$^{\Delta/\Delta}$ mice in comparison to control littermates (Figure 3.17A). Additionally, K14ERSin3A$^{\Delta/\Delta}$ mice appeared to salivate excessively resulting in a wet coat below the mouth (Figure 3.17B) and males had an enlarged testes region relative to control mice (Figure 3.17C). These exciting results led to further characterization of the skin phenotype observed in K14ERSin3A$^{\Delta/\Delta}$ mice.
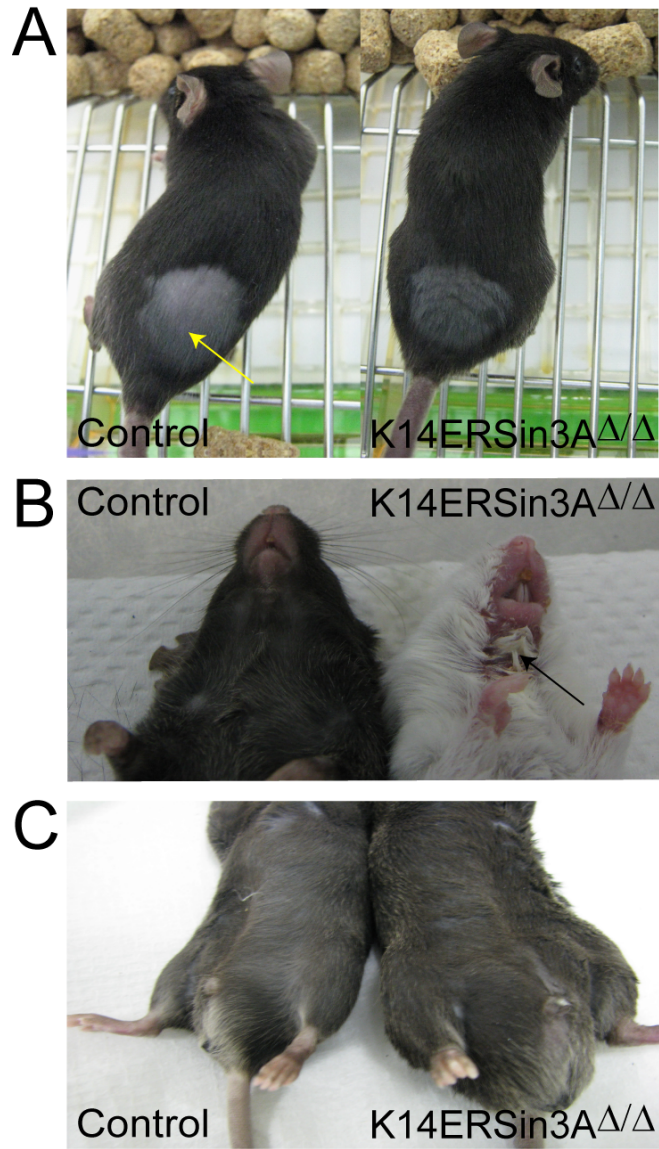
Figure 3.17: Deletion of Sin3A in adult skin leads to a severe phenotype. A) Back skin of K14ERSin3A$^{F/F}$ mice was shaved and subsequently treated with acetone (control) or 4-OHT (K14ERSin3A$^{\Delta/\Delta}$). The treated area of skin (indicated by yellow arrow) in K14ERSin3A$^{\Delta/\Delta}$ mice is increased in thickness relative to control. B) K14ERSin3A$^{\Delta/\Delta}$ mice salivate excessively relative to control mice, resulting in a wet coat below the mouth (black arrow). C) K14ERSin3A$^{\Delta/\Delta}$ mice have an enlarged testes region relative to control mice.

3.4.2 Depletion of Sin3A in the basal layer of the epidermis in adult skin leads to epidermal hyperplasia

To begin characterisation of the skin phenotype in K14ERSin3A$^{\Delta/\Delta}$ mice, 4-OHT was applied to the back skin in a time course experiment (Figure 3.18). Wild-type, K14ERSin3A$^{\Delta/\Delta}$ and R26K14ERLacZ back skin was treated with 4-OHT for 1 day, 5 days, 9 days or 15 days. The R26K14ERLacZ mouse was used as a reporter to analyse activation of Cre-recombinase (Figure 3.18A-D lower panels) and demonstrated homogenous recombination in the interfollicular epidermis after 5 days of treatment with 4-OHT (Figure 3.18B lower panel). To analyse the skin phenotype in these mice, skin samples were taken at each time point, sectioned and stained using H&E. Interestingly, after 9 days of treatment with 4-OHT, K14ERSin3A$^{\Delta/\Delta}$ skin exhibits an increase in thickness of the interfollicular epidermis and an enlargement of the sebaceous glands (Figure 3.18C middle panel) relative to Wild-type mice (Figure 3.18C upper panel). The increase in thickness of the interfollicular epidermis became most pronounced after 15 days of treatment (Figure 3.18D middle panel) in comparison to Wild-type controls (Figure 3.18 upper panel). The results of this time course experiment demonstrated that loss of Sin3A in the epidermis leads to an increase in the thickness of the interfollicular epidermis and an enlargement of the sebaceous glands.

To determine if the loss of Sin3A also had an impact on tail epidermis, I treated tail-skin of K14ERSin3A$^{F/F}$ with 4-OHT. Following 17 days of treatment with 4-OHT, the mice were sacrificed and tail skin samples collected and sectioned for analysis. Histological analysis using H&E staining revealed the same phenotype in the tail skin as in back skin, with an enlargement of the interfollicluar epidermis in K14ERSin3A$^{\Delta/\Delta}$ mice (Figure 3.19B) relative to that observed in Wild-type tail skin (Figure 3.19A). The causes driving this phenotype of epidermal hyperplasia required further investigation.
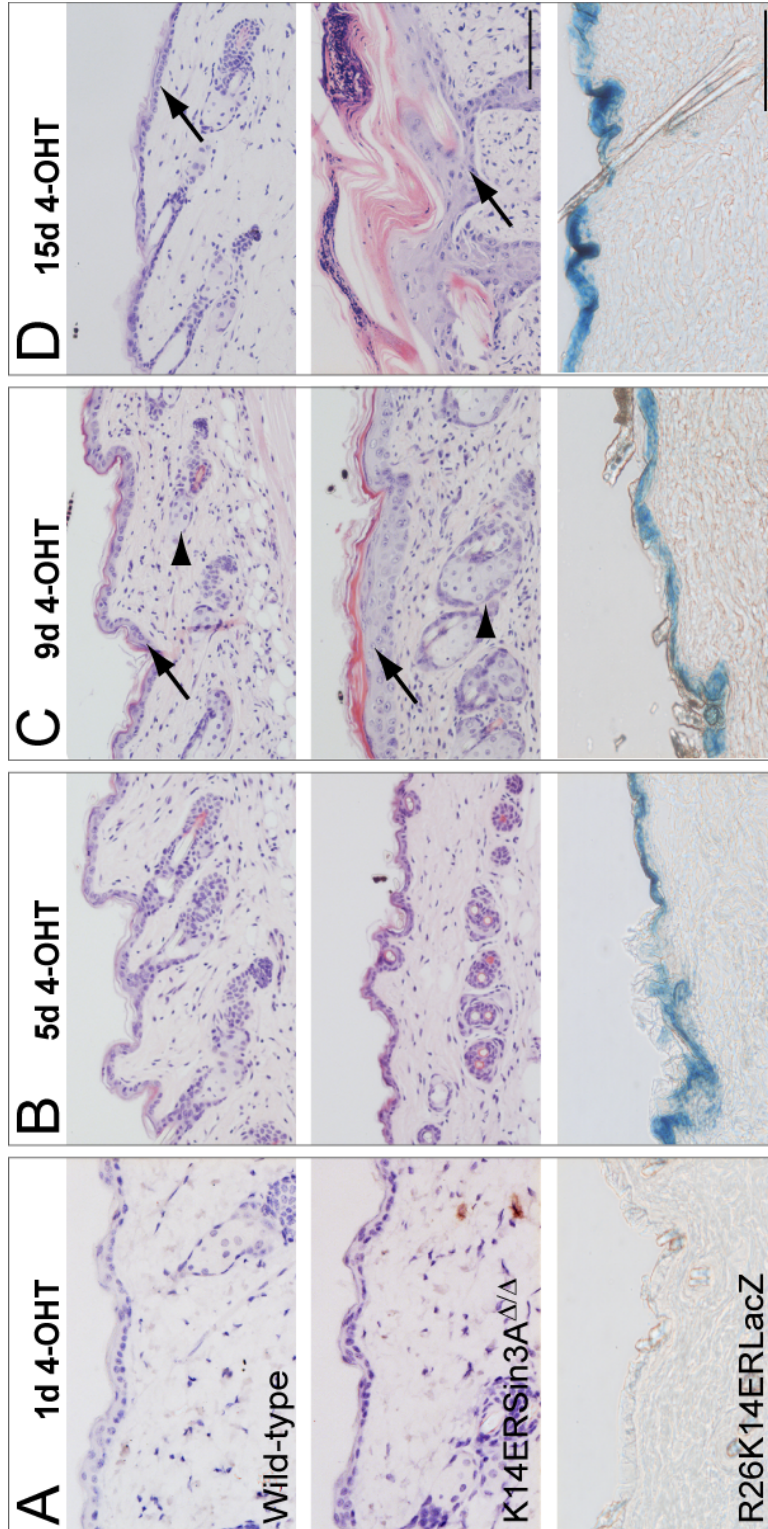
Figure 3.18: Effect of Sin3A loss in murine dorsal epidermis. Shaved dorsal-skin of Wild-type, K14ERSin3A$^{\Delta/\Delta}$ and Cre-recombinase reporter (R26K14ERLacZ) mice was treated with 4-OHT in a time-course experiment. Sections of dorsal skin from Wild-type and K14Sin3A$^{\Delta/\Delta}$ mice were stained for H&E. Sections of dorsal skin from R26K14ERLacZ mice were stained for β-galactosidase as a reporter for LacZ activity. A) Back skin sections from 1 day (d) treated mice. B) Back skin sections from 5 day treated mice C) Back skin sections from 9 day treated mice. D) Back skin sections from 15 day treated mice. Black arrows indicate increased thickness of the interfollicular epidermis in K14ERSin3A$^{\Delta/\Delta}$ mice relative to Wild-type mice. Black arrowheads show an enlargement of sebaceous glands in K14ERSin3A$^{\Delta/\Delta}$ mice relative to Wild-type mice. Scale Bars, 100μm.
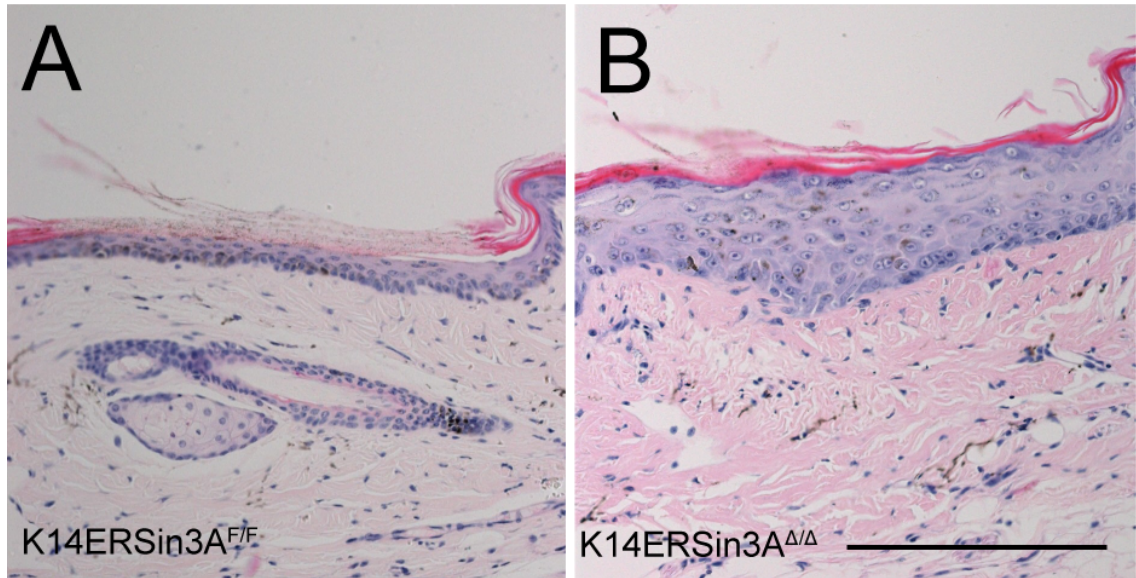
Figure 3.19: Effect of Sin3A loss in murine tail epidermis. Samples of tail skin of mice treated with 4-OHT were sectioned and stained using H&E. A) Tail skin section from control mice B) Tail skin section from K14ERSin3A$^{\Delta/\Delta}$ mice. Scale Bar, 100 μm.

3.4.3 Epidermal hyperplasia in Sin3A-depleted skin is driven by increased proliferation and differentiation

To determine if the epidermal hyperplasia observed in K14ERSin3A$^{\Delta/\Delta}$ skin was driven by an increase in proliferation, back skin sections from 4-OHT-treated control or K14ERSin3A$^{\Delta/\Delta}$ mice were stained for the proliferation marker Ki67 (Figure 3.20). The average number of Ki67-positive cells was significantly higher in the interfollicular epidermis (Figure 3.20C+G) and sebaceous glands (Figure 3.20F+H) in K14ERSin3A$^{\Delta/\Delta}$ mice relative to controls (Figure 3.20A, B, D, F+ H). To determine if this was also true in tail skin, BrdU incorporation was analysed by immunolabelling of whole mounts of tail epidermis (Figure 3.21). There was an increase in BrdU-positive nuclei in the interfollicular epidermis (Figure 3.21A) and the sebaceous glands (Figure 3.21B) of K14ERSin3A$^{\Delta/\Delta}$ mice relative to Wild-type mice. This provided the indication that proliferation was increased in interfollicular epidermis and sebaceous glands in both adult back and tail skin when Sin3A is lost.

To determine if the cell cycle was also impacted, cell cycle analysis was performed using cells isolated from K14ERSin3A$^{F/F}$and K14ERSin3A$^{\Delta/\Delta}$ back skin (Figure 3.22). Results from this analysis demonstrated that loss of Sin3A results in a significant increase of cells in the S and G2/M phases of the cell cycle (Figure 3.22A). This was confirmed by the detection of an increase in positively stained nuclei for key cell cycle factors: CyclinB1 (Figure 3.22B), whose expression peaks during G2/M phase [Miyazaki and Arai, 2007], UHRF1 (Figure 3.22C), which is required for cell cycle progression [Tien et al., 2011] and Mcm2 (Figure 3.22D), which is important in S phase [Bochman and Schwacha, 2009]. The accumulation of proteins involved in cell cycle progression and an increased number of cells in S and G2/M phases of the cell cycle indicates that loss of Sin3A from adult skin leads to an increase in actively cycling cells.
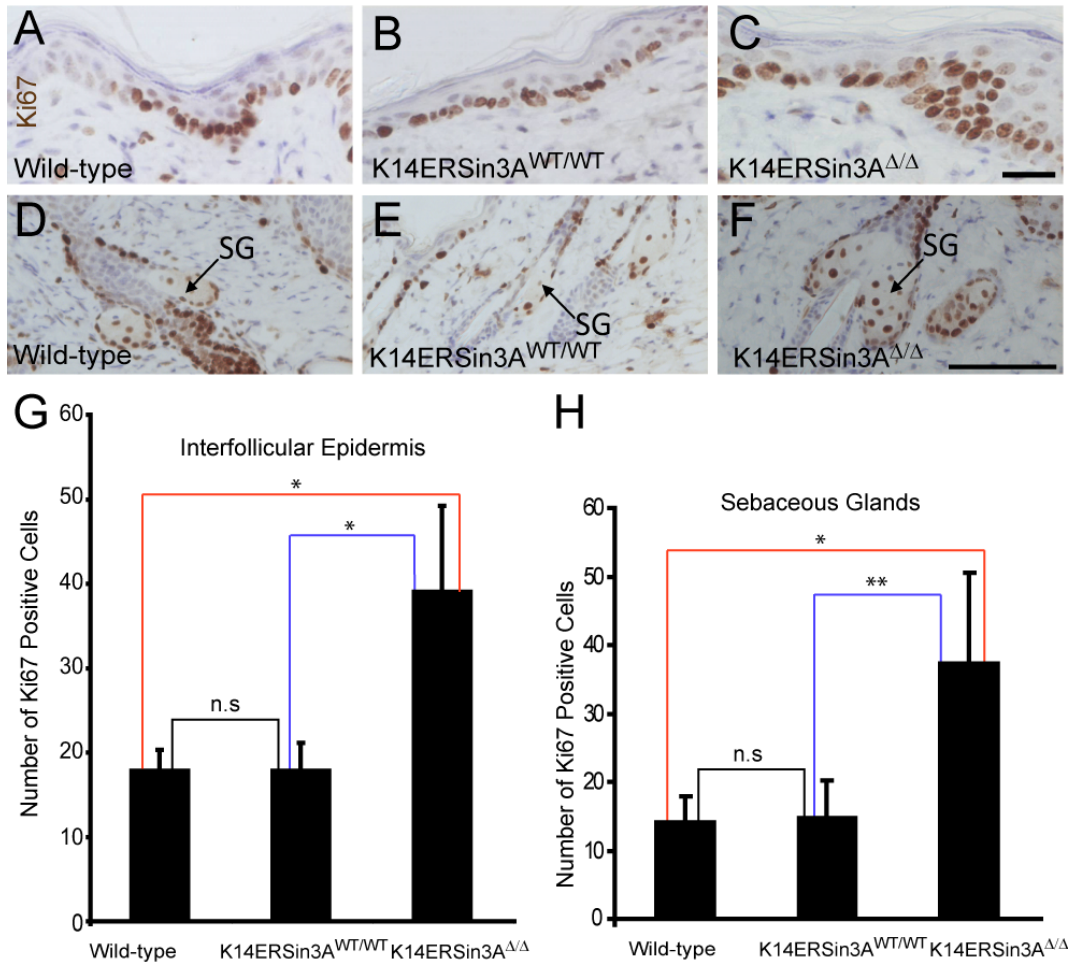
Figure 3.20: Deletion of Sin3A in adult back skin leads to increased proliferation. Samples of back skin of mice treated with 4-OHT were sectioned and stained for Ki67. A-C) Ki67-positive cells in 4-OHT-treated Wild-type, K14ERSin3A$^{WT/WT}$ and K14ERSin3A$^{\Delta/\Delta}$ interfollicular epidermis (IFE). D-F) Ki67-positive cells in 4-OHT-treated Wild-type, K14ERSin3A$^{WT/WT}$ and K14ERSin3A$^{\Delta/\Delta}$ sebaceous glands (SG). G) Quantification of Ki67-positive cells in the IFE. There is a significant increase in Ki67-positive cells in K14ERSin3A$^{\Delta/\Delta}$ IFE relative to controls. n.s p$>$0.05 * p$<$0.0006. H) Quantification of Ki67-positive cells in the SG. There is a significant increase in Ki67-positive cells in K14ERSin3A$^{\Delta/\Delta}$ SGs relative to controls. Error bars indicate standard deviation (n=5 animals of each mouse line) n.s p$>$0.05 * p$<$0.01 ** p$<$0.005. Scale Bars, A-C, 25 μm D-F, 100 μm.
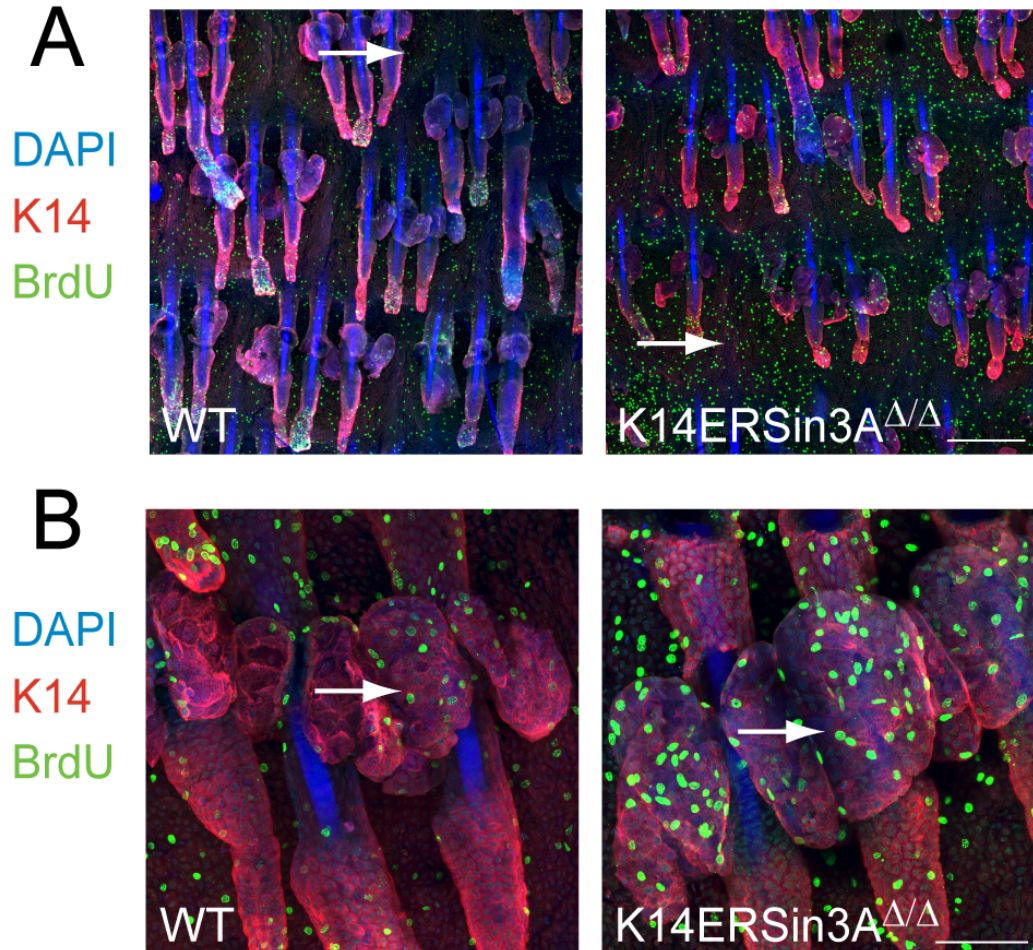
Figure 3.21: Deletion of Sin3A in adult tail skin leads to increased proliferation in interfollicular epidermis and sebaceous glands. BrdU incorporation was analysed in whole mounts of tail epidermis prepared from 4-OHT treated mice to identify cycling cells using antibodies for BrdU and K14. A) BrdU incorporation in whole mounts of tail epidermis in Wild-type (WT) mice (left panel) and K14ERSin3A$^{\Delta/\Delta}$ (right panel) indicates an increase in BrdU-positive cells in K14ERSin3A$^{\Delta/\Delta}$ interfollicular epidermis. B) BrdU incorporation in whole mounts of tail epidermis in WT mice (left panel) and K14ERSin3A$^{\Delta/\Delta}$ (right panel) indicates an increase in BrdU-positive cells in K14ERSin3A$^{\Delta/\Delta}$ sebceous glands. White arrows indicate BrdU positive nuclei in interfollicular epidermis A) and sebaceous glands B). Scale Bars, A) 250 μm, B) 75 μm.
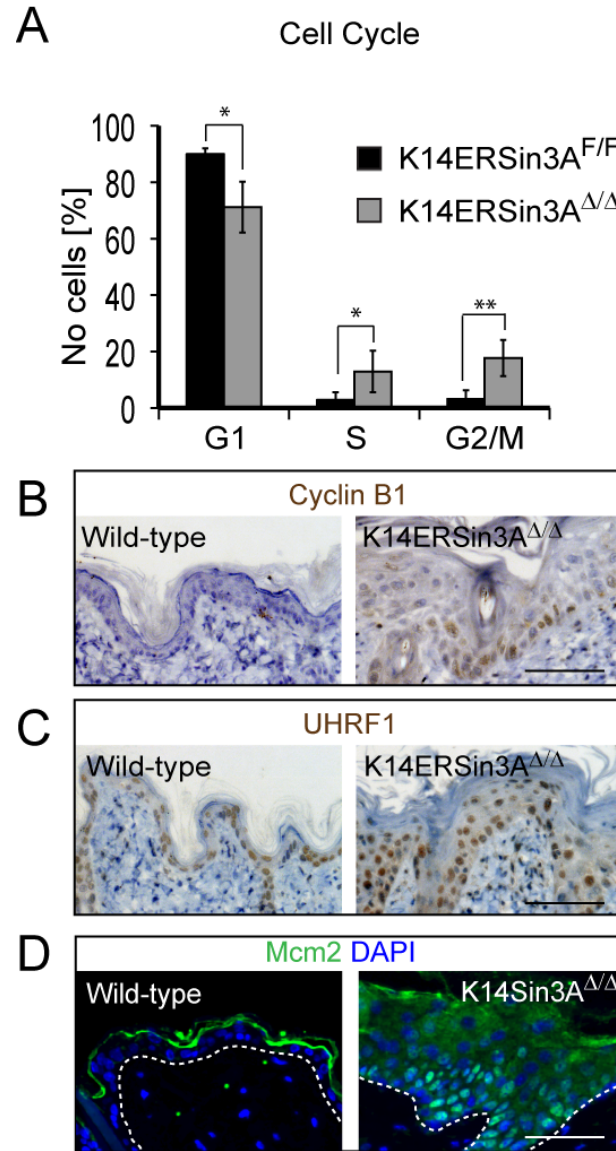
Figure 3.22: Deletion of Sin3A impacts the cell cycle. A) Cell cycle profiles of epidermal cells isolated from K14ERSin3A$^{F/F}$ and K14ERSin3A$^{\Delta/\Delta}$ back skin. B) Back skin sections from Wild-type and K14ERSin3A$^{\Delta/\Delta}$ back skin stained for Cyclin B1. C) Back skin sections from Wild-type and K14ERSin3A$^{\Delta/\Delta}$ back skin stained for UHRF1. D) Back skin sections from Wild-type and K14ERSin3A$^{\Delta/\Delta}$ back skin stained for Mcm2. Error bars indicate standard deviation (n=5 animals of each mouse line) * p<0.04 ** p<0.055. Scale Bar, 100 μm.

I next asked whether the promotion of proliferation observed when Sin3A expression is lost from adult skin leads to an induction of differentiation in the interfollicular epidermis. By answering this question, I could also determine whether Sin3A is necessary for the terminal differentiation program to be completed in the interfollicular epidermis. To do this, I looked at the expression of markers of both undifferentiated and differentiated cell layers in K14ERSin3A$^{\Delta/\Delta}$ skin.

I first examined the impact of Sin3A loss on the undifferentiated, basal layer of the interfollicular epidermis in K14ERSin3A$^{\Delta/\Delta}$ skin. In Sin3A-depleted skin, there is an increase in the thickness of the undifferentiated basal layer, as indicated by an increase in the expression of the basal marker Integrin $\alpha6$ in comparison to control skin (Figure 3.23A-D). The increase in expression of markers of undifferentiated cells when Sin3A expression is lost in adult skin was also true at the RNA level as shown by qPCR analysis (Figure 3.23E).

Deleting Sin3A from adult skin also increases the thickness of suprabasal layers, which contain differentiated cells (Figures 3.23, 3.24). There is an increase in the size of the spinous layer, as indicated by K10 staining (Figure 3.23A+B) and granular layer, as indicated by Involucrin staining (Figures 3.23C+D, 3.24) in K14ERSin3A$^{\Delta/\Delta}$ skin. RNA analysis indicated there is an increase in expression levels of differentiation markers including the granular layer markers Filaggrin, Loricrin and Involucrin [Blanpain and Fuchs, 2009; Eckert et al., 2004] and the cornified envelope marker Transglutaminase1 [Candi et al., 2005] (Figure 3.23 E).

Examination of markers of undifferentiated and differentiated cells at the RNA and protein level in Sin3A-depleted skin therefore demonstrates that there is an increase in expression of markers of both compartments and there is expansion of both differentiated and undifferentiated layers of the interfollicular epidermis. This evidence shows that Sin3A is not required for terminal differentiation in the interfollicular epidermis to be completed.
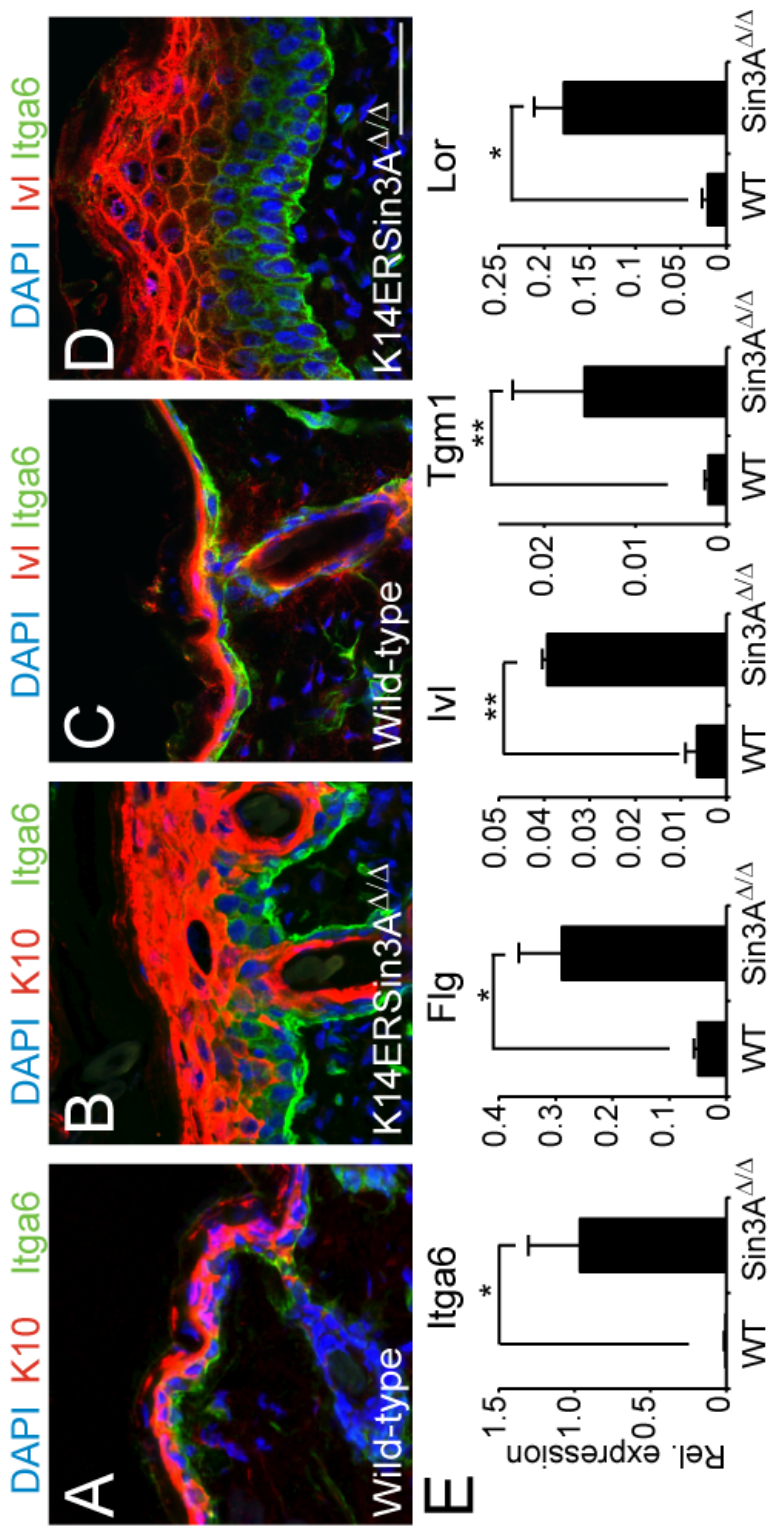
Figure 3.23: Sin3A is dispensable for epidermal differentiation. A-D) Sections of back skin from Wild-type (WT) and K14ERSin3A$^{\Delta/\Delta}$ back skin were labelled for suprabasal layers using the markers Keratin 10 (K10) and Involucrin (Ivl) and the basal layer using the marker Integrin α6 (Itgα6). E) RNA was isolated from back skin from WT and K14ERSin3A$^{\Delta/\Delta}$ mice and converted to cDNA. qPCR analysis was performed to compare RNA expression levels of Itgα6 (marker of undifferentiated cells) and differentiation markers Filaggrin (Flg), Involucrin (Ivl), Transglutaminase1 (Tgm1) and Loricrin (Lor) between WT and K14ERSin3A$^{\Delta/\Delta}$ samples. Results indicated that there was a significant increase in expression levels of markers of both differentiated and undifferentiated cells. Error bars indicate standard deviation (n=3 biological replicates averaged over 3 technical replicates). * P<0.05 ** P<0.001. Scale Bar, 100 μm.
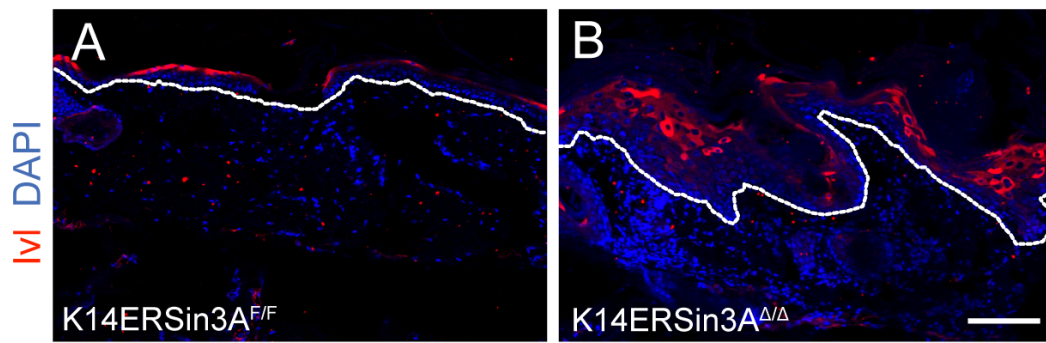
Figure 3.24: Sin3A deletion induces increased differentiation in tail skin Sections of tail skin from A) K14ERSin3A$^{F/F}$ and B) K14ERSin3A$^{\Delta/\Delta}$ were labelled using the suprabasal layer marker Involucrin (Ivl). Dashed white line represents the basal layer. Scale Bar, 100 μm.

3.5 Sin3A deletion leads to proliferation in other adult tissues

Deletion of Sin3A in adult skin induces proliferation, which contrasts results from studies using mouse embryonic fibroblasts, in which Sin3A deletion results in apoptosis and cell cycle arrest [Cowley et al., 2005; Dannenberg et al., 2005]. To determine if this effect was skin-specific or whether Sin3A deletion could promote proliferation in other tissues, I examined the impact of Sin3A deletion in the testis and salivary glands. I chose to analyse the effect of Sin3A deletion in the salivary glands and testis of K14ERSin3A$^{\Delta/\Delta}$ mice as these tissues express K14 and exhibited a phenotype as described above. Cre-recombinase activity following 4-OHT treatment was confirmed in the testis (Figure 3.25A) and salivary gland (Figure 3.26A) using the R26K14ERLacZ reporter line.

To determine if proliferation was impacted in testis and the salivary gland, sections were stained for Ki67 and the number of Ki67 cells were quantified in each tissue (Figures 3.25, 3.26). A small, yet significant, increase in Ki67-positive cells was observed in the testis of K14ERSin3A$^{\Delta/\Delta}$ mice (Figure 3.25D-F), indicating that proliferation was induced. A more marked effect was observed in the salivary gland, with nearly a 4-fold increase in the observed number of Ki67 positive cells in K14ERSin3A$^{\Delta/\Delta}$ mice relative to controls (Figure 3.26D-F). In similarity to the effect in skin, loss of Sin3A in Keratin 14 positive cells of the testis and salivary gland promotes proliferation. These results demonstrate that the induction of proliferation as a consequence of losing Sin3A is not a skin-specific effect.
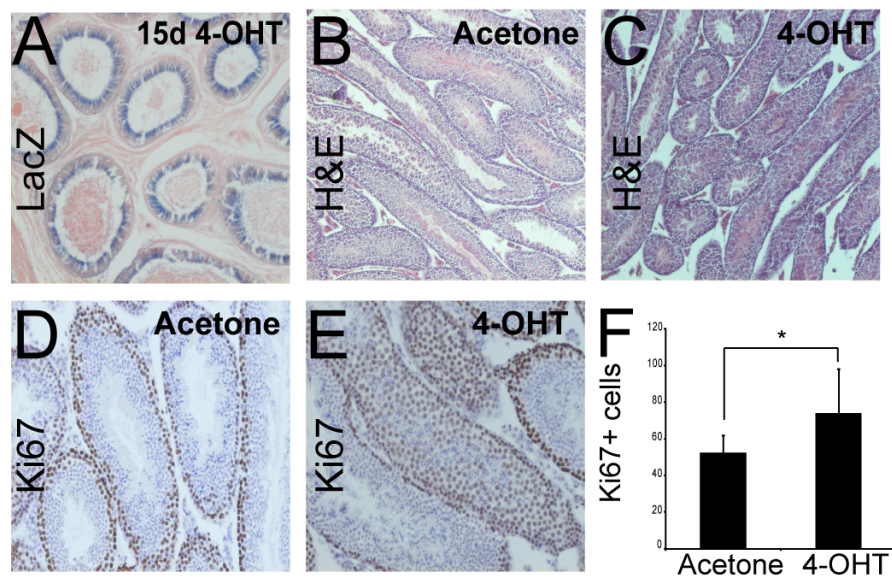
Figure 3.25: Sin3A deletion induces proliferation in testis. Sections of K14ERSin3A$^{\Delta/\Delta}$ testis were compared to acetone-treated control testis. A) LacZ staining indicating Cre-recombinase activity in the testis of R26K14ERLacZ mice B+C) H+E stained testis sections in control and K14ERSin3A$^{\Delta/\Delta}$ mice. D+E) Ki67 staining in testis sections from control and K14ERSin3A$^{\Delta/\Delta}$ mice. F) Quantification of Ki67 positive cells in control and K14ERSin3A$^{\Delta/\Delta}$ testis. A significant increase in Ki67 positive cells in K14ERSin3A$^{\Delta/\Delta}$ testis was observed. Error bars indicate standard deviation (n=5 animals per condition). * p<0.05).
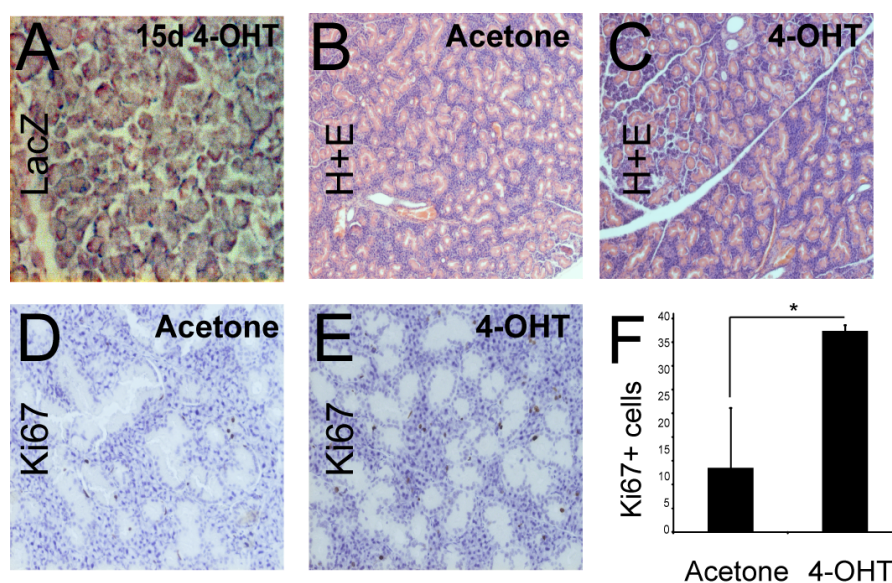
Figure 3.26: Sin3A deletion induces proliferation in salivary glands Sections of K14ERSin3A$^{\Delta/\Delta}$ tsalivary gland were compared to acetone-treated control salivary glands. A) LacZ staining indicating Cre-recombinase activity in the salivary glands of R26K14ERLacZ mice B+C) H&E stained salivary glands sections in control and K14ERSin3A$^{\Delta/\Delta}$ mice. D+E) Ki67 staining in salivary glands sections from control and K14ERSin3A$^{\Delta/\Delta}$ mice. F) Quantification of Ki67 positive cells in control and K14ERSin3A$^{\Delta/\Delta}$ salivary glands. A significant increase in Ki67 positive cells in K14ERSin3A$^{\Delta/\Delta}$ salivary glands was observed. Error bars indicate standard deviation (n=5 animals per condition). * p<0.03).

3.6 Sin3B is dispensable for epidermal homeostasis

Sin3A and Sin3B are the mammalian homologues of the Sin3 gene in yeast and have highly conserved domains for example the HID and PAH domains [Laherty et al., 1997]. As well as sharing homology, the Sin3A and Sin3B complexes share a number of core components, binding partners and gene targets [McDonel et al., 2009]. Due to the similarity between Sin3A and Sin3B, I hypothesised that Sin3B could also have a key role to play in adult skin. To determine the importance of Sin3B in adult skin, I generated the K14ERSin3B$^{F/F}$ mouse line, in which mice expressing CreER under the control of the K14 promoter were crossed with mice harbouring Sin3B floxed alleles. Upon topical application of 4-OHT to the skin of K14ERSin3B$^{F/F}$ mice Sin3B was deleted in undifferentiated epidermal cells, allowing me to begin to understand the nature of Sin3B's role in skin.

Following 28 days of 4-OHT treatment, samples of back skin from K14ERSin3B$^{\Delta/\Delta}$ mice were taken and analysed histologically (Figure 3.27). In this time-frame, no skin phenotype was observed and K14ERSin3B$^{\Delta/\Delta}$ back skin was not distinguishable from back skin from controls (Figure 3.27). This led to the conclusion that although Sin3A is vital for epidermal maintenance, its homologue Sin3B appears to be dispensable for epidermal homeostasis.
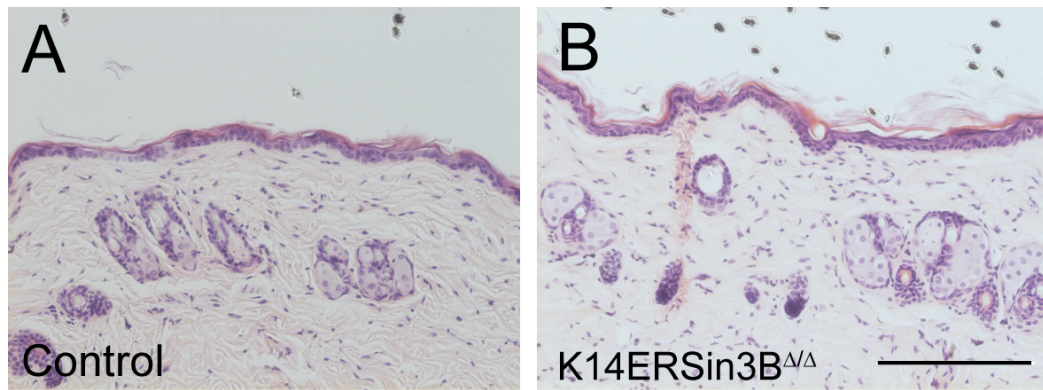
Figure 3.27: Sin3B is dispensable for epidermal homeostasis. K14ERSin3A$^{\text{F/F}}$ back skin was shaved and subsequently treated with acetone or 4-OHT for 28 days. Sectioned back skin samples were stained using H&E. A) Section of control back skin stained using H&E B) Section of K14ERSin3B$^{\Delta/\Delta}$ back skin. Skin from controls and K14ERSin3B$^{\Delta/\Delta}$ are indistinguishable. Scale Bar, 200 μm.

3.7   Summary

To examine whether Sin3A has a role in stem cell homeostasis in the skin I first generated a conditional mouse model in which Sin3A can be inducibly deleted in the hair follicle bulge, which is a well-characterised reservoir for quiescent stem cells [Li and Clevers, 2010]. This was achieved by crossing mice with floxed Sin3A alleles with mice expressing inducible Cre-recombinase under control of the Keratin 19 promoter (K19ERSin3A$^{F/F}$) . Following induction of Sin3A deletion in bulge stem cells via topical application of 4-OHT to the skin, I analysed the impact of Sin3A deletion in this cell population. These initial findings demonstrated that the loss of Sin3A from the quiescent bulge stem cell population does not induce proliferation or apoptosis and K19ERSin3A$^{\Delta/\Delta}$ hair follicles were phenotypically indistinguishable from K19ERSin3A$^{F/F}$ controls. At this stage, it appears that Sin3A is dispensable for bulge stem cell homeostasis.

As stem cells in the bulge region of the hair follicle are well-characterised as a quiescent stem cell population, it may be that Sin3A's functions in preventing excess proliferation are not revealed under normal homeostatic conditions. It may be that the nature of Sin3A's role in this region is revealed when the bulge stem cell population is induced to proliferate. Prior experiments by other research groups have revealed means by which proliferation of bulge stem cells can be induced. For example, it is known that upon wounding of the epidermis, stem cells localised in the hair follicle bulge proliferate and contribute to the wound repair process [Ito et al., 2005] and it is possible that Sin3A could be an important factor in this process. Additionally, application of TPA to the skin is known to induce proliferation in label retaining cells in the bulge region of the hair follicle, leading to a depletion of this cell population [Braun et al., 2003]. Following this protocol and analysing the impact of induction of proliferation in the bulge stem cell population in K19ERSin3A$^{\Delta/\Delta}$ skin would also provide new insights as to Sin3A function in this cell population. In the case that Sin3A is acting to repress genes involved in proliferation in this cell population, it may be that the loss of the label retaining cell population, which corresponds to bulge stem cells is accelerated in the absence of Sin3A.

Further insights into the role of Sin3A could be gained by analysing whether Sin3A is involved in the regulation of the hair cycle. The fact that mice undergo two esssentially synchronised hair cycles [Shimomura and Christiano, 2010] could be utilised to determine whether loss of Sin3A during specific phases of the hair cycle impacts hair cycle synchronisity or progression. Another possibility would be to delete Sin3A during postnatal hair morphogenesis, prior to entry into the hair cycle to determine if hair cycle entry and progression is impacted. Furthermore, since bulge stem cells are specified during embryogenesis [Nowak et al., 2008], inducing Sin3A deletion during embryonic development would reveal insights as to whether Sin3A deletion can lead to a disruption to the bulge stem cell population and hair morphogenesis.

However, at this stage I decided to focus on the role of Sin3A in undifferentiated cells in the basal layer of the epidermis as the use of *in vivo* models in which Sin3A is conditionally deleted yielded some highly interesting results that provide new insights into Sin3A's role in adult skin. Results from experiments using the K14Sin3A line suggest that in similarity to the complete knockout, loss of both alleles of Sin3A in K14-positive cells during embryogenesis leads to embryonic lethality [Cowley et al., 2005; Dannenberg et al., 2005], however, this is likely to be at a later stage than in these studies as K14 only begins to be expressed in the embryo at around E9.75 [Byrne et al., 1994; Lu et al., 2005]. As K14 is expressed in other tissues, such as the liver, as well as skin during embryogenesis, it is possible that Cre recombinase expression and therefore deletion of Sin3A could be occurring in other important tissues. Consequently, embryonic lethality when both alleles of Sin3A are deleted during embryogenesis using the K14Sin3A model could be due to effects in other tissues rather than resutling from a skin-specific defect [Byrne et al., 1994; Lu et al., 2005].

Loss of a single allele of Sin3A in K14-positive cells did not lead to a skin phenotype in adult mice, meaning that I moved on to an inducible system. K14ERSin3A$^{\Delta/\Delta}$ mice exhibited a severe phenotype which presented as skin thickening, excess salivation and an enlarged testis region in comparison to con-

trol mice. In contrast, K14ERSin3B$^{\Delta/\Delta}$ mice exhibited no phenotype, indicating that Sin3B, the paralog of Sin3A in mammalian systems, is not required in adult skin. It is possible that since Sin3A and Sin3B are known to share common targets in other tissues, Sin3A could compensate for the loss of Sin3B in adult skin. Sin3A must have independent roles to Sin3B in this tissue as the loss of Sin3A is not compensated for by Sin3B. These exciting initial results indicated that Sin3A has a key role to play in the epidermis and I further characterised the impact of the loss of Sin3A in skin.

Histological analysis of K14ERSin3A$^{\Delta/\Delta}$ skin showed that loss of Sin3A in adult skin leads to epidermal hyperplasia. I then demonstrated that thickening of the interfollicular epidermis and enlargement of the sebaceous glands was caused by increased proliferation in the absence of Sin3A. This in itself was interesting, as it contrasts results from Sin3A deletion in mouse embryonic fibroblasts, where it results in apoptosis and cell cycle arrest [Cowley et al., 2005; Dannenberg et al., 2005; McDonel et al., 2011]. I determined that this effect was not specific to skin and that Sin3A deletion also led to a promotion of proliferation in other adult tissues:- the testis and salivary glands.

The increase in proliferation in K14ERSin3A$^{\Delta/\Delta}$ skin drives an increase in differentiation. There is an increase in the size of the undifferentiated, basal layer of the interfollicular epidermis and also in the differentiated, suprabasal layers (as shown by markers of the spinous and granular layers). As all layers of the interfollicular epidermis were present and specified in the correct order, these results indicate that Sin3A is not required for the terminal differentiation program to be completed in interfollicular epidermis.

Taken together, results shown in this chapter demonstrate that Sin3A has a key role to play in maintaining balanced epidermal homeostasis. It is clear that in the absence of Sin3A, epidermal homeostasis is disrupted leading to an increase in proliferation and differentiation. Interestingly, the phenotype observed in K14ERSin3A$^{\Delta/\Delta}$skin mirrors that observed in skin in which Myc is overexpressed in K14 positive cells, as shown in the K14MycER mouse model [Arnold

and Watt, 2001; Waikel et al., 2001]. Given that Sin3A can bind to Myc targets at the EDC and the Sin3A complex has a role in transcriptional repression, I hypothesised that Sin3A could antagonise Myc function in the epidermis. If Sin3A's role is to abrogate Myc function via transcriptional repression, the phenotype in K14ERSin3A$^{\Delta/\Delta}$ skin could be driven by aberrant Myc activity. When Sin3A is absent, Myc would be free to bind to its EDC targets, leading to their expression thus driving the phenotype of increased proliferation and differentiation. To begin to determine if this was true, I next decided to analyse Myc activity in K14ERSin3A$^{\Delta/\Delta}$ skin.

Chapter 4

Deletion of Sin3A in adult skin leads to aberrant Myc activity at the EDC

4.1   Sin3A as a repressor of Myc

4.1.1   Myc expression is increased in K14ERSin3A$^{\Delta/\Delta}$ skin

In the previous chapter I demonstrated that the deletion of Sin3A in adult skin leads to an increase in proliferation and differentiation, which is highly similar to the phenotype observed when Myc is over-expressed in adult skin. This similarity and the prior knowledge that Sin3A can bind to Myc's targets at the EDC led to the hypothesis that Sin3A could antagonise Myc function in the epidermis. To test this hypothesis, I first decided to analyse Myc expression in K14ERSin3A$^{\Delta/\Delta}$ skin, with the idea that if Sin3A acts to repress Myc, Myc levels may increase in the epidermis when Sin3A is deleted. Staining for Myc in Wild-type and K14ERSin3A$^{\Delta/\Delta}$ skin revealed that there is an enrichment of nuclear Myc staining in the basal layer of the interfollicular epidermis in the absence of Sin3A expression (Figure 4.1).

It has previously been shown that acetylation of Myc at specific lysine residues by GCN5 and TIP60 increases stability of the Myc protein as well as its transacti-
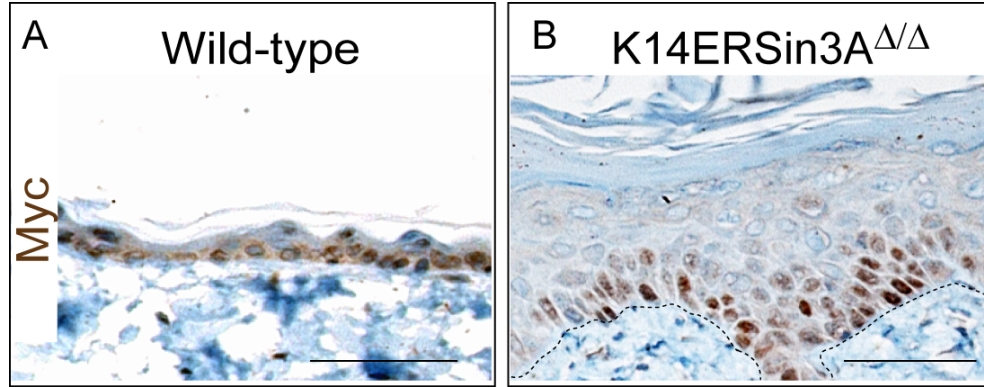
Figure 4.1: Myc expression increases in the absence of Sin3A in adult skin. Sections of skin from 4-OHT-treated Wild-type and K14ERSin3A$^{\Delta/\Delta}$ mice were stained for Myc protein. A) Myc expression in Wild-type skin B) Myc expression in K14ERSin3A$^{\Delta/\Delta}$ skin. There is an enrichment in Myc staining at the basal layer in these mice. Basal layer is indicated by dashed line. Scale Bars, 100 μm.

vation properties [Patel et al., 2004]. As the key enzymatic activity of the Sin3A complex is mediated by histone deacetylases, I hypothesised that the Sin3A complex could potentially deacetylate Myc, leading to a reduction in Myc stability. Conversely, in the absence of Sin3A, Myc acetylation status could increase, leading to an increase in protein stability, which might explain the increase in Myc levels observed in the basal layer of the interfollicular epidermis in K14ERSin3A$^{\Delta/\Delta}$ skin.

To begin to examine whether this is true, I compared the acetylation levels of Myc in epidermal cells isolated from K14ERSin3A$^{F/F}$ mice treated with EtOH (control) or tamoxifen (K14ERSin3A$^{\Delta/\Delta}$) (Figure 4.2). I first confirmed that Sin3A protein is deleted in K14ERSin3A$^{\Delta/\Delta}$ primary keratinocytes (Figure 4.2 top panel). I then performed immunoprecipiation for Myc and then western blots for acetylated-lysine residues and Myc (Figure 4.2 middle and bottom panels). There was an increase in Myc acetylation levels in K14ERSin3A$^{\Delta/\Delta}$ cells relative to control cells (Figure 4.2 middle panels). Using ImageJ, this increase was quantified as a 1.4-fold increase in Myc acetylation relative to total Myc levels in K14ERSin3A$^{\Delta/\Delta}$ cells in comparison to controls. This indicates that an increase in Myc acetylation status and therefore Myc stability could cause an increase in

Myc levels in K14ERSin3A$^{\Delta/\Delta}$ skin.
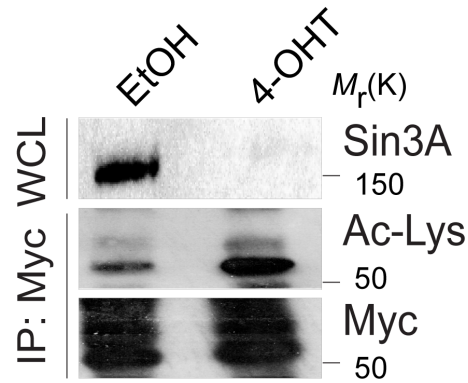
Figure 4.2: Myc acetylation levels increase in the absence of Sin3A. Primary keratinocytes were isolated from K14ERSin3A$^{\text{F/F}}$ and were treated with EtOH (vehicle control) or tamoxifen (K14ERSin3A$^{\Delta/\Delta}$). Protein was isolated from treated cells after 48 hours. Western blotting for Sin3A was performed using the whole cell lysate (WCL) to confirm that Sin3A was deleted in tamoxifen-treated (K14ERSin3A$^{\Delta/\Delta}$) cells (top panel). Western Blots for acetylated lysines (Ac-Lys, middle panel) and total Myc (bottom panel) were generated following immunoprecipitation of Myc.

4.1.2 Sin3A-Myc interaction leads to deacetylation and destabilisation of Myc

To further characterise the relationship between Sin3A and Myc, I tested whether they interact at the protein level. In collaboration with Salvador Aznar Benitah, FLAG-tagged MycER or FLAG-tagged ER constructs were introduced into 293T cells. Following treatment with tamoxifen, it was found via co-immunoprecipitation analysis that Sin3A binds to the FLAG-tagged MycER construct, but not with FLAG-tagged ER construct (Figure 4.3). These results demonstrate that Myc and Sin3A indeed interact *in vitro*. I then wanted to determine if this interaction could lead to Myc deacetylation thus targeting Myc for degradation.
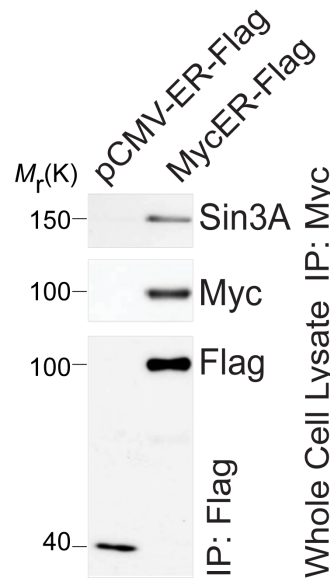
Figure 4.3: Sin3A and Myc interact. Cells expressing Flag-tagged MycER (MycER-Flag) or Flag-tagged-ER (pCMV-ER-Flag) were treated with tamoxifen and protein was isolated. Immunoprecipitation was performed using a Flag antibody and western blots were produced using antibodies for Flag, Myc and Sin3A. Sin3A and Myc co-immunoprecipitate with Flag-tagged MycER, but not Flag-tagged ER only, indicating that Sin3A and Myc interact. See [Nascimento et al., 2011].

4. Deletion of Sin3A in adult skin leads to aberrant Myc activity at the EDC

In collaboration with Shobbir Hussain, I further examined the impact of Sin3A on Myc acetylation and Myc stability. In agreement with prior work described by the McMahon group [Patel et al., 2004], over-expression of the histone acetyl-transferases GCN5 and TIP60 led to an increase in Myc acetylation in comparison to controls (Figure 4.4). In contrast, when Sin3A was over-expressed in conjunction with GCN5 or TIP60, acetylation levels of Myc were decreased, indicating that the Sin3A complex negates histone acetyl-transferase-mediated acetylation of the Myc protein (Figure 4.4). To determine if this effect impacted Myc protein stability, we transfected cells with the same constructs and then inhibited protein translation using cycloheximide (Figure 4.4). As expected, the half-life of Myc is increased when Myc and GCN5 are co-expressed in comparison to when Myc is expressed alone (Figure 4.5 top 3 panels). Interestingly, when Sin3A is over-expressed in conjunction with GCN5, there is a reduction in the half-life of the Myc protein (Figure 4.5 bottom panel). Taken together, these results demonstrate that Sin3A and Myc can interact and that this interaction targets Myc for degradation via de-acetylation of the Myc protein.
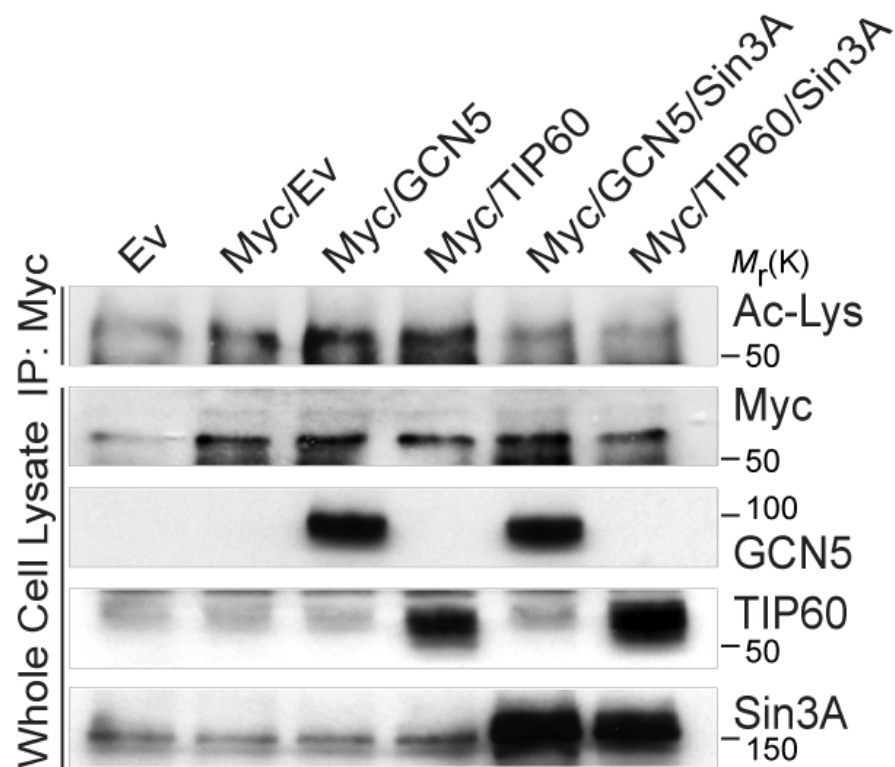
Figure 4.4: Sin3A leads to de-acetylation of Myc. Cells were transfected with the following constructs: Empty Vector (Ev), Myc and empty vector, Myc and GCN5, Myc and TIP60, Myc, GCN5 and Sin3A or Myc GCN5. Protein was extracted and western blots were performed to check protein levels of Myc, GCN5, TIP60 and Sin3A. Myc was immunoprecipitated (IP:Myc) and acetylated-lysine (Ac-Lys) levels were analysed via western blot. Over-expression of Sin3A blocks Myc acetylation mediated by the histone acetyl-transferases GCN5 and TIP60. See [Nascimento et al., 2011].
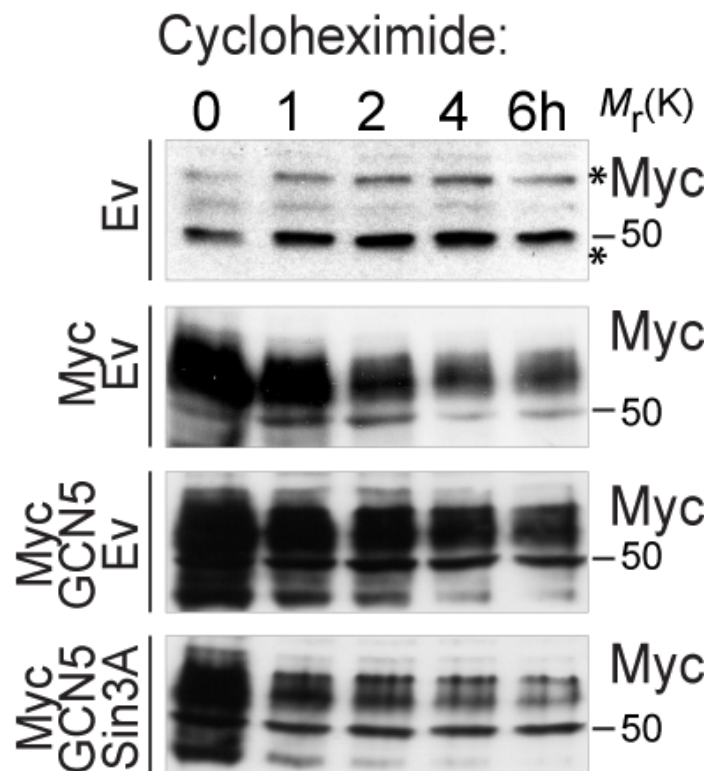
Figure 4.5: Sin3A reduces Myc protein stability. Cells were transfected with the following constructs: Empty Vector (Ev), Myc and empty vector (MycEV), Myc, GCN5 and empy vector (MycGCN5EV) or Myc, GCN5 and Sin3A (MycGCN5Sin3A). Following cycloheximide treatment for the number of hours (h) indicated, protein was extracted and western blots to detect Myc protein levels were performed. Over-expression of Sin3A leads to a reduction of Myc levels over time. Asterisks denote non-specific bands. See [Nascimento et al., 2011].

4.2 Loss of Sin3A leads to abberant Myc activity at the EDC

So far I have shown that in the absence of Sin3A, Myc levels are increased at the basal layer of the interfollicular epidermis due to an increase in Myc acetylation levels and therefore an increase in Myc protein stability. Sin3A can interact with Myc and target Myc protein for degradation, thus antagonising Myc function. Given these results and the fact that Sin3A binds to Myc targets at the EDC in a Wild-type scenario, Sin3A could act to repress Myc and its targets in this situation. In the case that Sin3A is deleted, Myc would be able to bind to its EDC target genes and induce target gene expression. If this was true, aberrant Myc activity might explain the phenotype of enhanced differentiation and proliferation in K14ERSin3A$^{\Delta/\Delta}$ skin. To shed some light on this possibility, I first decided to analyse Myc binding events at EDC genes in the absence of Sin3A in collaboration with Elisabete Nascimento.

In agreement with prior experiments by Elisabete Nascimento, binding of Sin3A to EDC genes was at its highest in Wild-type mice (Figure 4.6A, red bars), absent in K14MycER mice (Figure 4.6B, red bars) and importantly was absent in K14ERSin3A$^{\Delta/\Delta}$ mice. Myc binds to EDC genes in the opposite fashion, with highest occurence of Myc in K14MycER mice (Figure 4.6B, blue bars) and lowest in Wild-type mice (Figure 4.6A, blue bars). The highlight of these experiments was the demonstration that binding of endogenous Myc to the EDC was enriched in K14ERSin3A$^{\Delta/\Delta}$ mice (Figure 4.6C, blue bars). This indicates that in the absence of Sin3A, Myc is free to bind to its EDC target genes. This could explain the increase in differentiation in K14ERSin3A$^{\Delta/\Delta}$ skin. To add evidence to this theory, we next decided to analyse mRNA expression levels of EDC genes in K14ERSin3A$^{\Delta/\Delta}$ mice relative to Wild-type mice to determine if Myc binding to EDC targets influences their expression in these mice.

When Sin3A is depleted, gene expression at EDC target genes is impacted, as demonstrated by differential expression of EDC genes in K14ERSin3A$^{\Delta/\Delta}$ skin relative to Wild-type skin (Figure 4.7, red bars). Remarkably, the fold changes

Figure 4.6: Myc binds EDC targets when Sin3A is deleted from adult skin. A) Binding of Myc (blue bars) and Sin3A (red bars) at EDC target genes in Wild-type skin. B) Binding of Myc (blue bars) and Sin3A (red bars) at EDC target genes in K14MycER skin. C) Binding of Myc (blue bars) and Sin3A (red bars) at EDC target genes in K14ERSin3A$^{\Delta/\Delta}$ skin. Myc binds to its EDC genes in K14ERSin3A$^{\Delta/\Delta}$ skin in a comparable manner to when Myc is over-expressed in the K14MycER mouse model. See [Nascimento et al., 2011].

exhibited in K14ERSin3A$^{\Delta/\Delta}$ skin samples were highly similar to those observed when Myc is over-expressed as shown by expression of EDC genes in K14MycER skin samples (Figure 4.7). These results were highly exciting as they provide the information that when Sin3A is lost in adult skin, not only is Myc occupancy of EDC genes enhanced, gene expression at this locus parallels that seen in K14MycER samples. Thus there is the indication that enhanced differentiation in K14ERSin3A$^{\Delta/\Delta}$ skin appears to be due to the ability of Myc to bind to its EDC targets and impact their expression.

Figure 4.7: Repression of Myc EDC target genes is lost when Sin3A is deleted. mRNA expression levels of EDC genes in K14ERSin3A$^{\Delta/\Delta}$skin relative to Wild-type (WT) mice are denoted by red bars. mRNA expression levels of EDC genes in K14MycER mice relative to Wild-type mice are denoted by blue bars. A comparison between mRNA expression levels of EDC target genes in K14ERSin3A$^{\Delta/\Delta}$ mice and Wild-type mice demonstrates similar changes relative to Wild-type in the two mouse models. See [Nascimento et al., 2011].

4.3   Summary

To build on the results from the previous chapter in which I demonstrated that Sin3A is essential for maintenance of epidermal homeostasis as in its absence there is increased proliferation and differentiation, I further explored Sin3A function in adult skin, particularly in connenction to its relatationship with Myc. Due to the high similarity of the phenotype of K14ERSin3A$^{\Delta/\Delta}$ and K14MycER skin, I considered that Sin3A could normally act to repress Myc and its targets, in particular at the EDC, in adult skin leading to aberrant Myc activity when Sin3A is deleted. I took a number of different approaches to determine if this hypothesis was correct.

I first demonstrated that when Sin3A is lost in adult skin, there is an increase in Myc protein levels in the basal layer of the interfollicular epidermis and that there is an increase in levels of acetylated Myc in K14ERSin3A$^{\Delta/\Delta}$ skin. As previously mentioned, acetylation of Myc by the histone acetyltransferases TIP60 and GCN5 leads to increased stability of the Myc protein, which could explain the enrichment of Myc in K14ERSin3A$^{\Delta/\Delta}$ skin. Theoretically, in a Wild-type scenario, Sin3A could therefore act to block Myc acetylation, as the key enzymatic activity of the Sin3A complex is mediated by histone deactylases. Intriguingly, Sin3A can interact with Myc and when Sin3A is over-expressed, acetylation of Myc protein is decreased, which also leads to a decrease in stability of Myc at the protein level. This is interesting as destabilisation and targeting of Myc for degradation by Sin3A could explain work by Elisabete Nascimento [Nascimento et al., 2011], which demonstrated that Myc is displaced from its EDC target genes in a Wild-type scenario thus allowing Sin3A and associated repressors for example Mxi-1, to bind in Myc's place. This would also fit in with Sin3A's known function as a transcriptional co-repressor.

If Sin3A truly acts to repress Myc and its targets at the EDC, Myc would be free to bind to the EDC and influence target gene expression in K14ERSin3A$^{\Delta/\Delta}$ skin thus explaining the enhancement of differentiation in these mice. I investigated this in conjunction with Elisabete Nascimento by combining ChIP-

chip and gene expression analysis. Results using these approaches demonstrated that in K14ERSin3A$^{\Delta/\Delta}$, Myc binds to its EDC targets and influences EDC target expression in a highly similar manner to that observed in K14MycER skin. These results demonstrated that the differentiation phenotype observed in K14ERSin3A$^{\Delta/\Delta}$ skin is driven by aberrant Myc activity at the EDC, leading to a recapitulation of the K14MycER phenotype. Further evidence has shown that Sin3A and Myc can bind to genes involved in proliferation and cell growth in addition to those genes that act to control epidermal differentiation [Nascimento et al., 2011]. Given these results, it is possible that Myc could also be driving excessive proliferation when Sin3A is deleted in adult skin.

Overall, my results so far demonstrate that Sin3A can act as an antagonist of Myc function in the epidermis as when Sin3A is deleted, there is an increase in Myc protein, enhanced binding of Myc to EDC targets and a de-repression of Myc target genes leading to enhanced differentiation and proliferation. It is interesting to note that recent work by Das and colleagues has demonstrated that Sin3A also acts to oppose Myc function in *Drosophila* [Das et al., 2012]. It is plausible that the opposing functions of Sin3A and Myc must be balanced in order for harmonious epidermal homeostasis to be maintained as disrupting this balance via deleting Sin3A or increasing Myc expression levels leads to divergence from normal proliferation and differentiation levels culminating in epidermal catastrophe. In order to truly demonstrate that the skin phenotype in K14ERSin3A$^{\Delta/\Delta}$ is exclusively driven by erroneous Myc activity, tfurther work was necessary. As such subsequent experiments were focussed on further dissecting the role of relationship between Sin3A and Myc in adult skin.

Chapter 5

Balanced epidermal homeostasis is restored upon deletion of Myc in K14ERSin3A$^{\triangle/\triangle}$ skin

5.1 Concurrent deletion of Sin3A and Myc in adult skin restores epidermal thickness to normal levels

To build on prior results indicating that erroneous Myc activity and expression of its targets leads to the skin phenotype in K14ERSin3A$^{\triangle/\triangle}$ mice, I wanted to determine if Myc is the sole driver behind the phenotype in K14ERSin3A$^{\triangle/\triangle}$ skin. In order to address this, I wanted to delete Myc in K14ERSin3A$^{\triangle/\triangle}$ skin, as if Myc is responsible for the excess proliferation and differentiation in K14ERSin3A$^{\triangle/\triangle}$ skin, deleting Myc should resolve these problems. As such I crossed K14ERSin3A$^{F/F}$ mice with mice harbouring Myc floxed alleles (Myc$^{F/F}$), resulting in the creation of the K14ERSin3A$^{F/F}$Myc$^{F/F}$ line. This enabled me to concurrently delete Sin3A and Myc in adult skin upon topical application of 4-OHT.

5. Balanced epidermal homeostasis is restored upon deletion of Myc in K14ERSin3A$^{\Delta/\Delta}$ skin

As K14ERSin3A$^{\Delta/\Delta}$ mice display epidermal hyperplasia, I first decided to treat the skin of K14ERSin3A$^{F/F}$Myc$^{F/F}$ mice with 4-OHT and analyse the thickness of the skin in comparison to K14ERSin3A$^{\Delta/\Delta}$ skin and relevant controls (Figure 5.1). This would begin to answer the question as to whether Myc is driving the epidermal hyperplasia observed in K14ERSin3A$^{\Delta/\Delta}$ skin. Remarkably, K14ERSin3A$^{\Delta/\Delta}$Myc$^{\Delta/\Delta}$ skin (Figure 5.1B) resembled control skin (Figure 5.1C+D), with comparable epidermal thickness to controls rather than the marked increase in epidermal thickness observed in K14ERSin3A$^{\Delta/\Delta}$ skin (Figure 5.1A). These results further intimated that Myc is the primary force behind the epidermal hyperplasia phenoype observed in K14ERSin3A$^{\Delta/\Delta}$ skin.

I next wanted to confirm that expression of Sin3A and Myc is down-regulated in K14ERSin3A$^{\Delta/\Delta}$Myc$^{\Delta/\Delta}$ skin. I performed qPCR analysis, which confirmed that Myc levels are reduced in K14ERSin3A$^{\Delta/\Delta}$Myc$^{\Delta/\Delta}$ skin in comparison to K14ERSin3A$^{\Delta/\Delta}$ and Sin3A$^{F/F}$Myc$^{F/F}$ controls (Figure 5.2). A reduction in Sin3A expression in K14ERSin3A$^{\Delta/\Delta}$Myc$^{\Delta/\Delta}$ skin relative to Sin3A$^{F/F}$Myc$^{F/F}$ and K14ERSin3A$^{WT/\Delta}$Myc$^{\Delta/\Delta}$ controls was also confirmed by qPCR analysis (Figure 5.3). Complete loss of Sin3A and Myc was not observed as RNA was isolated from whole skin samples whereas Sin3A and Myc expression was only lost in K14-positive cells.

These results confimed that K14ERSin3A$^{\Delta/\Delta}$Myc$^{\Delta/\Delta}$ mice have down-regulation of both Sin3A and Myc and that deletion of Myc in K14ERSin3A$^{\Delta/\Delta}$ skin reverts skin thickness to normal levels. My next experiments were performed to reveal whether deletion of Myc in K14ERSin3A$^{\Delta/\Delta}$ skin also restores proliferation levels to the normal levels observed in controls.
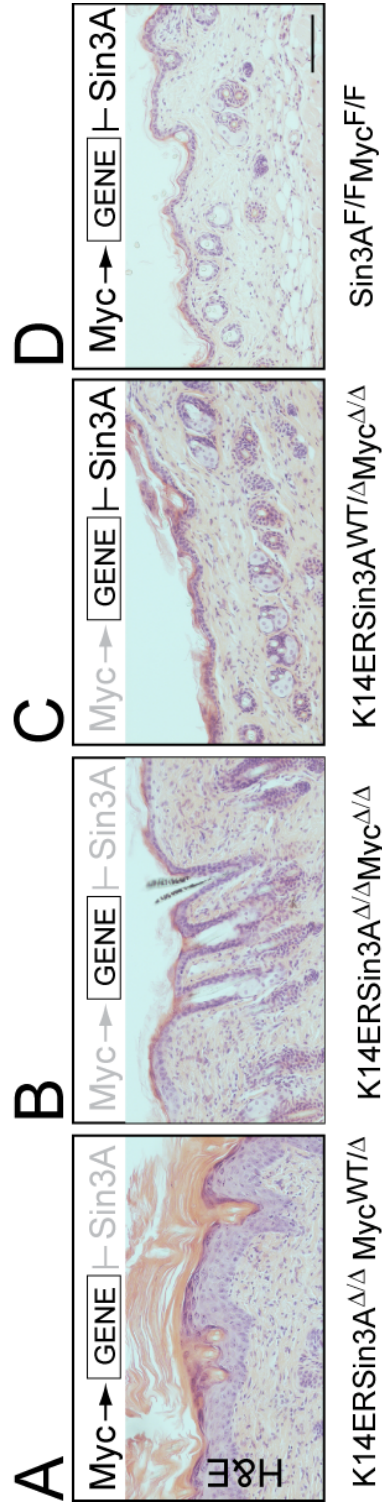
Figure 5.1: Epidermal thickness is comparable to normal in K14ERSin3A$^{\Delta/\Delta}$Myc$^{\Delta/\Delta}$ skin. H&E staining of sections of A) Sin3A deleted skin (K14ERSin3A$^{\Delta/\Delta}$), B) Sin3A and Myc deleted skin (K14ERSin3A$^{\Delta/\Delta}$Myc$^{\Delta/\Delta}$), C) skin with Myc only deleted (K14ERSin3A$^{WT/\Delta}$Myc$^{\Delta/\Delta}$) and D) skin where no Cre-recombinase is expressed (Sin3A$^{F/F}$Myc$^{F/F}$). The upper row indicates the impact of the genotype on Myc or Sin3A gene expression. Scale Bar, 100 μm.
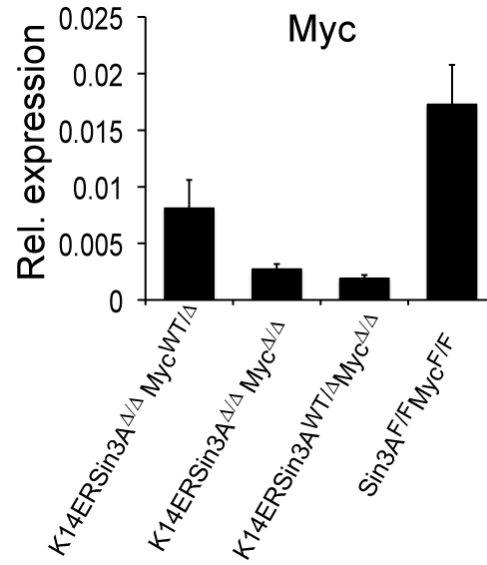
Figure 5.2: Confirmation of Myc down-regulation in K14ERSin3A$^{\Delta/\Delta}$Myc$^{\Delta/\Delta}$ skin. qPCR analysis was performed using RNA from skin samples of the mice indicated to determine Myc expression levels. Myc was significantly down-regulated in K14ERSin3A$^{WT/\Delta}$Myc$^{\Delta/\Delta}$ and K14ERSin3A$^{\Delta/\Delta}$Myc$^{\Delta/\Delta}$ skin in comparison to Sin3A$^{F/F}$Myc$^{F/F}$ skin (P<0.005). Error bars indicate standard deviation (n=3 biological replicates averaged over three technical replicates for each mouse line).
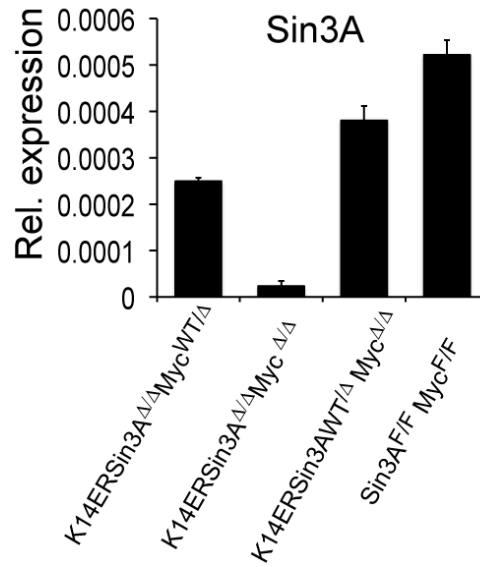
Figure 5.3: **Confirmation of Sin3A down-regulation in K14ERSin3A$^{\Delta/\Delta}$Myc$^{\Delta/\Delta}$ skin**. qPCR analysis was performed using RNA from skin samples of the mice indicated to determine Sin3A expression levels. Sin3A was significantly downregulated in K14ERSin3A$^{\Delta/\Delta}$Myc$^{WT/\Delta}$ and K14ERSin3A$^{\Delta/\Delta}$Myc$^{\Delta/\Delta}$ skin in comparison to Sin3A$^{F/F}$Myc$^{F/F}$ skin (P<0.01). Error bars indicate standard deviation (n=3 biological replicates averaged over three technical replicates for each mouse line).

5.2 Deletion of Myc in K14ERSin3A$^{\Delta/\Delta}$ skin leads to restoration of normal proliferation levels

To examine whether that in addition to epidermal size, proliferation levels were also returned to a normal state in K14ERSin3A$^{\Delta/\Delta}$Myc$^{\Delta/\Delta}$ skin, skin sections from K14ERSin3A$^{\Delta/\Delta}$Myc$^{\Delta/\Delta}$ and control mice were labelled for the proliferation marker, Ki67 (Figure 5.4). Quantification of the number of Ki67 cells in K14ERSin3A$^{\Delta/\Delta}$Myc$^{\Delta/\Delta}$ skin sections was performed and compared to the number of Ki67 positive cells in K14ERSin3A$^{\Delta/\Delta}$, Sin3A$^{F/F}$Myc$^{F/F}$ and K14ERSin3A$^{WT/\Delta}$Myc$^{\Delta/\Delta}$ skin sections (Figure 5.5). The results from this analysis demonstrated that numbers of Ki67-positive cells and therefore levels of proliferation in K14ERSin3A$^{\Delta/\Delta}$Myc$^{\Delta/\Delta}$ skin were strikingly similar to those observed in Sin3A$^{F/F}$Myc$^{F/F}$ and K14ERSin3A$^{WT/\Delta}$Myc$^{\Delta/\Delta}$ control skin samples (Figure 5.4, 5.5). It follows, and was observed, that the number of Ki67 positive cells counted in K14ERSin3A$^{\Delta/\Delta}$Myc$^{\Delta/\Delta}$ skin was significantly lower than those observed in K14ERSin3A$^{\Delta/\Delta}$ skin (Figure 5.4, 5.5). These results indicated that deletion of Myc in skin in which Sin3A is deleted leads to restoration of proliferation to control levels.

I then peformed gene expression analysis of proliferation and cell cycle genes shown to be impacted by Sin3A deletion [Nascimento et al., 2011] (Figure 5.6, 5.7). These experiments and subsequent analysis was carried out in conjunction with Elisabete Nascimento. In agreement with the results shown by Ki67 staining, gene expression levels of proliferation and cell cycle genes were reduced in K14ERSin3A$^{\Delta/\Delta}$Myc$^{\Delta/\Delta}$ skin relative to expression levels in K14ERSin3A$^{\Delta/\Delta}$ skin and much more comparable to Wild-type expression levels (Figure 5.6, 5.7).
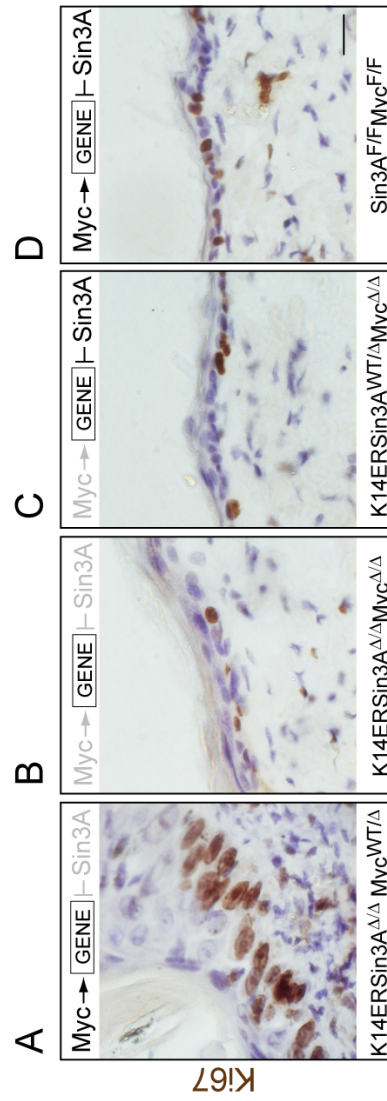
Figure 5.4: Proliferation is comparable to normal levels in K14ERSin3A$^{\Delta/\Delta}$Myc$^{\Delta/\Delta}$ skin. Ki67 staining of sections of A) Sin3A deleted skin (K14ERSin3A$^{\Delta/\Delta}$Myc$^{WT/\Delta}$), B) Sin3A and Myc deleted skin (K14ERSin3A$^{\Delta/\Delta}$Myc$^{\Delta/\Delta}$), C) skin with Myc only deleted (K14ERSin3A$^{WT/\Delta}$Myc$^{\Delta/\Delta}$) and D) skin where no cre recombinase is expressed Sin3A$^{F/F}$Myc$^{F/F}$. The upper row indicates the impact of the genotype on Myc or Sin3A gene expression. Scale Bar, 25 μm.
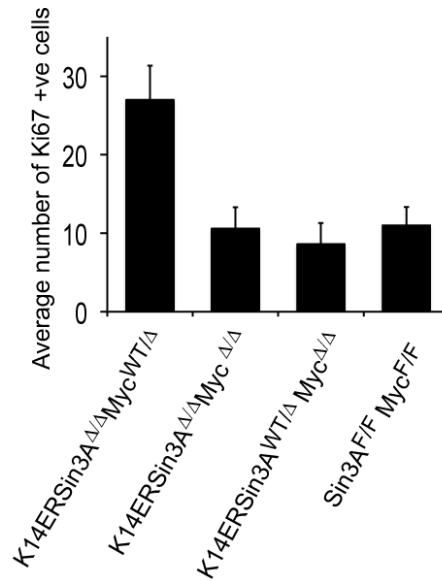
Figure 5.5: Quantification of Ki67-positive cells in 4-OHT-treated skin. The number of Ki67-positive cells in sections of Sin3A deleted skin (K14ERSin3A$^{\Delta/\Delta}$Myc$^{WT/\Delta}$, Sin3A and Myc deleted skin (K14ERSin3A$^{\Delta/\Delta}$Myc$^{\Delta/\Delta}$), Myc only deleted skin (K14ERSin3A$^{WT/\Delta}$Myc$^{\Delta/\Delta}$) and skin where no Cre-recombinase is expressed Sin3A$^{F/F}$Myc$^{F/F}$ were quantified. Numbers of Ki67-positive cells in K14ERSin3A$^{\Delta/\Delta}$Myc$^{\Delta/\Delta}$ skin are comparable to controls (n.s P>0.05) and are significantly lower than in K14ERSin3A$^{\Delta/\Delta}$Myc$^{WT/\Delta}$ skin (P< 0.002). Error bars indicate standard deviation (n=5 animals per mouse line).
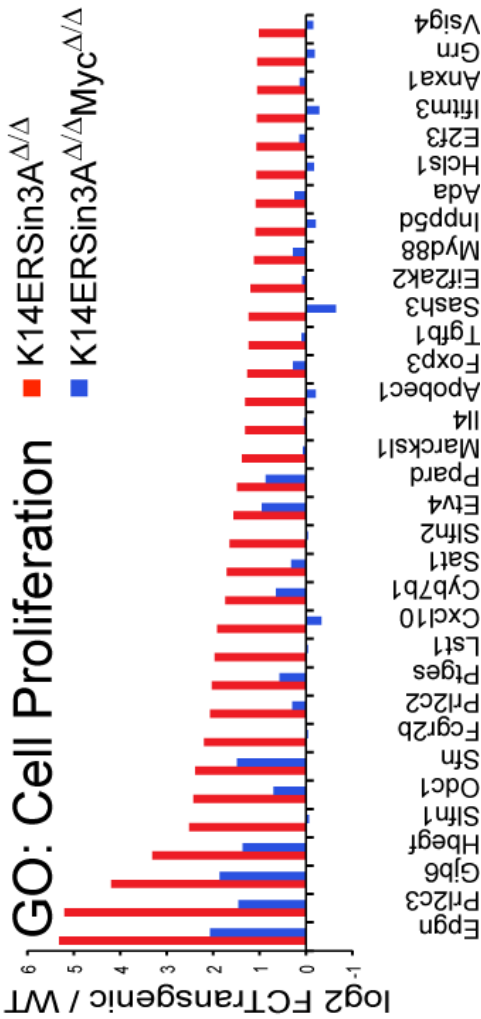
Figure 5.6: Expression levels of proliferation genes are comparable to normal levels when Myc is deleted in K14ERSin3A$^{\Delta/\Delta}$ skin. RNA expression levels of genes categorised as cell proliferation genes was analysed in K14ERSin3A$^{\Delta/\Delta}$ and K14ERSin3A$^{\Delta/\Delta}$Myc$^{\Delta/\Delta}$ skin. Fold change in gene expression of the cell proliferation genes is shown for K14ERSin3A$^{\Delta/\Delta}$ (red bars) and K14ERSin3A$^{\Delta/\Delta}$Myc$^{\Delta/\Delta}$ (blue bars), normalised to Wild-type expression levels. GO=Gene Ontology. See [Nascimento et al., 2011].

Figure 5.7: Expression levels of cell cycle genes are restored to normal when Myc is deleted from K14ERSin3A$^{\Delta/\Delta}$ skin. RNA expression of genes categorised as cell cycle genes via gene ontology (GO) was analysed in K14ERSin3A$^{\Delta/\Delta}$ and K14ERSin3A$^{\Delta/\Delta}$Myc$^{\Delta/\Delta}$ skin. Fold change of gene expression of the cell cycle genes is shown for K14ERSin3A$^{\Delta/\Delta}$ (red bars) and K14ERSin3A$^{\Delta/\Delta}$Myc$^{\Delta/\Delta}$ (blue bars) skin, normalised to Wild-type expression levels. See [Nascimento et al., 2011].

5. Balanced epidermal homeostasis is restored upon deletion of Myc in K14ERSin3A$^{\Delta/\Delta}$ skin

Results from Ki67 staining and gene expression analysis of genes involved in proliferation and cell cycle progression combined demonstrate that proliferation levels are returned to normal when Myc is deleted from K14ERSin3A$^{\Delta/\Delta}$ skin. Since epidermal proliferation as well as the size of the epidermis were returned to normal in K14ERSin3A$^{\Delta/\Delta}$Myc$^{\Delta/\Delta}$ skin, I next wanted to examine whether differentiation was also restored.

5.3 Differentiation is returned to normal levels when Myc is deleted from K14ERSin3A$^{\Delta/\Delta}$ skin.

I have already shown that epidermal thickness and proliferation levels are reduced to normal levels when Myc is depleted from K14ERSin3A$^{\Delta/\Delta}$ skin, but had not yet addressed whether normal differentiation was resumed. To address this, I first decided to analyse expression of EDC genes in K14ERSin3A$^{\Delta/\Delta}$Myc$^{\Delta/\Delta}$ skin and then compare this expression to the pattern of EDC gene expression in K14ERSin3A$^{\Delta/\Delta}$ skin, since I knew that EDC gene expression is perturbed in K14ERSin3A$^{\Delta/\Delta}$ skin. This work was carried out in collaboration with Elisabete Nascimento. Via this analysis, we observed that EDC gene expression, which is disrupted in a similar manner to K14MycER skin in K14ERSin3A$^{\Delta/\Delta}$ skin, is comparable to Wild-type expression levels in K14ERSin3A$^{\Delta/\Delta}$Myc$^{WT/\Delta}$ skin (Figure 5.8).

Leading on from this finding, I decided to analyse the protein expression of markers of both undifferentiated and differentiated layers in sections of K14ERSin3A$^{\Delta/\Delta}$Myc$^{\Delta/\Delta}$ skin, with the aim of establishing whether the balance of undifferentiated and differentiated layers is also returned to normal.

I first decided to analyse expression of markers of the undifferentiated, basal layer of the interfollicular epidermis (Figure 5.9). Examination of the basal markers K14 and Integrin $\alpha6$ expression in sections of K14ERSin3A$^{\Delta/\Delta}$Myc$^{\Delta/\Delta}$ skin showed that undifferentiated layers are returned back to normal and are much more comparable to Wild-type skin in comparison to K14ERSin3A$^{\Delta/\Delta}$Myc$^{WT/\Delta}$ skin (Figure 5.9).
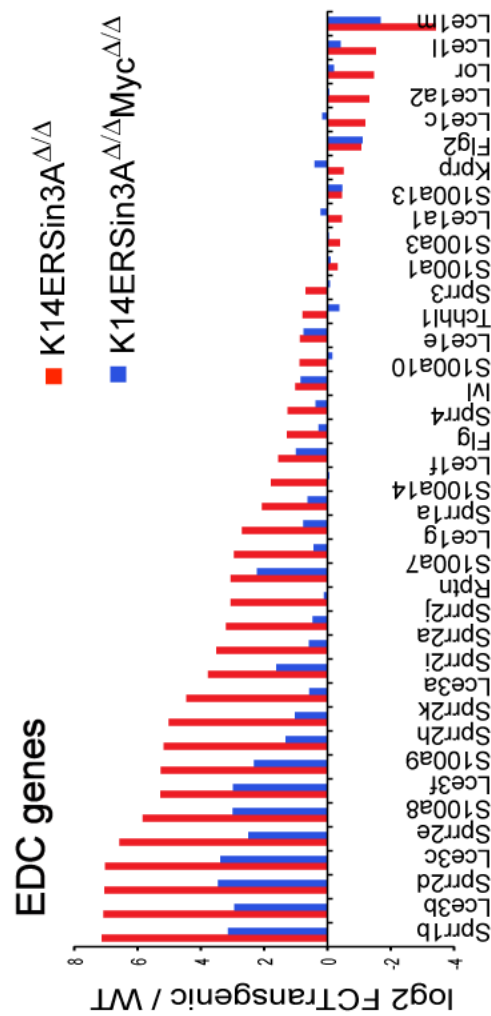
Figure 5.8: Expression levels of EDC genes are comparative to normal when Myc is deleted from K14ERSin3A$^{\Delta/\Delta}$ skin. RNA expression of EDC genes was analysed in K14ERSin3A$^{\Delta/\Delta}$ and K14ERSin3A$^{\Delta/\Delta}$Myc$^{\Delta/\Delta}$ skin. Fold change of gene expression of EDC genes is shown for K14ERSin3A$^{\Delta/\Delta}$ (red bars) and K14ERSin3A$^{\Delta/\Delta}$Myc$^{\Delta/\Delta}$ (blue bars), normalised to Wild-type expression levels. See [Nascimento et al., 2011].
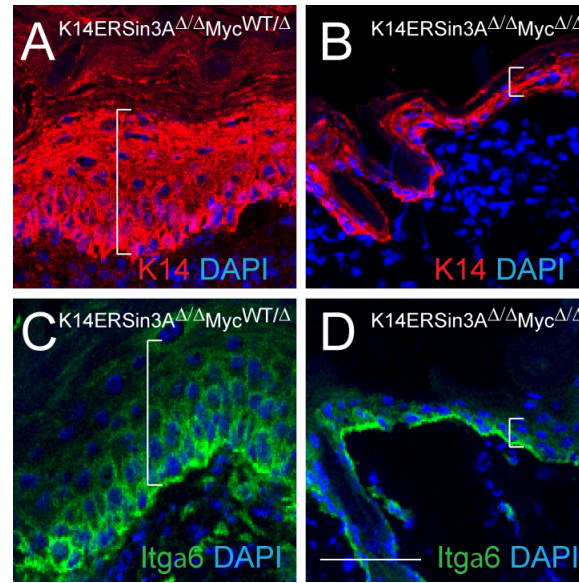
Figure 5.9: Undifferentiated layers are returned to normal when Myc is deleted from K14ERSin3A$^{\Delta/\Delta}$ skin. Sections of 4-OHT-treated A) K14ERSin3A$^{\Delta/\Delta}$MyctextsuperscriptWT/Δ skin or B) K14ERSin3A$^{\Delta/\Delta}$Myc$^{\Delta/\Delta}$ skin labelled with the basal layer marker K14 (K14). Sections of 4-OHT-treated C) K14ERSin3A$^{\Delta/\Delta}$MyctextsuperscriptWT/Δ or D) K14ERSin3A$^{\Delta/\Delta}$Myc$^{\Delta/\Delta}$ skin labelled with the basal layer marker Integrin α6 (Itga6). White bars indicate the thickness of the interfollicular epidermis. Scale Bar, 50μm.

5. Balanced epidermal homeostasis is restored upon deletion of Myc in K14ERSin3A$^{\Delta/\Delta}$ skin

I wanted to determine if deleting Myc in K14ERSin3A$^{\Delta/\Delta}$ skin had the same impact on differentiated layers, therefore I examined expression of markers of the suprabasal layer, K10 and Filaggrin (Figure 5.10). K10-and Filaggrin-expressing layers are reduced to levels comparable to Wild-type in K14ERSin3A$^{\Delta/\Delta}$Myc$^{\Delta/\Delta}$ skin and are much reduced when compared to K14ERSin3A$^{\Delta/\Delta}$Myc$^{WT/\Delta}$ skin, demonstrating that differentiated layers are also returned to normal (Figure 5.10).
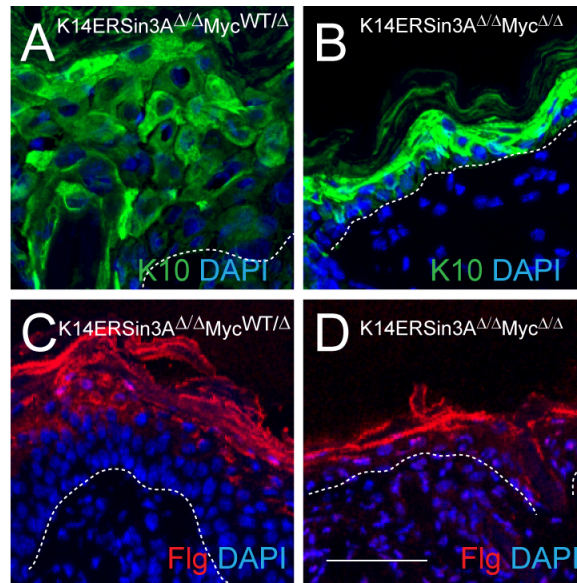
Figure 5.10: Differentiation is returned to normal when Myc is deleted from K14ERSin3A$^{\Delta/\Delta}$ skin. A) Sections of 4-OHT-treated K14ERSin3A$^{\Delta/\Delta}$Myc$^{WT/\Delta}$ skin labelled with the suprabasal marker Keratin10 (K10) B) Sections of 4-OHT-treated K14ERSin3A$^{\Delta/\Delta}$Myc$^{\Delta/\Delta}$ skin labelled with the suprabasal layer marker K10 C) Sections of 4-OHT-treated K14ERSin3A$^{\Delta/\Delta}$Myc$^{WT/\Delta}$ skin labelled with the suprabasal layer marker Filaggrin (Flg) D) Sections of 4-OHT-treated K14ERSin3A$^{\Delta/\Delta}$Myc$^{\Delta/\Delta}$ skin were labelled with the suprabasal layer marker Flg. Dotted white lines indicate the basement membane. Scale Bar, 50 μm.

The results from gene expression analysis and staining for differentiation markers as well as markers for undifferentiated layers intimate that the balance of differentiated and undifferentiated layers observed in K14ERSin3A$^{\Delta/\Delta}$ mice is restored to normal when Myc is also deleted.

5.4 Sin3A and Myc are vital for epidermal homeostasis

I next wanted to determine what the longer term impact of deleting Sin3A and Myc simultaneously has on skin homeostasis. To address this, I topically treated K14Sin3A$^{F/F}$, K14ERSin3A$^{\Delta/\Delta}$, K14ERSin3A$^{\Delta/\Delta}$Myc$^{\Delta/\Delta}$ skin with TPA, which is an agent known to induce epidermal proliferation, thus inducing an increased rate of turnover in the same time period as with topical application of 4-OHT or acetone alone. An increase in epidermal thickness and proliferation was observed in K14Sin3A$^{F/F}$ skin as expected (Figure 5.11A+D), a phenotype which was exacerbated in Sin3A depleted skin (Figure 5.11B+E). However, in TPA-treated K14ERSin3A$^{\Delta/\Delta}$Myc$^{\Delta/\Delta}$ skin , the response to TPA is altered with the outermost layers of the interfollicular epidermis beginning to slough off and a wound-like situation being observed (Figure 5.11C+F). In K14Sin3A$^{F/F}$, K14ERSin3A$^{\Delta/\Delta}$ skin treated with TPA, differentiation can still proceed as shown by labelling for the suprabasal marker Filaggrin (Figure 5.11G+H). In contrast, there is a disruption to Filaggrin-expressing layers when both Sin3A and Myc are depleted (Figure 5.11I). The disruption to K14ERSin3A$^{\Delta/\Delta}$Myc$^{\Delta/\Delta}$ skin homeostasis and lack of induced epidermal hyperplasia does not appear to be due to induced apoptosis, as increased cleaved Caspase 3 is not detected (Figure 5.11L).

Challenging epidermal homeostasis in K14ERSin3A$^{\Delta/\Delta}$Myc$^{\Delta/\Delta}$ skin via induction of proliferation using topical application of TPA has shown that although deletion of Myc and Sin3A reverts the proliferation and differentiation phenotype observed when Sin3A alone is depleted, the epidermis is not entirely normal. These results reinforce the hypothesis that the balanced expression of Myc and Sin3A and consequently their targets is absolutely required and that these two factors are highly important in skin maintenance.
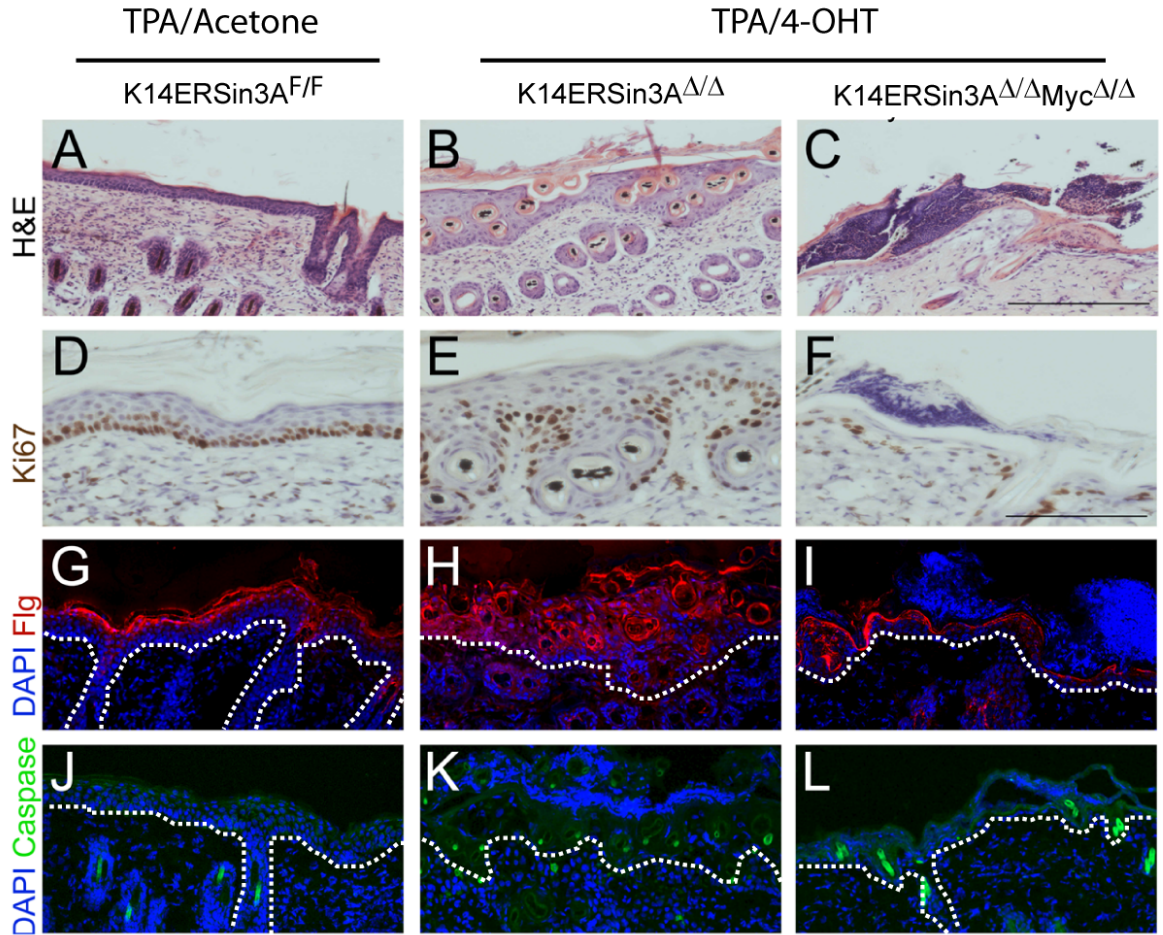
Figure 5.11: TPA-induced proliferation disrupts K14ERSin3A$^{\Delta/\Delta}$Myc$^{\Delta/\Delta}$ skin homeostasis. H&E-stained sections of TPA-treated A) K14ERSin3A$^{F/F}$, B) K14ERSin3A$^{\Delta/\Delta}$ and C) K14ERSin3A$^{\Delta/\Delta}$Myc$^{\Delta/\Delta}$ skin. Ki67-labelled TPA-treated D) K14ERSin3A$^{F/F}$ skin, E) K14ERSin3A$^{\Delta/\Delta}$ skin and F) K14ERSin3A$^{\Delta/\Delta}$Myc$^{\Delta/\Delta}$. Skin sections from TPA-treated G) K14ERSin3A$^{F/F}$ skin, H) K14ERSin3A$^{\Delta/\Delta}$ skin and I) K14ERSin3A$^{\Delta/\Delta}$Myc$^{\Delta/\Delta}$ skin labelled for the differentiation marker Filaggrin (Flg, red), counter-stained with DAPI (blue). Skin sections from TPA-treated J) K14ERSin3A$^{F/F}$, K) K14ERSin3A$^{\Delta/\Delta}$ and L) K14ERSin3A$^{\Delta/\Delta}$Myc$^{\Delta/\Delta}$ skin labelled for the apoptosis marker cleaved Caspase 3 (Caspase, green), counter-stained with DAPI (blue). Scale Bars , 100 μm. Dashed white lines indicate the basal layer of the IFE.

5.5   Summary

Throughout this chapter I have aimed to determine that Myc is the primary driver behind the phenotype of enhanced differentiation and proliferation in Sin3A-depleted skin. I had previously shown that in the absence of Sin3A, Myc can bind to its EDC genes, resulting in enhanced expression of these targets. Further evidence suggested that Myc could also be the cause behind the push towards proliferation in the absence of Sin3A in the epidermis. My approach to determine whether errant Myc activity is truly the cause of the K14ERSin3A$^{\Delta/\Delta}$ phenotype was to use a mouse model in which we could delete Myc as well as Sin3A in the epidermis. This approach was fruitful and yielded some highly exciting results.

Deletion of Myc in K14ERSin3A$^{\Delta/\Delta}$ skin led to a dramatic rescue of the skin phenotype observed, with epidermal thickness returning to normal levels. As shown by examination of gene expression at the RNA level, levels of expression of genes involved in proliferation and the cell cycle are reduced and there is a remarkable reduction of proliferation, as demonstrated by Ki67 quantification, in K14ERSin3A$^{\Delta/\Delta}$Myc$^{\Delta/\Delta}$ skin relative to K14ERSin3A$^{\Delta/\Delta}$ skin. Moreover, examination of differentiation markers indicated that the balance between differentiated and undifferentiated layers was returned to normality in K14ERSin3A$^{\Delta/\Delta}$Myc$^{\Delta/\Delta}$ skin. These results were particularly important as they show that when Myc is removed from K14ERSin3A$^{\Delta/\Delta}$ skin, the skin phenotype of excess proliferation and enhanced differentiation is no longer present.

Given that I have shown that balanced Sin3A and Myc activity is essential for the mainteance of epidermal homeostasis, it was somewhat surprising that deletion of both of these key factors simultaneously produced a relatively normal epidermis. However, the results that we were obtained were limited to the analysis of short-term homeostasis. In order to examine the longer-term impacts of loss of Sin3A and Myc, I decided to challenge the system to proliferate excessively via the topical application of TPA, K14ERSin3A$^{\Delta/\Delta}$Myc$^{\Delta/\Delta}$ skin, which is known to induce hyperplasia. In this scenario, the skin from K14ERSin3A$^{\Delta/\Delta}$Myc$^{\Delta/\Delta}$ skin is not normal and the system cannot cope, thus demonstrating the importance

of the presence of Sin3A and Myc to maintain the epidermis.

The implications of these results is that Myc is the cause of the phenotype in skin in which Sin3A is absent and that a balance of Sin3A and Myc is required for harmonious epidermal homeostasis. The results indicate that although Sin3A is dispensable for terminal differentiation, Sin3A acts to antagonise Myc function and can inhibit Myc-mediated activity thus preventing excess proliferation and differentiation from occurring. Sin3A and Myc share target genes, but their roles are antagonistic, meaning that levels of Sin3A and Myc must be balanced (Figure 5.12). A perturbation of Sin3A or Myc expression leads to disruption of the careful balance between cell-loss and cell-division that is vital for maintaining homeostasis and a functional tissue. It follows that the opposing effects of Myc and Sin3A on gene transcription are essential to maintain epidermal homeostasis.
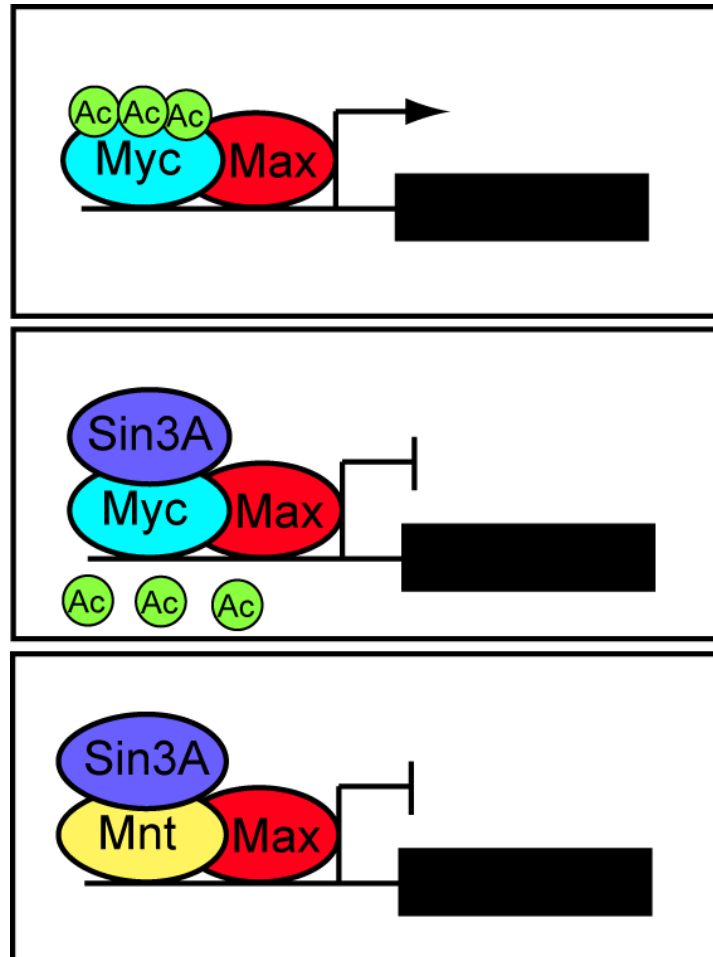
Figure 5.12: Opposing roles of Sin3A and Myc at their target genes. Upper panel: When Myc binds to its target genes in the skin with its obligate binding partner Max, gene expression is induced. Middle panel: Acetylation of the Myc protein enhances its stability. Sin3A can lead to the deacetylation of the Myc protein, decreasing its stability and targeting the Myc protein for degradation. The exact mechanism of degradation needs further investigation to be determined. This would ultimately lead to the repression of shared target genes. Lower Panel: Sin3A itself has no intrinsic DNA binding activity and so would be recruited to the DNA of target genes by specific transcription factors e.g. the Myc antagonist Mnt, to mediate gene repression. The opposing activities of Myc (gene activation) and Sin3A (gene repression) must be carefully balanced to avoid disruption of tissue homeostasis. For example, when Sin3A expression is lost in skin, Myc is erroneously active leading to excess proliferation and differentiation.

Chapter 6

Sin3A and tumour susceptibility in skin

6.1 Sin3A and tumour susceptibility in skin: short term pilot experiments

As demonstrated in my results so far, a major phenotype when Sin3A expression is lost from the interfollicular epidermis is excessive proliferation and prior studies implicated Sin3A as a potential tumour supressor [Suzuki et al., 2008]. These findings and the knowledge that Sin3A is recruited by known tumour suppressors to mediate their function [Goeman et al., 2005; Rampalli et al., 2005], prompted me to investigate whether Sin3A influences susceptibility to tumourigenesis in skin. Since K14ERSin3A$^{\Delta/\Delta}$ mice have to be sacrificed after 15 days of treatment with 4-OHT due to ill health, this mouse model was not suitable for analysis of tumour generation. It has been previously demonstrated that loss of a single allele of Sin3A is sufficient to increase susceptibility to tumor formation in other tissues, for example with non small cell lung cancer [Suzuki et al., 2008], therefore I decided to utilise the K14Sin3A$^{WT/\Delta}$ mouse model in pilot experiments in order to examine the role of Sin3A in skin tumour susceptibility.

It is known that short term exposure of skin to UVB radiation induces skin reddening or sunburn [Matsumura and Ananthaswamy, 2004]. UVB radiation

comprises the wavelengths 280-320nm of the solar spectrum and is absorbed into the skin [Matsumura and Ananthaswamy, 2004]. The response of the epidermis to a single dose of UVB radiation is well established and is schematically represented in Figure 6.1. As such, I decided to perform a pilot experiment to determine whether the loss of a single allele of Sin3A impacts how the epidermis reacts following short term exposure to UVB radiation (Figure 6.1).

To analyse the skin of K14Sin3A$^{\text{WT}/\Delta}$ following UVB irradiation, I first performed histological analyses on skin sections obtained 24 or 48 hours after UVB treatment (Figures 6.2, 6.3). The results from this analysis were highly interesting as the thickness of the interfollicular epidermis of K14Sin3A$^{\text{WT}/\Delta}$ skin (Figure 6.2C) was markedly increased in comparison to the interfollicular epidermis of control skin collected 24 hours after exposure to UVB radiation (Figure 6.2B) as well as K14Sin3A$^{\text{WT}/\Delta}$ skin that has not been irradiated (Figure 6.2A). This finding was particularly exciting as it appears that the phenotype of epidermal hyperplasia observed in K14ERSin3A$^{\Delta/\Delta}$ skin is recapitulated. By 48 hours post-UVB irradiation, the interfollicular epidermis in K14Sin3A$^{\text{WT}/\Delta}$ skin (Figure 6.3C) is still thicker than irradiated control skin (Figure 6.3B) although the difference is less stark.
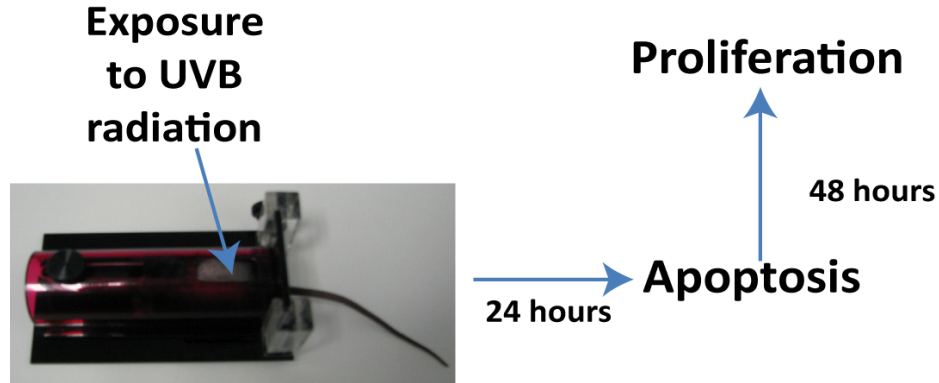
Figure 6.1: Schematic representation of short-term UVB exposure experiment. Mice were restrained as shown and exposed to one dose of UVB radiation. Protective restraints are necessary to provide protection against damage to the eyes and ears by the UVB radiation [Workman et al., 2010]. Dorsal skin was collected after 24 hours or 48 hours post-UV treatment. The standard response of skin to one exposure of UVB radiation is well characterised. 24 hours post-exposure, apoptosis is at its highest while after 48 hours proliferation is induced to replace those cells that have been lost through apoptosis [Ouhtit et al., 2000].
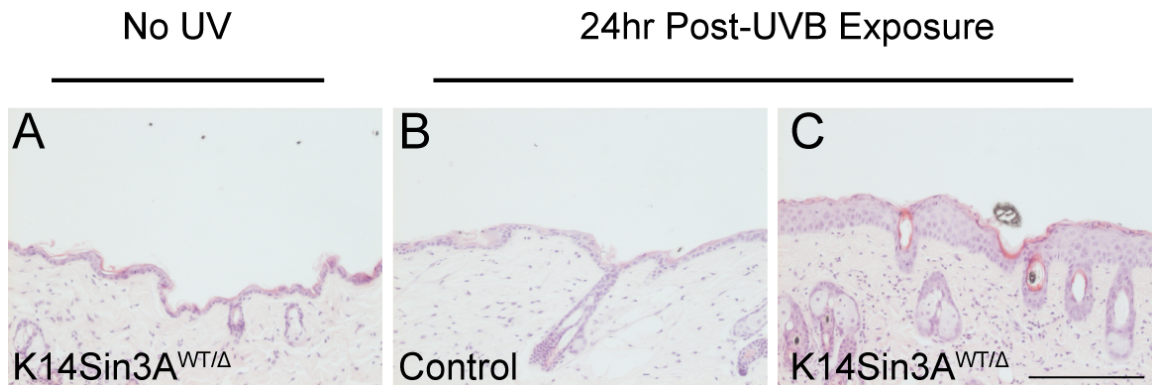
Figure 6.2: Impact of loss of a single Sin3A allele in skin 24 hours after UV irradiation. Mice were exposed to one dose of UVB radiation. Dorsal skin was collected 24 hours (hr) post-exposure and was subsequently sectioned. Skin sections from A) K14Sin3A$^{WT/\Delta}$ mice not exposed to UVB, B) Control mice exposed to UVB radiation and C) K14Sin3A$^{WT/\Delta}$ mice exposed to UVB radiation were stained for histological analysis using standard H&E staining. Scale bar, 200μm.
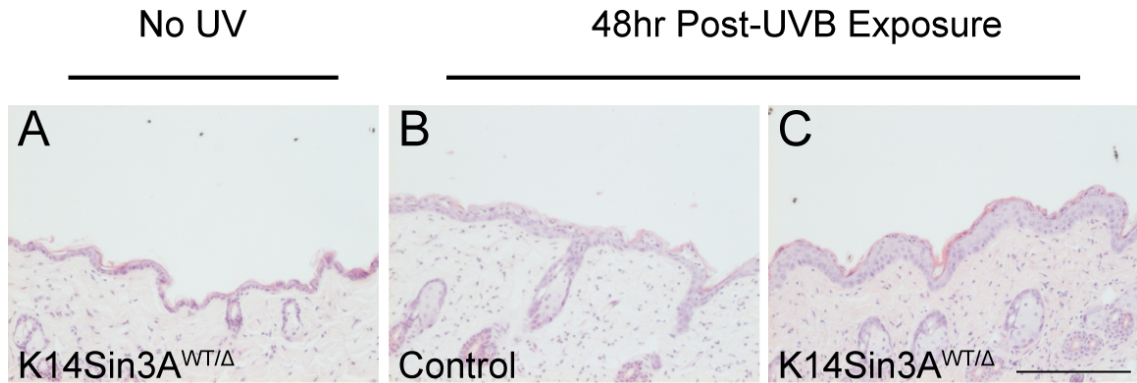
Figure 6.3: Impact of loss of a single Sin3A allele in skin 48 hours after UV irradiation. Mice were exposed to one dose of UVB radiation and dorsal skin was collected 48 hours (hr) post-exposure. Skin samples were subsequently sectioned. Skin sections from A) K14Sin3A$^{WT/\Delta}$ mice not exposed to UVB, B) Control mice exposed to UVB radiation and C) K14Sin3A$^{WT/\Delta}$ mice exposed to UVB radiation were stained for histological analysis using standard H&E staining. Scale bar, 200 μm.

I next determined if this increase in thickness of the interfollicular epidermis in irradiated K14Sin3A$^{WT/\Delta}$ skin in comparison to control irradiated skin is due to an alteration in the induction of proliferation in this region. To this end I labelled sections of control irradiated skin or K14Sin3A$^{WT/\Delta}$ skin, collected 24 or 48 hours post-exposure to UVB radiation, with the proliferation maker Ki67 (Figure 6.4). As expected, the number of Ki67-positive cells, and thus levels of proliferation, in the interfollicular epidermis of control skin collected 24 hours post-irradiation is low (Figure 6.4 upper left panel), as apoptosis peaks at this time point (Figure 6.1). The average number of Ki67-positive cells is significantly increased in the interfollicular epidermis of K14Sin3A$^{WT/\Delta}$ skin, collected at the same point (Figures 6.4 upper right panel, 6.5), indicating that proliferation is possibly induced erroneously. Levels of Ki67-positive cells are comparable between control and K14Sin3A$^{WT/\Delta}$ irradiated skin collected 48 hours post-exposure (Figures 6.4 lower panels, 6.5). It is well characterised that proliferation peaks 48 hours post-exposure to a single dose of UVB radiation (Figure 6.1), so the increase in proliferation in control skin at this time point was expected. It is interesting that the levels of proliferation in K14Sin3A$^{WT/\Delta}$ irradiated skin are consistent at 24 hours and 48 hours post-exposure and differs from the normal response of skin

to UVB irradiation (Figures 6.4 right hand panels, 6.5).

Figure 6.4: Impact of loss of a single Sin3A allele on proliferation in UVB irradiated skin. Mice were exposed to one dose of UVB radiation. Dorsal skin was collected either 24 hours (upper panels) or 48 hours (lower panels) post-exposure and was subsequently sectioned. Skin sections from control (K14Sin3A$^{WT/WT}$) mice (left panels) and K14Sin3A$^{WT/\Delta}$ mice (right panels) exposed to UVB were stained for the proliferation marker Ki67. Dashed lines outline the basal layer of the interfollicular epidermis. Scale bar, 50 μm.
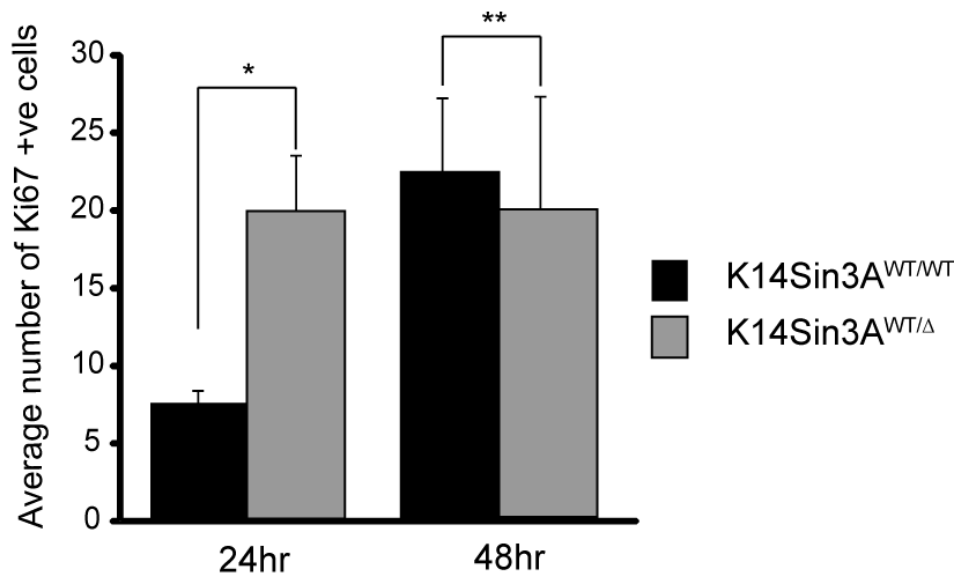
Figure 6.5: Quantification of Ki67-positive cells in UVB irradiated skin. The average number of Ki67-positive (+ve) cells was quantified in sections of dorsal skin collected from control (K14Sin3A$^{WT/WT}$) or K14Sin3A$^{WT/\Delta}$ mice either 24 hours (24hr) or 48 hours (48hr) post-exposure to a single dose of UVB radiation. Error bars represent standard deviation (n=5 biological replicates per mouse line for each time point). * p<0.0001 ** p>0.05.

As the UV response in K14Sin3A$^{WT/\Delta}$ skin appears to be altered in terms of increased thickness of the interfollicular epidermis and enhanced proliferation 24 hours post-exposure to UVB irradiation, I also decided to assess the impact on induction of p53 following UVB irradiation. It is known that p53 is induced as a consequence of UV radiation in the skin and is important in UVB irradiation-induced apoptosis [Hildesheim et al., 2002; Kulms and Schwarz, 2000]. Additionally, levels of apoptosis and correspondingly p53 peak at 24 hours post-irradiation (Figure 6.1). As such, I labelled skin sections collected from control and K14Sin3A$^{WT/\Delta}$ skin either 24 or 48 hours post-irradiation using a p53 antibody (Figure 6.6).

As expected, control skin collected 24 hours post-UVB irradiation exhibited high levels of p53-positive cells (Figure 6.6 upper left panel). However, the number of p53-positive cells detected in the interfollicular epidermis of K14Sin3A$^{WT/\Delta}$ skin collected 24 hours post-UVB irradiation (Figure 6.6 upper right panel) was markedly reduced in comparison to control skin at this point (Figure 6.7). This suggests that p53 induction after UVB irradiation of K14Sin3A$^{WT/\Delta}$ skin is impaired when compared to control samples. I also examined skin collected from control skin and K14Sin3A$^{WT/\Delta}$ 48 hours post-UVB irradiation that was labelled for p53 (Figure 6.6 lower panels). As anticipated, levels of p53 in control skin collected at the 48 hour time point (Figure 6.6 lower left panel) were much reduced at this time point in comparison to at the 24 hour time point (Figures 6.6 upper left panel, 6.7). In contrast, levels of p53-expressing cells in K14Sin3A$^{WT/\Delta}$ skin were comparable at the 24 hour and 48 hour time points (Figures 6.6 right panels, 6.7). At the 48 hour time point there was a significantly higher number of p53 positive cells in K14Sin3A$^{WT/\Delta}$ interfollicular epidermis in comparison to controls (Figures 6.6 lower panels, 6.7), further indicating that the loss of a single allele of Sin3A is sufficient to cause abnormalities in UVB irradiated skin.

Taken together, these results imply that the response to short-term UV radiation exposure is defective in K14Sin3A$^{WT/\Delta}$ mice in comparison to control mice. The induction of p53 in K14Sin3A$^{WT/\Delta}$ skin is markedly reduced while proliferation appears to peak at an earlier stage than in control skin. The phenotype of epidermal hyperplasia post UV-irradiation is remarkably similar to that observed in
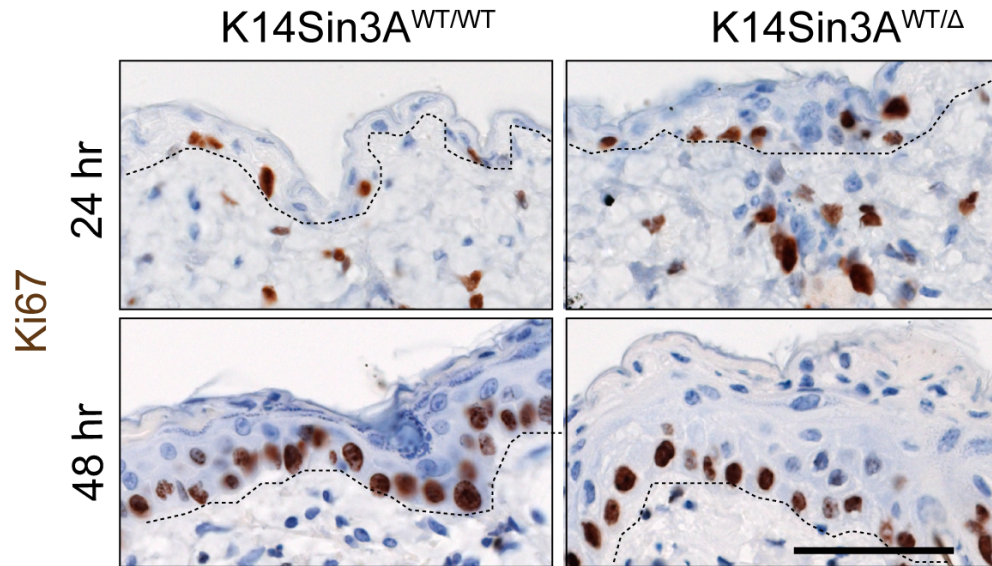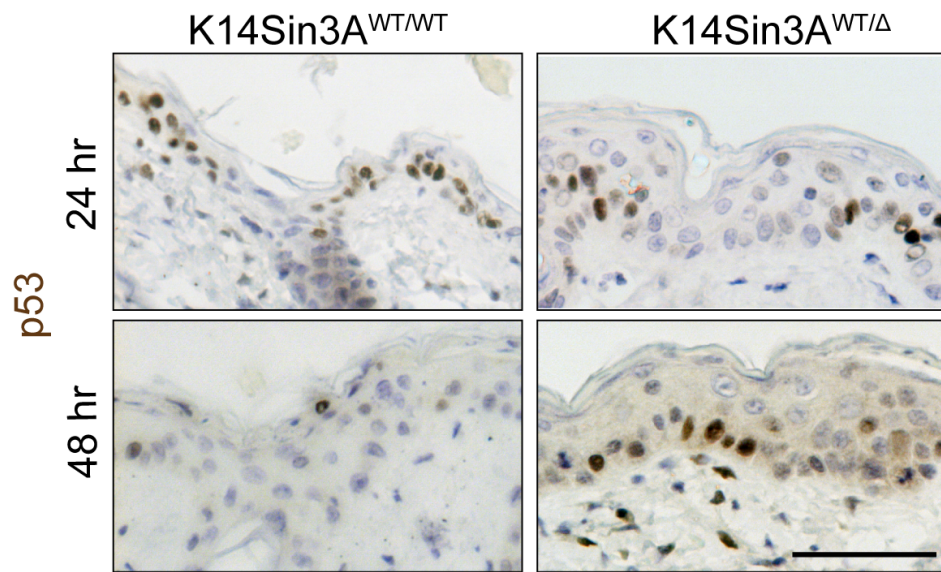
Figure 6.6: Impact of loss of a single Sin3A allele on p53 induction in skin post-UVB irradiation. Mice were exposed to one dose of UVB radiation. Dorsal skin was collected either 24 hours (upper panels) or 48 hours (lower panels) post-exposure and was subsequently sectioned. Skin sections from control (K14Sin3A$^{\mathrm{WT/WT}}$) mice (left panels) and K14Sin3A$^{\mathrm{WT/\Delta}}$ mice (right panels) exposed to UVB were stained using a p53 antibody. Scale bar, 50 μm.
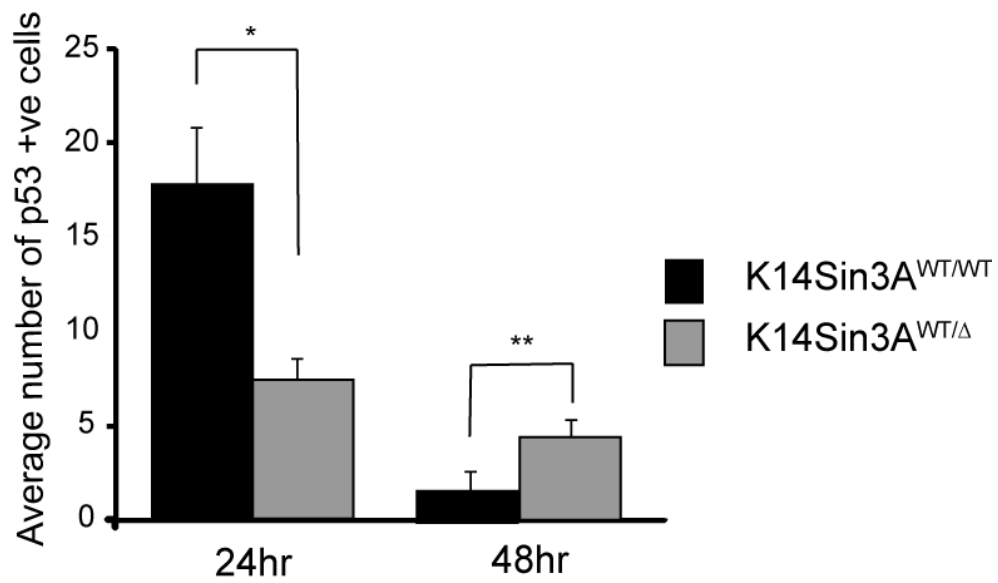
Figure 6.7: Quantification of p53-positive cells in UVB irradiated skin. The average number of p53-positive (+ve) cells was quantified in sections of dorsal skin collected from control (K14Sin3A$^{WT/WT}$) or K14Sin3A$^{WT/\Delta}$ mice either 24 hours (24hr) or 48 hours (48hr) post-exposure to a single dose of UVB radiation. Error bars represent standard deviation (n=5 biological replicates per mouse line for each time point). * p<0.0001 ** p<0.002.

K14ERSin3A$^{\Delta/\Delta}$ skin. As a phenotype was observed at this time point, I decided to examine the impact of long term exposure to UVB radiation on K14Sin3A$^{\text{WT}/\Delta}$ skin.

6.2 Sin3A and tumour susceptibility in skin: long term pilot experiments

It is well established that long-term exposure of mouse skin to UVB radiation leads to the generation of skin cancer [Berg et al., 1996]. Consequently I decided to perform pilot experiments to begin to establish whether there is a difference in tumour development in the skin of K14Sin3A$^{WT/\Delta}$ mice in comparison to skin of control mice. I aimed to expose the back skin of control and K14Sin3A$^{WT/\Delta}$ mice to UVB radiation over a time period of up to 30 weeks in order to induce tumour formation. The experimental design is represented schematically in Figure 6.8. However, in practice, a number of problems with this approach came to light. Due to negative impacts on animal welfare caused by the use of restraints, the length of time between UVB treatment was increased as advised by a veterinarian. At 25 weeks due to adverse effects unrelated to the UVB irradiation, a number of mice had to be culled, therefore I analysed the skin at this time point instead.

Dorsal skin obtained from control and K14Sin3A$^{WT/\Delta}$ mice after 25 weeks of exposure to UVB radiation was sectioned and then stained using H&E (Figure 6.9). No skin tumours were observed in either control or K14Sin3A$^{WT/\Delta}$ skin at this time point. The interfollicular epidermis of K14Sin3A$^{WT/\Delta}$ skin (Figure 6.9B) was increased in thickness in comparison to control skin (Figure 6.9A). This increase in thickness of the interfollicular epidermis coincided with a significant increase in the average number of Ki67-positive cells in K14Sin3A$^{WT/\Delta}$ interfollicular epidermis (Figure 6.10B) in comparison to control interfollicular epidermis (Figure6.10A+E). Finally, there is a decrease in the average number of p53-positive cells in K14Sin3A$^{WT/\Delta}$ interfollicular epidermis (Figure 6.10D) in comparison to those observed in control interfollicular epidermis (Figure 6.10C+F).
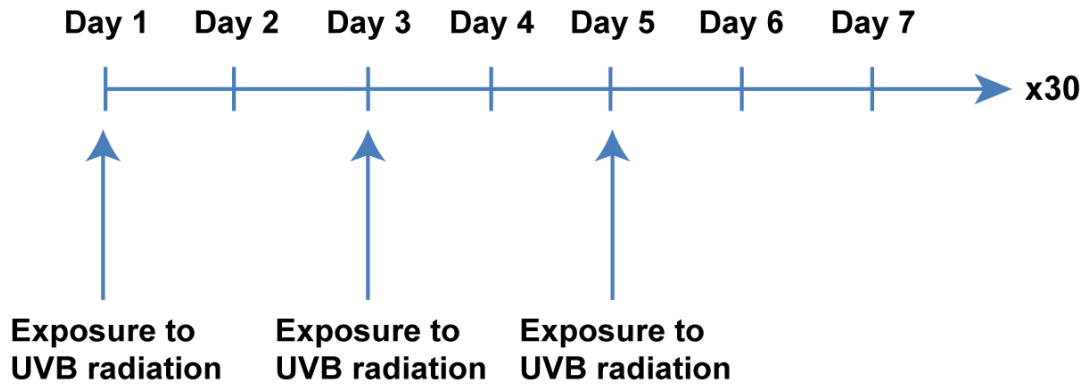
Figure 6.8: Schematic representation of experimental design using long-term UVB exposure. To assess the impact of loss of a single allele of Sin3A on tumour susceptibility in skin, I designed a pilot experiment in which mice would be exposed to one dose of UVB radiation, three times a week for up to 30 weeks.
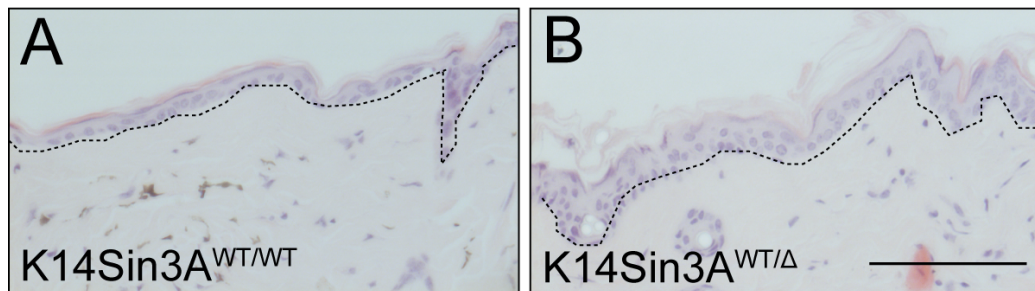
Figure 6.9: Impact of loss of a single Sin3A allele on skin subjected to long-term UVB exposure. Dorsal skin was collected from mice exposed to UVB radiation over a 25 week period. Skin sections from A) control (K14Sin3A$^{\text{WT/WT}}$ mice and B) K14Sin3A$^{\text{WT/}\Delta}$ skin were stained using H&E. Dashed lines outline the interfollicular epidermis. Scale bar, 100 μm.
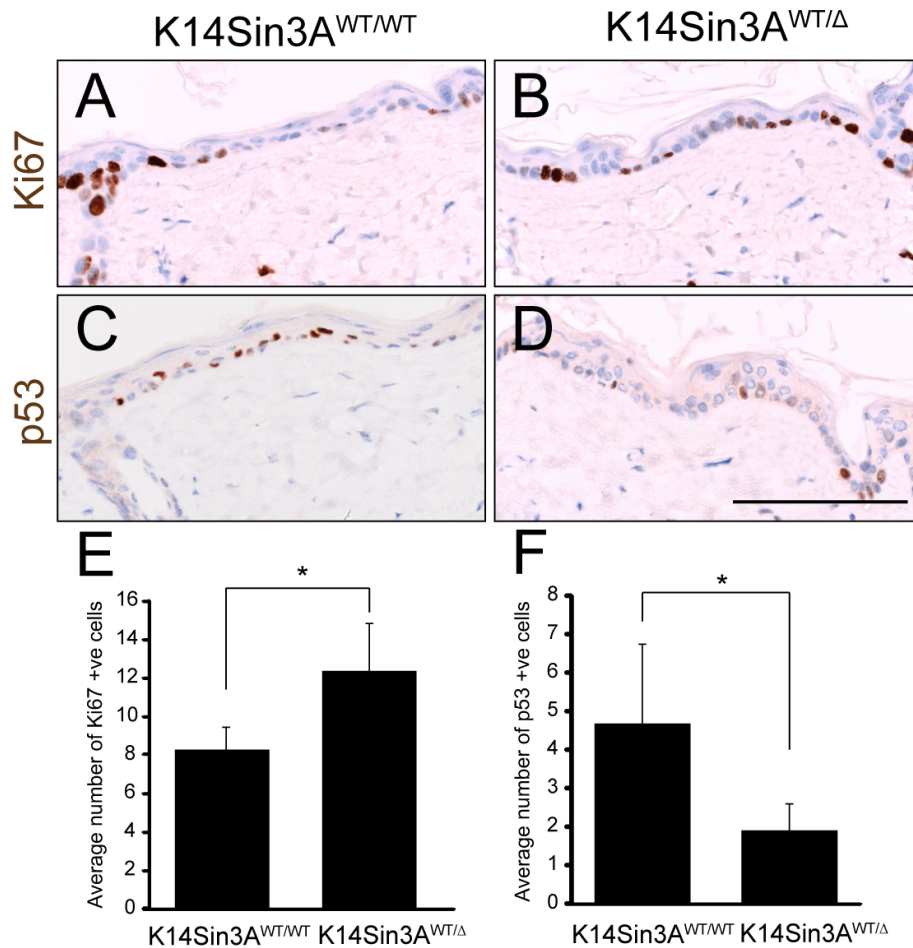
Figure 6.10: Impact of loss of a single Sin3A allele on levels of proliferation and p53 in UVB-irradiated skin. Dorsal skin was collected from mice exposed to UVB radiation over a 25 week period. Skin sections from A) control mice (K14Sin3A$^{WT/WT}$) and B) K14Sin3A$^{WT/\Delta}$ skin were labelled for Ki67 or C+D) p53. The number of E) Ki67-positive (+ve) or F) p53-positive (+ve) cells were quantified and are represented graphically. Error bars represent standard deviation (n=average of 5 IFE fields selected at random, counted from 2 biological replicates). * p<0.03. Scale bar, 50 μm.

In summary, pilot experiments in which mice were exposed to UVB radiation over a 25 week time period did not lead to the generation of skin tumours. The potential causes for this lack of tumour generation will be discussed in the chapter summary below. Analysis of skin obtained at this time point revealed that there is a visual increase in the thickness of the interfollicular epidermis in K14Sin3A$^{\text{WT}/\Delta}$ skin in comparison to control skin, which coincides with an increase in proliferation and a reduction in p53 levels. Further experiments are necessary to reveal whether Sin3A influences tumour susceptibility.

6.3 Summary

In the above chapter I began to explore the role of Sin3A in the context of Sin3A acting as a potential tumour suppressor in skin. Pilot experiments using short term exposure of skin to UVB radiation revealed that there is a differential response between control skin and K14Sin3A$^{\text{WT}/\Delta}$. Epidermal thickness and proliferation is increased in K14Sin3A$^{\text{WT}/\Delta}$ skin in comparison to controls and there is a lower induction of p53 and potentially apoptosis as a consequence.

A well established effect of UVB radiation is the induction of DNA damage, for example, thymine dimer formation which in turn leads to activation of p53 as a transcription factor, with increased p53 levels being detectable in the nucleus [Marrot and Meunier, 2008; Matsunaga et al., 2008]. The induction of p53 in response to DNA damage has two main outcomes, either cell cycle arrest to allow for repair of mutated DNA for example via nucleotide excision repair or apoptosis [Siliciano et al., 1997]. As lower levels of p53 are observed in K14Sin3A$^{\text{WT}/\Delta}$ mice it would be interesting to determine if expression and activity of components involved in p53-dependent cell cycle arrest for example P21 [Bunz et al., 1998] and DNA repair processes such as Gadd45 [Smith et al., 1994] and p48 [Sengupta and Harris, 2005] are disrupted in K14Sin3A$^{\text{WT}/\Delta}$ skin. DNA damage caused by UVB irradiation also results in the induction of Mdm2, which is both a target and also a regulator of p53 [Wang and Jiang, 2012; Wu and Levine, 1997]. Part of the role of Mdm2 in the regulation of p53 is via the promotion of degradation of p53 via a p53-Mdm2-negative feedback loop [Marine et al., 2006]. It would be interesting to determine whether Mdm2 levels are increased in K14Sin3A$^{\text{WT}/\Delta}$ mice in comparision to controls and if this is the case to then examine the possibility that Sin3A has a role in repressing Mdm2.

The most striking aspect of this experiment was the recapitulation of the phenotype observed in K14ERSin3A$^{\Delta/\Delta}$ skin. It is possible that the absence of a single allele of Sin3A is sufficient to allow Myc activity to be increased and its target genes to be activated in UV irradiated skin. It is of interest to note that Myc over-expressing skin is resistant to UVB-induced apoptosis [Waikel et al.,

1999] and it is possible that the loss of a single allele of Sin3A in skin can lead the recapitulation of this phenoype as there is a lower induction of p53. It would be interesting to determine if resistance to apoptosis is cause of the increase in epidermal thickness in K14Sin3A$^{\text{WT}/\Delta}$ mice after short term exposure to UVB radiation. Analysis of apoptosis using specific markers for example active caspase 3 or caspase 9 [Schuler et al., 2000] would be necessary to determine if apoptosis levels are different when a single allele of Sin3A is lost in comparison to control skin. Further experiments are necessary to investigate the impact of loss of Sin3A on Myc behaviour in UVB-irradiated skin, for example examination of expression levels of known Myc target genes in comparison to control skin.

The positive results from the short term pilot experiments prompted me to perform long term pilot experiments in which mice were exposed to UVB radiation over a number of weeks. In this pilot study, examination of skin obtained following 25 weeks of treatment demonstrated that despite prolonged exposure to UVB radiation, no skin tumours had developed in either control or K14Sin3A$^{\text{WT}/\Delta}$ skin. However, an increase in epidermal thickness and proliferation was observed in K14Sin3A$^{\text{WT}/\Delta}$ skin in comparison to control skin. It can be speculated that if exposure had been continued for a longer time period, this increase in proliferation could have been sufficient to increase tumour susceptibility in K14Sin3A$^{\text{WT}/\Delta}$ skin in comparison to controls.

The long term pilot experiments illuminated some problems that may have resulted in a lack of tumour formation in the time frame of treatment. For the possibility of skin tumour development induced by UVB radiation, skin hyperplasia must be maintained over a 12-15 week period [Workman et al., 2010]. The problems incurred during the pilot experiments may have meant that skin hyperplasia was not maintained and therefore tumours did not develop. The use of protective restraints was necessary to avoid damage to the eyes and ears of experimental animals. However, the restraints used caused adverse effects on animal welfare unrelated to UVB radiation that resulted in the length of time between UVB treatments being increased as advised by a veterinarian. Another problem was that due to the nature of the restraints, it is possible that the exact area of skin

was not irradiated with each dose of UVB irradiation. Another point to consider is that the experiments were performed using mice of a mixed genetic background. Some mouse strains, for example mice that are homozygous for the spontaneous Hr^{hr} mutation, are more susceptible to tumour development following long term UV irradiation experiments while the C57BL/6J line is more resistant as judged by a longer exposure time needed before tumours develop [Kripke, 1977; Perez et al., 2012].The use of a mixed genetic background, including the more resistant C57BL/6J line, could have led to a reduced susceptibility of the K14Sin3A line to tumour development and a longer time period of UV exposure (over 30 weeks) necessary before tumour development could be observed. These three issues together may have led to a lack of maintenance of hyperplasia and the subsequent lack of tumour development. If this procedure was refined and the genetic background of the mice was taken into account when planning future experiments, it could prove useful to go beyond pilot experiments and use larger numbers of mice.

An alternative approach could involve the use of two-stage chemical carcinogenesis to induce skin tumours using 7,12-dimethylbenz(a)anthracene (DMBA) and TPA. This technique has long been used to induce skin carcinogenesis [Filler et al., 2007] and determination as to whether there is differential susceptibility between control and K14Sin3A$^{WT/\Delta}$ skin using this approach could yield interesting results. Pilot experiments would be necessary to establish appropriate doses of DMBA and TPA for tumour initiation and promotion. Further experiments could include the evaluation of levels of Sin3A expression in skin tumours obtained from either experimental mice or human patients. Recent observations by Das et al have demonstrated that expression levels of Sin3A are reduced in a number of human tumours including lung, renal and liver tumours [Das et al., 2012]. If Sin3A acts a tumour suppressor in skin it could be hypothesised that Sin3A levels could be reduced in skin tumour samples in similarity to the other tissues analysed by Das and colleagues [Das et al., 2012]. Finally, another possibility to evaluate the influence of Sin3A on tumour susceptibility in skin could be to cross K14Sin3A$^{WT/\Delta}$ mice with a mouse model in which Ras is activated as Ras is known to have a key role in skin carcinogenesis [Caulin et al., 2007]. For example, RasGRP1 transgenic mice spontaneously develop both papillomas and cutaneous

squamous cell carcinomas [Diez et al., 2009; Oki-Idouchi and Lorenzo, 2007]. The deletion of Sin3A in this genetic background and assessing the speed of tumour development, tumour type and severity and number of tumours in comparison to controls could be a useful approach. In the scope of my PhD project it was not feasible to create another mouse line, but I believe that this approach could lead to some interesting results.

Overall, initial pilot experiments described in this chapter have yielded some promising results despite some setbacks. As loss of a single allele of Sin3A leads to epidermal hyperplasia and an increase in proliferation in these pilot experiments, the initial signs that Sin3A is important in carcinogenesis are promising. Further investigations as described above including alternative approaches or refinement of the UVB radiation techniques would be useful to establish whether Sin3A has a role has a tumour suppressor in skin.

Chapter 7

Conclusions and future perspectives

The aims of my thesis were to establish a role for the transcriptional functions of Sin3A in skin and to determine if Sin3A played a role as an opposing factor to Myc in this region. In order to meet these aims I used a number of transgenic mouse models to conditionally delete Sin3A in skin and analysed the resultant phenotypes using a variety of techniques. The approaches I used yielded a number of highly interesting result and provided new insights into the role of Sin3A in a complex mammalian tissue.

Preliminary analyses demonstrate that Sin3A appears to be dispensable for bulge stem cell homeostasis, however, it is possible that more in depth investigations could reveal a role for Sin3A in the bulge region of the HF. It would be interesting to examine the impact of loss of Sin3A in the bulge region under non-homeostatic situations such as in the case of wounding. It is known that bulge stem cells are activated and contribute to the wound repair process in the IFE following skin injury [Ito et al., 2005]. Lineage tracing experiments have demonstrated that the progeny of bulge stem cells can be detected in the early parts of the wound healing process, around 5 days after injury, while the number of progeny detected rapidly decreases by 20 days after injury [Ito et al., 2005] leading to the suggestion that bulge stem cells are part of an 'emergency response' to epidermal repair [Plikus et al., 2012]. As part of this process, bulge stem cell progeny exhibits greater plasticity in fate as under normal homeostatic conditions these stem cells

only give rise to cells of the HF [Plikus et al., 2012] and it is possible that bulge stem cells lacking Sin3A could be defective in this scenario. Performing wounding experiments similar to those performed by Ito and colleagues ([Ito et al., 2005]) using K19ERSin3A$^{\Delta/\Delta}$ mice and appropriate controls to determine whether the wound healing repair process is analogous to controls when Sin3A is lost from the bulge could yield some highly exciting results. Additionally, application of TPA to the skin is known to induce proliferation in label retaining cells in the bulge region of the hair follicle, leading to a depletion of this cell population [Braun et al., 2003]. Following this protocol and analysing the impact of induction of proliferation in the bulge stem cell population in K19ERSin3A$^{\Delta/\Delta}$ skin would also provide new insights as to Sin3A function in this cell population. In the case that Sin3A is acting to repress genes involved in proliferation in this cell population, it may be that the loss of the label retaining cell population, which corresponds to bulge stem cells is accelerated in the absence of Sin3A.

In order to establish a role for Sin3A in the HF it could also be interesting to analyse the role of Sin3A in normal bulge homeostasis in a more controlled manner. As the first two hair cycles are synchronised in the back skin of mice, Sin3A could be deleted from the bulge at specific stages of the hair cycle i.e. catagen, anagen or telogen to examine the impact of Sin3A loss on hair cycle progression as well as on hair follicle morphology at specific stages. One potential point of consideration when planning these experiments is that treatment with 4-OHT has been known to cause hair cycle delay of up to three weeks when mice are treated with 4-OHT in the first telogen (P21-28), leading to an extended telogen stage before entry into anagen (Cedric Blanpain, Kim Jensen, personal communication). In this case, it would be more feasible to compare 4-OHT-treated skin from K19ERSin3A$^{\Delta/\Delta}$ mice with 4-OHT treated skin K19ERSin3A$^{\text{WT/WT}}$ from age and sex matched controls rather than acetone-treated K19ERSin3A$^{\text{F/F}}$ littermates. However, this hair cycle delay upon 4-OHT treatment is a phenomenon that has not been observed in my hands, possibly due to a lower concentration of 4-OHT being used (1.5mg per application).

As mentioned in my introduction, the hair follicle is home to numerous stem cell

populations and as such it is possible that Sin3A could have a role in other hair follicle stem cell populations aside from the bulge. The question as to whether Sin3A does govern aspects of stem cell behaviour in the hair follicle outside of the bulge is not yet answered. To begin to address this question, Sin3A$^{F/F}$ could be crossed with mice expressing inducible Cre-recombinase under the control of lineage-specific promoters. For example Sin3A$^{F/F}$ mice could be crossed with the Lgr6tm2.1(cre/ERT2)Cle mouse line (The Jackson Laboratory, [Snippert et al., 2010]) allowing Sin3A to be deleted in Lgr6-expressing stem cells, which reside in the isthmus region of the hair follicle, upon application of 4-OHT to the skin. Alternatively, Sin3A$^{F/F}$ mice could be crossed with the Lrig1tm1.1(cre/ERT2)Rjc mouse line (The Jackson Laboratory, [Powell et al., 2012], which would lead to Sin3A deletion in the infundibulum upon application of 4-OHT. The assessment of the phenotype observed when Sin3A is deleted from these stem cell populations initially by histological analysis, gene expression analysis and for expression of hair follicle markers could provide more exciting results about Sin3A's role in hair follicle homeostasis.

As I did not establish a role for Sin3A in hair follicle stem cells, I next wanted to determine if Sin3A could have a role in governing homeostasis in the interfollicular epidermis. To address this I used a mouse model in which I deleted Sin3A in the undifferentiated cells in this region. An initial approach involving conditional deletion of Sin3A in K14-positive cells yielded no K14Sin3A$^{\Delta/\Delta}$ pups leading to the conclusion that loss of Sin3A in K14 positive cells during embryogenesis leads to embryonic lethality. It is possible that embryonic lethality is not due to skin-specific deletion of Sin3A as K14 and therefore Cre-recombinase is expressed in other tissues during embryogenesis . To investigate the stage at which embryonic lethality occurs, timed matings using K14Sin3A$^{WT/\Delta}$ mice could be set up in order for embryos to be collected at specific time points during embryogenesis. As K14 expression begins at around E9.75 in the embryo [Byrne et al., 1994; Lu et al., 2005], embryos could be collected from E9 onwards and genotyped to try and detect K14Sin3A$^{\Delta/\Delta}$ embryos. If identified, K14Sin3A$^{\Delta/\Delta}$ embryos could then be compared to control embryos to determine any abnormalities that could lead to lethality. It is noteworthy that loss of a single allele of Sin3A did not

lead to a phenotype in skin as judged by comparisons of K14Sin3A$^{\text{WT}/\Delta}$ skin to control skin. This concurs with results from studies of deletion of a single Sin3A allele during embryogenesis using the Sin3A floxed allele, which demonstrated that embryos with this genotype are indistinguishable from Wild-type whereas complete loss of Sin3A leads to lethality [Dannenberg et al., 2005; McDonel et al., 2011].

On account of these results, I then turned to an inducible model in which the deletion of Sin3A could be controlled temporally as well as spatially to begin to unravel the functions of Sin3A in the interfollicular epidermis. The initial outcomes of these experiments were highly intriguing as K14ERSin3A$^{\Delta/\Delta}$ mice presented with a severe phenotype, namely thickened skin, excess salivation and an enlargement of the testes region in males. Upon further investigation of the skin phenotype, I showed that when Sin3A is deleted in this tissue there is hyperproliferation in the interfollicular epidermis and sebaceous glands and enhanced differentiation in the interfollicular epidermis. This was highly interesting as up to this point, aside from functions in muscle [VanOevelen et al., 2010] and testis [Pellegrino et al., 2012], Sin3A's role in adult tissues has been poorly defined.

An interesting aspect of the phenotype of excess proliferation when Sin3A is deleted is that this is not limited only to skin and can be observed in the salivary glands and the testis. Additional experiments to determine the exact impact of Sin3A loss in these tissues would be intriguing. The determination of the exact cell types impacted by Sin3A loss and perhaps examining the effects on expression of Sin3A targets would be intriguing to perform. In particular, determination of the cell types affected in the testis and and the examination of the impact of Sin3A-loss in these K14-expressing cells in this region could be quite fascinating as fertility could be affected. Furthermore prior analyses by other groups have demonstrated that deletion of Sin3A in testis impacts Sertoli cells [Payne et al., 2010; Pellegrino et al., 2012], which provide a niche for germ cells in the testis [Grover et al., 2004] providing a basis that Sin3A is important in certain cell types in this region. However, I believe that a different approach to topical application of 4-OHT to the back skin to generate K14ERSin3A$^{\Delta/\Delta}$ tissues could be

better to target the testis region more efficiently. A possibility would to be inject the 4-OHT via the intraperitoneal route, however, as judged by the severity of the phenotype when 4-OHT is applied topically, it is possible that injection of 4-OHT could lead to more severe side effects more quickly, making experiments to examine fertility difficult. Further examination of the K14ERSin3A$^{\Delta/\Delta}$ testis phenotype would be useful to determine if the results concur with those recently published by Pellegrino and colleagues who show that Sin3A expresssion is required for the germ cell lineage in the mouse [Pellegrino et al., 2012].

Since there is a severe phenotype when Sin3A is deleted in K14-positive cells, at this point I decided to perform experiments using a transgenic mouse model in which the mammalian homologue of Sin3A, Sin3B, was deleted in undifferentiated cells of the epidermis upon application of tamoxifen. As a consequence of a lack of revelation of a skin phenotype in these experiments, Sin3B appears to be non-essential in skin. This is not altogether surprising as despite the high homology between Sin3A and Sin3B, these two factors have independent roles in other processes for example embryogenesis and muscle development [Cowley et al., 2005; Dannenberg et al., 2005; David et al., 2008; McDonel et al., 2009; VanOevelen et al., 2010] and thus could act independently in skin. However, the possibility that Sin3B does have some function in the skin that is compensated for by Sin3A in the absence of Sin3B can not be completely discarded. Further experiments could include crossing the K14ERSin3A and K14Sin3B lines to generate K14ERSin3A$^{F/F}$Sin3B$^{F/F}$ mice in which both Sin3A and Sin3B could be deleted in the epidermis concurrently upon 4-OHT application to the skin and subsequent analysis of the skin phenotpe observed. It may be that Sin3B could compensate for some features of Sin3A loss and that a more extreme phenotype would be observed upon removal of both of these factors.

I next wanted to probe the causes of the enhanced differentation and increased proliferation phenotype observed in K14ERSin3A$^{\Delta/\Delta}$ skin. As explained in my research aims, I belived that Sin3A could act as an antagonist to Myc in the epidermis and as a consequence I wanted to determine if aberrant Myc activity could be contributing to excess proliferation and increased differentiation when

Sin3A is lost in skin. Via a combination of microarray and ChIP-chip analysis I provided some enlightenment as to causes of this phenotype and Sin3A's relationship with Myc. Results from these analyses revealed that in the absence of Sin3A in the interfollicular epidermis, Myc aberrantly binds its target genes at the EDC leading to their activation and a push towards differentiation. Furthermore, Myc also activates genes involved in growth and proliferation when Sin3A is deleted, leading to epidermal hyperplasia.

It is also interesting to note that the presence of Sin3A leads to de-acetylation and a reduction in stability of the Myc protein. However, ChIP-chip experiments revealed that Sin3A is absent from promoter regions in a scenario of Myc over-expression. This indicates that when high levels of Myc are bound, Sin3A is unable to form a stable repressor complex on chromatin. Consequently, the *in vivo* interaction of Sin3A and Myc is likely to occur indirectly via core complex components or mediating the de-acetylase enzymatic activity or other interacting proteins rather than directly with the Sin3A protein. This differs from Mad family repressors, which interact with Sin3A's PAH2 domain via their SID [Laherty et al., 1997]. Investigations into the mechanism by which this occurs are necessary. One possible candidate for this role is Yin Yang 1, which has been demonstrated to interact with Sin3A to mediate transcriptional repression [Lu et al., 2011] and has been implicated in Myc degradation [Parija and Das, 2003]. It is known that Myc acetylation leads to a reduction of ubiquitination of the Myc protein [Popov et al., 2010; Vervoorts et al., 2003] thus it is possible that de-acetylation has the opposing impact on Myc ubqiquitination and could be linked to the ubiquitin proteosome pathway. Experiments to examine the effect of Sin3A loss on Myc ubiquitination could therefore yield interesting results.

In a similar scenario to Sin3A's impact on c-Myc, Sin3A has been shown to be able to deacetylate STAT3 [Icardi et al., 2012]. Interestingly, studies have revealed that STAT3 activation in skin leads to skin defects such as squamous cell carcinoma and psoriasis while repression of STAT3 can improve these conditions [Aggarwal et al., 2006]. The investigation of Sin3A's relationship with STAT3 specifically in the skin has not been examined in detail and it could be

exciting to determine if Sin3A can lead to STAT3 repression specifically in skin. Firstly, simply determining whether STAT3 is up-regulated in K14ERSin3A$^{\Delta/\Delta}$ via qPCR, western blotting or immunostaining could provide some insight as to whether there is a relationship between these factors in skin. Following on from this, examining whether Sin3A and STAT3 can interact in keratinocytes and examination of the acetylation status in K14ERSin3A$^{\Delta/\Delta}$ keratinocytes versus control keratinocytes could yield new, interesting information about the roles of Sin3A in skin.

Evidence that Myc is the primary driver behind the phenotype in the absence of Sin3A was cemented by the lack of epidermal hyperplasia and excess differentiation when Myc is deleted in Sin3A-depleted skin. Moreover, expression levels of EDC genes and genes involved in proliferation and the cell cycle are close to normality in skin in which Myc and Sin3A have been deleted. However, when the system is challenged by an induction of proliferation, the interfollicular epidermis responds in an abnormal fashion, indicating that the Sin3A/Myc network is not dispensable in the interfollicular epidermis.

These highly exciting results demonstrated that Sin3A and Myc share target genes within the EDC and beyond and that a transcriptional regulatory network governs behaviour in the interfollicular epidermis. This system must be carefully balanced as misregulation causes disruption to epidermal homeostasis. This means that the transcriptionally activating powers of Myc must be opposed by the transcriptionally repressing activities of the Sin3A repressor complex at shared target genes in a balanced manner. Interestingly, Sin3A has also been shown to oppose *Drosophila* Myc activity [Das et al., 2012] so this relationship between Sin3A and Myc could be conserved in other tissues and organisms.

Aside from revealing the relationship with Sin3A and Myc in skin, the results that I have obtained to date have demonstrated that Sin3A appears to inhibit proliferation. At the same time it appears that Sin3A is dispensable for the terminal differentiation program to occur in the interfollicular epidermis. It would be interesting to further probe the role of Sin3A in the interfollicular epidermis to

determine if Sin3A acts to prevent differentiation. For example, over-expressing Sin3A specifically in basal keratinocytes either *in vitro* or *in vivo* could give insights into Sin3A's role in the differentiation process. It could be hypothesised that over-expression of Sin3A in this cell-type specifically leads to a block of differentiation in this tissue.

In addition to impacts in the interfollicular epidermis, I revealed that Sin3A deletion leads to increased size and proliferation of sebceous glands, however, this phenotype was not fully explored during my project, leaving some questions unanswered. For example, it would also be of interest to determine if Sin3A has a conserved function in the sebaceous glands in terms of opposing proliferation and possibly differentiation induced by Myc. This could be the case as it is known that Myc activation induces sebocyte differentiation in both human and mouse epidermis [Arnold and Watt, 2001; Frye et al., 2003; LoCelso et al., 2008; Waikel et al., 2001]. Examination of K14ERSin3A$^{\Delta/\Delta}$ sebaceous glands in more detail to determine what sebaceous gland cell types are impacted by the loss of Sin3A for example are there increased numbers of undifferentiated or differentiated cells in this region?

Disruption of the balance of Sin3A and Myc in the interfollicular epidermis could potentially lead to diseases involving hyper-proliferation such as cancer and psoriasis [Gudjonsson and Elder, 2007]. Building on the pilot experiments that were performed using UVB radiation in Sin3A-depleted skin would provide insights into Sin3A's possible function as a tumour suppressor. One approach could involve the use of two-stage chemical carcinogenesis to induce skin tumours using DMBA and TPA, which is an established technique used to induce skin carcinogenesis [Filler et al., 2007]. Determination as to whether there is differential susceptibility between control and K14Sin3A$^{\mathrm{WT}/\Delta}$ skin using this approach could provide information as to whether or not Sin3A acts as a tumour suppressor in skin. Pilot experiments would be necessary to establish appropriate doses of DMBA and TPA for tumour initiation and promotion.

Further experiments could include the evaluation of levels of Sin3A expression in

skin tumours obtained from either experimental mice or human patients. Recent observations by Das et al have demonstrated that expression levels of Sin3A are reduced in a number of human tumours including lung, renal and liver tumours [Das et al., 2012]. If Sin3A acts a tumour suppressor in skin it could be hypothesised that Sin3A levels could be reduced in skin tumour samples in similarity to the other tissues analysed by Das and colleagues [Das et al., 2012]. Finally, another possibility to evaluate the influence of Sin3A on tumour susceptibility in skin could be to cross K14Sin3A$^{\text{WT}/\Delta}$ mice with a mouse model in which Ras is activated as Ras is known to have a key role in skin carcinogenesis [Caulin et al., 2007]. For example, RasGRP1 transgenic mice spontaneously develop both papillomas and cutaneous squamous cell carcinomas [Diez et al., 2009; Oki-Idouchi and Lorenzo, 2007]. The deletion of Sin3A in this genetic background and assessing the speed of tumour development, tumour type and severity and number of tumours in comparison to controls could be a useful approach.

It would also be interesting to analyse the role of Sin3A in other hyper-proliferative skin diseases such as psoriasis. From the results I have obtained indicating that Sin3A acts to suppress proliferation, it could be hypothesised that loss of Sin3A function for example via decreased expression or mutation could lead to excess proliferation, therefore contributing to these diseases. One approach could be to examine Sin3A expression levels in samples of psoriatic skin from human patients and compare these levels to those observed in normal skin. An alternative approach could take advantage of the existence of a number of appropriate mouse models for psoriasis, such as K5.Stat3C mice, which are transgenic mice with keratinocytes expressing a constitutively active STAT3, [Gudjonsson et al., 2007; Sano et al., 2004]. Skin from these mice could then be examined for Sin3A expression, loss or mutations to establish a role for Sin3A in disease processes.

The maintenance of homeostasis in mammalian tissues requires a balance between cell loss and replacement to avoid diseases such as cancer or tissue failure due to over-proliferation or under-proliferation. The results that I have produced have demonstrated that the presence of Sin3A is essential for the maintenance of balanced homeostasis in skin, a complex mammalian tissue. Furthermore, I found

that Sin3A is antagonistic to Myc function in the interfollicular epidermis and is necessary to prevent hyperproliferation or excess differentiation in this tissue. As a whole, the work completed in this thesis indicates that a complex interplay between chromatin regulators, in this case Sin3A, and transcription factors, in this case Myc, are of key importance in dictating epidermal cell fate and behaviour. Sin3A and Myc are two key regulators in mammalian epidermis whose opposing functions provide a balance between transcriptional activation and repression to govern proliferation and differentiation. The interplay between these factors must be tightly controlled to ensure that epidermal homeostasis is maintained.

References

B.B. Aggarwal, S. Shishodia, et al. Molecular targets of dietary agents for prevention and therapy of cancer. *Biochemical pharmacology*, 71(10):1397–1421, 2006. 162

L Alland, R Muhle, H Hou, J Potes, L Chin, N Schreiber-Agus, and R DePinho. Role for N-CoR and histone deacetylase in Sin3-mediated transcriptional repression. *Nature*, 387(1):49–55, 1997. 29

L. Alland, G. David, H. Shen-Li, J. Potes, R. Muhle, H.C. Lee, H. Hou Jr, K. Chen, and R.A. DePinho. Identification of mammalian sds3 as an integral component of the sin3/histone deacetylase corepressor complex. *Molecular and cellular biology*, 22(8):2743–2750, 2002. 29

L. Alonso and E. Fuchs. The hair cycle. *Journal of cell science*, 119(3):391–393, 2006. 10

I Arnold and F Watt. c-Myc activation in transgenic mouse epidermis results in mobilization of stem cells and differentiation of their progeny. *Current Biology*, 11(8):558–568, 2001. 23, 24, 104, 164

D Ayer, Q Lawrence, and R Eisenman. Mad-Max transcriptional repression is mediated by ternary complex formation with mammalian homologs of yeast repressor Sin3. *Cell*, 80(5):767–776, 1995. 26, 28

D.E. Ayer. Histone deacetylases: transcriptional repression with siners and nurds. *Trends in cell biology*, 9(5):193–198, 1999. 29

G.A. Baltus, M.P. Kowalski, A.V. Tutter, and S. Kadam. A positive regulatory role for the msin3a-hdac complex in pluripotency through nanog and sox2. *Journal of Biological Chemistry*, 284(11):6998–7006, 2009. 31

B. Beck and C. Blanpain. Mechanisms regulating epidermal stem cells. *The EMBO Journal*, 31(9):2067–2075, 2012. 14, 16, 17, 70

S.A. Benitah and M. Frye. Stem cells in ectodermal development. *Journal of Molecular Medicine*, pages 1–8, 2012. 5, 10, 13

R.J. Berg, H.J. Van Kranen, H.G. Rebel, A. De Vries, W.A. Van Vloten, CF Van Kreijl, J.C. Van Der Leun, and FR De Gruijl. Early p53 alterations in mouse skin carcinogenesis by uvb radiation: immunohistochemical detection of mutant p53 protein in clusters of preneoplastic epidermal cells. *Proceedings of the National Academy of Sciences*, 93(1):274, 1996. 149

C Blanpain and E Fuchs. Epidermal homeostasis: a balancing act of stem cells in the skin. *Nature Reviews in Molecular Cell Biology*, 10(3):207–217, 2009. 94

C Blanpain, W Lowry, A Geoghegan, L Polak, and E Fuchs. Self-renewal, multipotency, and the existence of two cell populations within an epithelial stem cell niche. *Cell*, 118(5):635–648, 2004. 16

C. Blanpain, W.E. Lowry, H.A. Pasolli, and E. Fuchs. Canonical notch signaling functions as a commitment switch in the epidermal lineage. *Genes & development*, 20(21):3022–3035, 2006. 18

M.L. Bochman and A. Schwacha. The mcm complex: unwinding the mechanism of a replicative helicase. *Microbiology and Molecular Biology Reviews*, 73(4): 652–683, 2009. 90

V.A. Botchkarev, M.R. Gdula, A.N. Mardaryev, A.A. Sharov, and M.Y. Fessing. Epigenetic regulation of gene expression in keratinocytes. *Journal of Investigative Dermatology*, 2012. 21, 22

K Braun, C Niemann, U Jensen, J Sundberg, V Silva-Vargas, and F Watt. Manipulation of stem cell proliferation and lineage commitment: visualisation of

label-retaining cells in wholemounts of mouse epidermis. *Development*, 130 (21):5241–55, 2003. 55, 102, 158

A. Brehm, E.A. Miska, D.J. McCance, J.L. Reid, A.J. Bannister, and T. Kouzarides. Retinoblastoma protein recruits histone deacetylase to repress transcription. *nature*, 391(6667):597–601, 1998. 26

M Broome, D Ryan, and R Eckert. S100 Protein Subcellular Localization During Epidermal Differentiation and Psoriasis. *Journal of Histochemistry & Cytochemistry*, 51(5):675–685, 2003. 7

S Brown, C Tilli, B Jackson, A Avilion, M MacLeod, L Maltais, R Lovering, and C Byrne. Rodent Lce gene clusters; new nomenclature, gene organization, and divergence of human and rodent genes. *The Journal of Investigative Dermatology*, 127(7):1782–1786, 2007. 7

K. Brubaker, S.M. Cowley, K. Huang, L. Loo, G.S. Yochum, D.E. Ayer, R.N. Eisenman, and I. Radhakrishnan. Solution structure of the interacting domains of the mad–sin3 complex: Implications for recruitment of a chromatin-modifying complex. *Cell*, 103(4):655–665, 2000. 28

F. Bunz, A. Dutriaux, C. Lengauer, T. Waldman, S. Zhou, JP Brown, JM Sedivy, KW Kinzler, and B. Vogelstein. Requirement for p53 and p21 to sustain g2 arrest after dna damage. *Science*, 282(5393):1497–1501, 1998. 153

C. Byrne, M. Tainsky, and E. Fuchs. Programming gene expression in developing epidermis. *Development*, 120(9):2369–2383, 1994. 4, 5, 103, 159

E Candi, R Schmidt, and G Melino. The cornified envelope: a model of cell death in the skin. *Nature Reviews in Molecular Cell Biology*, 6(4):328–340, 2005. 94

C. Caulin, T. Nguyen, G.A. Lang, T.M. Goepfert, B.R. Brinkley, W.W. Cai, G. Lozano, D.R. Roop, et al. An inducible mouse model for skin cancer reveals distinct roles for gain-and loss-of-function p53 mutations. *Journal of Clinical Investigation*, 117(7):1893–1901, 2007. 155, 165

E Clayton, D Doupé, A Klein, D Winton, B Simons, and P Jones. A single type of progenitor cell maintains normal epidermis. *Nature*, 446(7132):185–189, 2007. 15

G. Cotsarelis. Epithelial stem cells: a folliculocentric view. *Journal of investigative dermatology*, 126(7):1459–1468, 2006. 15

G Cotsarelis, T Sun, and R Lavker. Label-retaining cells reside in the bulge area of pilosebaceous unit: implications for follicular stem cells, hair cycle, and skin carcinogenesis. *Cell*, 61(7):1329–1337, 1990. 15

S.M. Cowley, B.M. Iritani, S.M. Mendrysa, T. Xu, P.F. Cheng, J. Yada, H.D. Liggitt, and R.N. Eisenman. The msin3a chromatin-modifying complex is essential for embryogenesis and t-cell development. *Molecular and cellular biology*, 25 (16):6990–7004, 2005. 28, 30, 31, 97, 103, 104, 161

X. Dai and J.A. Segre. Transcriptional control of epidermal specification and differentiation. *Current opinion in genetics & development*, 14(5):485–491, 2004. 9

J Dannenberg, G David, S Zhong, J Torre, W Wong, and R Depinho. mSin3A corepressor regulates diverse transcriptional networks governing normal and neoplastic growth and survival. *Genes & Development*, 19(13):1581–1595, 2005. 28, 30, 31, 34, 97, 103, 104, 160, 161

TK Das, J. Sangodkar, N. Negre, G. Narla, and RL Cagan. Sin3a acts through a multi-gene module to regulate invasion in drosophila and human tumors. *Oncogene*, 2012. 118, 155, 163, 165

R. DasGupta and E. Fuchs. Multiple roles for activated lef/tcf transcription complexes during hair follicle development and differentiation. *Development*, 126(20):4557–4568, 1999. 20

H.R. Dassule, P. Lewis, M. Bei, R. Maas, and A.P. McMahon. Sonic hedgehog regulates growth and morphogenesis of the tooth. *Development*, 127(22):4775–4785, 2000. 34

G. David, G.M. Turner, Y. Yao, A. Protopopov, and R.A. DePinho. msin3-associated protein, msds3, is essential for pericentric heterochromatin formation and chromosome segregation in mammalian cells. *Genes & development*, 17(19):2396–2405, 2003. 29

G. David, K.B. Grandinetti, P.M. Finnerty, N. Simpson, G.C. Chu, and R.A. DePinho. Specific requirement of the chromatin modifier msin3b in cell cycle exit and cellular differentiation. *Proceedings of the National Academy of Sciences*, 105(11):4168, 2008. 28, 161

C. de Guzman Strong, S. Conlan, C.B. Deming, J. Cheng, K.E. Sears, and J.A. Segre. A milieu of regulatory elements in the epidermal differentiation complex syntenic block: implications for atopic dermatitis and psoriasis. *Human molecular genetics*, 19(8):1453–1460, 2010. 7, 9

F.R. Diez, A.A. Garrido, A. Sharma, C.T. Luke, J.C. Stone, N.A. Dower, J.M. Cline, and P.S. Lorenzo. Rasgrp1 transgenic mice develop cutaneous squamous cell carcinomas in response to skin wounding: potential role of granulocyte colony-stimulating factor. *The American journal of pathology*, 175(1):392–399, 2009. 156, 165

D.P. Doupé and P.H. Jones. Interfollicular epidermal homeostasis: dicing with differentiation. *Experimental Dermatology*, 2012. 13, 15

I. Driskell, H. Oda, S. Blanco, E. Nascimento, P. Humphreys, and M. Frye. The histone methyltransferase setd8 acts in concert with c-myc and is required to maintain skin. *The EMBO journal*, 31(3):616–629, 2011. 21, 23

R Eckert, J Crish, T Efimova, S Dashti, A Deucher, F Bone, G Adhikary, G Huang, R Gopalakrishnan, and S Balasubramanian. Regulation of involucrin gene expression. *The Journal of Investigative Dermatology*, 123(1):13–22, 2004. 94

R.L. Eckert, A.M. Broome, M. Ruse, N. Robinson, D. Ryan, and K. Lee. S100 proteins in the epidermis. *Journal of investigative dermatology*, 123(1):23–33, 2003. 9

E. Ezhkova, H.A. Pasolli, J.S. Parker, N. Stokes, I. Su, G. Hannon, A. Tarakhovsky, E. Fuchs, et al. Ezh2 orchestrates gene expression for the stepwise differentiation of tissue-specific stem cells. *Cell*, 136(6):1122–1135, 2009. 22

E. Ezhkova, W.H. Lien, N. Stokes, H.A. Pasolli, J.M. Silva, and E. Fuchs. Ezh1 and ezh2 cogovern histone h3k27 trimethylation and are essential for hair follicle homeostasis and wound repair. *Genes & Development*, 25(5):485–498, 2011. 22

M.Y. Fessing, A.N. Mardaryev, M.R. Gdula, A.A. Sharov, T.Y. Sharova, V. Rapisarda, K.B. Gordon, A.D. Smorodchenko, K. Poterlowicz, G. Ferone, et al. p63 regulates satb1 to control tissue-specific chromatin remodeling during development of the epidermis. *The Journal of Cell Biology*, 194(6):825–839, 2011. 5, 21

R.B. Filler, S.J. Roberts, and M. Girardi. Cutaneous two-stage chemical carcinogenesis. *Cold Spring Harbor Protocols*, 2007(9):pdb–prot4837, 2007. 155, 164

T.C. Fleischer, U.J. Yun, and D.E. Ayer. Identification and characterization of three new components of the msin3a corepressor complex. *Molecular and cellular biology*, 23(10):3456–3467, 2003. 29

M Frye, C Gardner, E Li, I Arnold, and F Watt. Evidence that Myc activation depletes the epidermal stem cell compartment by modulating adhesive interactions with the local microenvironment. *Development*, 130(12):2793–2808, 2003. 23, 24, 164

M Frye, A Fisher, and F Watt. Epidermal stem cells are defined by global histone modifications that are altered by Myc-induced differentiation. *PloS One*, 2(1): e763, 2007. 23

E Fuchs. Scratching the surface of skin development. *Nature*, 445(7130):834–842, 2007. 4, 5, 10, 12

E. Fuchs. Skin stem cells: rising to the surface. *The Journal of cell biology*, 180 (2):273–284, 2008. 2, 7, 10

E Fuchs and V Horsley. More than one way to skin . . . *Genes & Development*, 22(8):976–985, 2008. 1

E. Fuchs and S. Raghavan. Getting under the skin of epidermal morphogenesis. *Nature Reviews Genetics*, 3(3):199–209, 2002. 3

A Gebhardt, M Frye, S Herold, S Benitah, K Braun, B Samans, F Watt, H-P Elsässer, and M Eilers. Myc regulates keratinocyte adhesion and differentiation via complex formation with Miz1. *The Journal of Cell Biology*, 172(1):139–149, 2006. 23

F. Goeman, D. Thormeyer, M. Abad, M. Serrano, O. Schmidt, I. Palmero, and A. Baniahmad. Growth inhibition by the tumor suppressor p33ing1 in immortalized and primary cells: involvement of two silencing domains and effect of ras. *Molecular and cellular biology*, 25(1):422–431, 2005. 139

A. Grover, M.R. Sairam, C.E. Smith, and L. Hermo. Structural and functional modifications of sertoli cells in the testis of adult follicle-stimulating hormone receptor knockout mice. *Biology of reproduction*, 71(1):117–129, 2004. 160

C.M. Grozinger, S.L. Schreiber, et al. Deacetylase enzymes-biological functions and the use of small-molecule inhibitors. *Chemistry and Biology-Kidlington*, 9 (1):3–16, 2002. 29

A. Grzenda, G. Lomberk, J.S. Zhang, and R. Urrutia. Sin3: Master scaffold and transcriptional corepressor. *Biochimica et Biophysica Acta (BBA)-Gene Regulatory Mechanisms*, 1789(6-8):443–450, 2009. 26, 28, 29, 30

J.E. Gudjonsson and J.T. Elder. Psoriasis: epidemiology. *Clinics in dermatology*, 25(6):535–546, 2007. 164

J.E. Gudjonsson, A. Johnston, M. Dyson, H. Valdimarsson, and J.T. Elder. Mouse models of psoriasis. *Journal of Investigative Dermatology*, 127(6):1292–1308, 2007. 165

C Hassig, T Fleischer, A Billin, S Schreiber, and D Ayer. Histone deacetylase activity is required for full transcriptional repression by mSin3A. *Cell*, 89(3): 341–347, 1997. 26, 29

C.A. Higgins, G.E. Westgate, and C.A.B. Jahoda. From telogen to exogen: mechanisms underlying formation and subsequent loss of the hair club fiber. *Journal of Investigative Dermatology*, 129(9):2100–2108, 2009. 12

J. Hildesheim, D.V. Bulavin, M.R. Anver, W.G. Alvord, M.C. Hollander, L. Vardanian, and A.J. Fornace. Gadd45a protects against uv irradiation-induced skin tumors, and promotes apoptosis and stress signaling via mapk and p53. *Cancer research*, 62(24):7305, 2002. 145

S Hoffjan and S Stemmler. On the role of the epidermal differentiation complex in ichthyosis vulgaris, atopic dermatitis and psoriasis. *The British Journal of Dermatology*, 157(3):441–449, 2007. 9

C Hooker and P Hurlin. Of Myc and Mnt. *Journal of Cell Science*, 119(Pt 2): 208–216, 2006. 23

V Horsley, D O'Carroll, R Tooze, Y Ohinata, M Saitou, T Obukhanych, M Nussenzweig, A Tarakhovsky, and E Fuchs. Blimp1 defines a progenitor population that governs cellular input to the sebaceous gland. *Cell*, 126(3): 597–609, 2006. 12, 17

V. Horsley, A.O. Aliprantis, L. Polak, L.H. Glimcher, and E. Fuchs. Nfatc1 balances quiescence and proliferation of skin stem cells. *Cell*, 132(2):299–310, 2008. 18, 19

L. Icardi, R. Mori, V. Gesellchen, S. Eyckerman, L. De Cauwer, J. Verhelst, K. Vercauteren, X. Saelens, P. Meuleman, G. Leroux-Roels, et al. The sin3a repressor complex is a master regulator of stat transcriptional activity. *Proceedings of the National Academy of Sciences*, 2012. 29, 162

M Ito, Y Liu, Z Yang, J Nguyen, F Liang, R Morris, and G Cotsarelis. Stem cells in the hair follicle bulge contribute to wound repair but not to homeostasis of the epidermis. *Nature Medicine*, 11(12):1351–1354, 2005. 102, 157, 158

V Jaks, N Barker, M Kasper, J Es, H Snippert, H Clevers, and R Toftgå rd. Lgr5 marks cycling, yet long-lived, hair follicle stem cells. *Nature Genetics*, 40(11): 1291–1299, 2008. 16

V Jaks, M Kasper, and R Toftgå rd. The hair follicle-a stem cell zoo. *Experimental Cell Research*, 316(8):1422–1428, 2010. 16

P. Janich, G. Pascual, A. Merlos-Suárez, E. Batlle, J. Ripperger, U. Albrecht, H.Y.M. Cheng, K. Obrietan, L. Di Croce, and S.A. Benitah. The circadian molecular clock creates epidermal stem cell heterogeneity. *Nature*, 480(7376): 209–214, 2011. 19

K Jensen, C Collins, E Nascimento, D Tan, M Frye, S Itami, and F Watt. Lrig1 expression defines a distinct multipotent stem cell population in mammalian epidermis. *Cell Stem Cell*, 4(5):427–439, 2009. 16

K Jensen, R Driskell, and F Watt. Assaying proliferation and differentiation capacity of stem cells using disaggregated adult mouse epidermis. *Nature Protocols*, 5(5):898–911, 2010. 39

M. Kashiwagi, B.A. Morgan, and K. Georgopoulos. The chromatin remodeler mi-2β is required for establishment of the basal epidermis and normal differentiation of its progeny. *Development*, 134(8):1571–1582, 2007. 21

C.K. Kaufman, P. Zhou, H.A. Pasolli, M. Rendl, D. Bolotin, K.C. Lim, X. Dai, M.L. Alegre, and E. Fuchs. Gata-3: an unexpected regulator of cell lineage determination in skin. *Genes & development*, 17(17):2108–2122, 2003. 19

H. Korkeamäki, K. Viiri, M.K. Kukkonen, M. Mäki, and O. Lohi. Alternative mrna splicing of sap30l regulates its transcriptional repression activity. *FEBS letters*, 582(2):379–384, 2008. 28

M.I. Koster and D.R. Roop. The role of p63 in development and differentiation of the epidermis: Tanioku kihei memorial lecture. *Journal of dermatological science*, 34(1):3–9, 2004. 4, 5, 6

T. Kouzarides. Acetylation: a regulatory modification to rival phosphorylation? *Science's STKE*, 19(6):1176, 2000. 29

K. Kretzschmar and F.M. Watt. Lineage tracing. *Cell*, 148(1):33–45, 2012. 16

M.L. Kripke. Latency, histology, and antigenicity of tumors induced by ultraviolet light in three inbred mouse strains. *Cancer research*, 37(5):1395–1400, 1977. 155

D. Kulms and T. Schwarz. Molecular mechanisms of uv-induced apoptosis. *Photodermatology, photoimmunology & photomedicine*, 16(5):195–201, 2000. 145

D. Kurek, G.A. Garinis, J.H. Van Doorninck, J. Van Der Wees, and F.G. Grosveld. Transcriptome and phenotypic analysis reveals gata3-dependent signalling pathways in murine hair follicles. *Development*, 134(2):261–272, 2007. 19

A. Kuzmichev, Y. Zhang, H. Erdjument-Bromage, P. Tempst, and D. Reinberg. Role of the sin3-histone deacetylase complex in growth regulation by the candidate tumor suppressor p33ing1. *Molecular and cellular biology*, 22(3):835–848, 2002. 28

C Laherty, W Yang, J Sun, J Davie, E Seto, and R Eisenman. Histone deacetylases associated with the mSin3 corepressor mediate Mad Transcriptional Repression with the mSin3 Corepressor Mediate Mad Transcriptional Repression. *Cell*, 89:349–356, 1997. 26, 100, 162

A. Lai, B.K. Kennedy, D.A. Barbie, N.R. Bertos, X.J. Yang, M.C. Theberge, S.C. Tsai, E. Seto, Y. Zhang, A. Kuzmichev, et al. Rbp1 recruits the msin3-histone deacetylase complex to the pocket of retinoblastoma tumor suppressor family proteins found in limited discrete regions of the nucleus at growth arrest. *Molecular and cellular biology*, 21(8):2918–2932, 2001. 28

X. Le Guezennec, M. Vermeulen, and H.G. Stunnenberg. Molecular characterization of sin3 pah-domain interactor specificity and identification of pah partners. *Nucleic acids research*, 34(14):3929–3937, 2006. 28

M. LeBoeuf, A. Terrell, S. Trivedi, S. Sinha, J.A. Epstein, E.N. Olson, E.E. Morrisey, and S.E. Millar. Hdac1 and hdac2 act redundantly to control p63 and p53 functions in epidermal progenitor cells. *Developmental cell*, 19(6): 807–818, 2010. 20

G Legube, L Linares, C Lemercier, M Scheffner, S Khochbin, and D Trouche. Tip60 is targeted to proteasome-mediated degradation by Mdm2 and accumulates after UV irradiation. *The European Molecular Biology Organization Journal*, 21(7):1704–1712, 2002. 49

E Li, D Owens, P Djian, and F Watt. Expression of involucrin in normal, hyperproliferative and neoplastic mouse keratinocytes. *Experimental Dermatology*, 9 (6):431–8, 2000. 55

L Li and H Clevers. Coexistence of quiescent and active adult stem cells in mammals. *Science*, 327(5965):542–555, 2010. 102

K.K. Lin, V. Kumar, M. Geyfman, D. Chudova, A.T. Ihler, P. Smyth, R. Paus, J.S. Takahashi, and B. Andersen. Circadian clock genes contribute to the regulation of hair follicle cycling. *PLoS genetics*, 5(7):e1000573, 2009. 19

C LoCelso, M Berta, K Braun, M Frye, S Lyle, C Zouboulis, and F Watt. Characterization of bipotential epidermal progenitors derived from human sebaceous gland: contrasting roles of c-Myc and beta-catenin. *Stem Cells*, 26(5):1241–1252, 2008. 164

R Lopez, S Garcia-Silva, S Moore, O Bereshchenko, A Martinez-Cruz, O Ermakova, E Kurz, J Paramio, and C Nerlov. C/EBPalpha and beta couple interfollicular keratinocyte proliferation arrest to commitment and terminal differentiation. *Nature Cell Biology*, 11(10):1181–1190, 2009. 9

H. Lu, M. Hesse, B. Peters, and T.M. Magin. Type ii keratins precede type i keratins during early embryonic development. *European journal of cell biology*, 84(8):709–718, 2005. 103, 159

P. Lu, I.L. Hankel, B.S. Hostager, J.A. Swartzendruber, A.D. Friedman, J.L. Brenton, P.B. Rothman, J.D. Colgan, P. Lu, I.L. Hankel, et al. The developmental regulator protein gon4l associates with protein yy1, co-repressor sin3a, and histone deacetylase 1 and mediates transcriptional repression. *Journal of Biological Chemistry*, 286(20):18311–18319, 2011. 162

N.M. Luis, L. Morey, S. Mejetta, G. Pascual, P. Janich, B. Kuebler, G. Roma, E. Nascimento, M. Frye, L. Di Croce, et al. Regulation of human epidermal stem cell proliferation and senescence requires polycomb-dependent and-independent functions of cbx4. *Cell stem cell*, 9(3):233–246, 2011. 21

N.M. Luis, L. Morey, L. Di Croce, and S.A. Benitah. Polycomb in stem cells: Prc1 branches out. *Cell Stem Cell*, 11(1):16–21, 2012. 21

J.A. Mack, S. Anand, and E.V. Maytin. Proliferation and cornification during development of the mammalian epidermis. *Birth Defects Research Part C: Embryo Today: Reviews*, 75(4):314–329, 2005. 4, 5

J.C. Marine, S. Francoz, M. Maetens, G. Wahl, F. Toledo, and G. Lozano. Keeping p53 in check: essential and synergistic functions of mdm2 and mdm4. *Cell Death & Differentiation*, 13(6):927–934, 2006. 153

P.A. Marks, T. Miller, and V.M. Richon. Histone deacetylases. *Current opinion in pharmacology*, 3(4):344–351, 2003. 29

L. Marrot and J.R. Meunier. Skin dna photodamage and its biological consequences. *Journal of the American Academy of Dermatology*, 58(5):S139–S148, 2008. 153

G. Mascré, S. Dekoninck, B. Drogat, K.K. Youssef, S. Brohée, P.A. Sotiropoulou, B.D. Simons, and C. Blanpain. Distinct contribution of stem and progenitor cells to epidermal maintenance. *Nature*, 2012. 15

Y. Matsumura and H.N. Ananthaswamy. Toxic effects of ultraviolet radiation on the skin. *Toxicology and applied pharmacology*, 195(3):298–308, 2004. 139, 140

T. Matsunaga, K. Hieda, and O. Nikaido. Wavelength dependent formation of thymine dimers and (6-4) photoproducts in dna by monochromatic ultraviolet light ranging from 150 to 365 nm. *Photochemistry and photobiology*, 54(3): 403–410, 2008. 153

V. MBoneko and H.J. Merker. Development and morphology of the periderm of mouse embryos (days 9–12 of gestation). *Cells Tissues Organs*, 133(4):325–336, 1988. 5

P. McDonel, I. Costello, and B. Hendrich. Keeping things quiet: roles of nurd and sin3 co-repressor complexes during mammalian development. *The international journal of biochemistry & cell biology*, 41(1):108–116, 2009. 21, 26, 27, 29, 100, 161

P. McDonel, J. Demmers, D.W.M. Tan, F. Watt, and B.D. Hendrich. Sin3a is essential for the genome integrity and viability of pluripotent cells. *Developmental Biology*, 2011. 30, 34, 49, 74, 104, 160

J.A. McGrath and J. Uitto. The filaggrin story: novel insights into skin-barrier function and disease. *Trends in molecular medicine*, 14(1):20–27, 2008. 7

A.L. Means, Y. Xu, A. Zhao, K.C. Ray, and G. Gu. A ck19creert knockin mouse line allows for conditional dna recombination in epithelial cells in multiple endodermal organs. *Genesis*, 46(6):318–323, 2008. 35

S. Mejetta, L. Morey, G. Pascual, B. Kuebler, M.R. Mysliwiec, Y. Lee, R. Shiekhattar, L. Di Croce, and S.A. Benitah. Jarid2 regulates mouse epidermal stem cell activation and differentiation. *The EMBO Journal*, 30(17): 3635–3646, 2011. 22

B.J. Merrill, U. Gat, R. DasGupta, and E. Fuchs. Tcf3 and lef1 regulate lineage differentiation of multipotent stem cells in skin. *Genes & development*, 15(13): 1688, 2001. 20

N. Meyer and L.Z. Penn. Reflecting on 25 years with myc. *Nature Reviews Cancer*, 8(12):976–990, 2008. 23

M.L. Mikkola. Genetic basis of skin appendage development. In *Seminars in cell & developmental biology*, volume 18, pages 225–236. Elsevier, 2007. 1

A.A. Mills, B. Zheng, X.J. Wang, H. Vogel, D.R. Roop, A. Bradley, et al. p63 is a p53 homologue required for limb and epidermal morphogenesis. *Nature*, 398 (6729):708–713, 1999. 4

T. Miyazaki and S. Arai. Two distinct controls of mitotic cdk1/cyclin b1 activity requisite for cell growth prior to cell division. *Cell Cycle-Landes Bioscience-*, 6(12):1419, 2007. 90

U. Moehren, U. Dressel, C.A. Reeb, S. Väisänen, T.W. Dunlop, C. Carlberg, and A. Baniahmad. The highly conserved region of the co-repressor sin3a functionally interacts with the co-repressor alien. *Nucleic acids research*, 32 (10):2995–3004, 2004. 30

M. Moriyama, A.D. Durham, H. Moriyama, K. Hasegawa, S.I. Nishikawa, F. Radtke, and M. Osawa. Multiple roles of notch signaling in the regulation of epidermal development. *Developmental cell*, 14(4):594–604, 2008. 18

R Morris, Y Liu, L Marles, Z Yang, C Trempus, S Li, J Lin, J Sawicki, and G Cotsarelis. Capturing and profiling adult hair follicle stem cells. *Nature Biotechnology*, 22(4):411–417, 2004. 15

S. Müller-Röver, B. Handjiski, C. van der Veen, S. Eichmüller, K. Foitzik, I.A. McKay, K.S. Stenn, and R. Paus. A comprehensive guide for the accurate classification of murine hair follicles in distinct hair cycle stages. *Journal of investigative dermatology*, 117(1):3–15, 2001. 10, 70

M. Murphy, J. Ahn, K.K. Walker, W.H. Hoffman, R.M. Evans, A.J. Levine, and D.L. George. Transcriptional repression by wild-type p53 utilizes histone deacetylases, mediated by interaction with msin3a. *Genes & development*, 13 (19):2490, 1999. 26

M Nair, A Teng, V Bilanchone, A Agrawal, B Li, and X Dai. Ovol1 regulates the growth arrest of embryonic epidermal progenitor cells and represses c-myc transcription. *The Journal of Cell Biology*, 173(2):253–264, 2006. 9

E.M. Nascimento, C.L. Cox, S. MacArthur, S. Hussain, M. Trotter, S. Blanco, M. Suraj, J. Nichols, B. Kübler, S.A. Benitah, et al. The opposing transcriptional functions of sin3a and c-myc are required to maintain tissue homeostasis. *Nature Cell Biology*, 13(12):1395–1405, 2011. 7, 23, 24, 52, 61, 109, 111, 112, 114, 116, 117, 118, 124, 127, 128, 131

H. Nguyen, B.J. Merrill, L. Polak, M. Nikolova, M. Rendl, T.M. Shaver, H.A. Pasolli, and E. Fuchs. Tcf3 and tcf4 are essential for long-term homeostasis of skin epithelia. *Nature genetics*, 41(10):1068–1075, 2009. 20

J.G.W. Nijhof, K.M. Braun, A. Giangreco, C. Van Pelt, H. Kawamoto, R.L. Boyd, R. Willemze, L.H.F. Mullenders, F.M. Watt, F.R. de Gruijl, et al. The cell-surface marker mts24 identifies a novel population of follicular keratinocytes with characteristics of progenitor cells. *Development*, 133(15):3027–3037, 2006. 16

J Nowak, L Polak, H Pasolli, and E Fuchs. Hair follicle stem cells are specified and function in early skin morphogenesis. *Cell Stem Cell*, 3(1):33–43, 2008. 19, 103

C.E. Oki-Idouchi and P.S. Lorenzo. Transgenic overexpression of rasgrp1 in mouse epidermis results in spontaneous tumors of the skin. *Cancer research*, 67(1): 276, 2007. 156, 165

K.M. Osorio, S.E. Lee, D.J. McDermitt, S.K. Waghmare, Y.V. Zhang, H.N. Woo, and T. Tumbar. Runx1 modulates developmental, but not injury-driven, hair follicle stem cell activation. *Development*, 135(6):1059–1068, 2008. 19

K.M. Osorio, K.C. Lilja, and T. Tumbar. Runx1 modulates adult hair follicle stem cell emergence and maintenance from distinct embryonic skin compartments. *The Journal of Cell Biology*, 193(1):235–250, 2011. 19

A. Ouhtit, H.K. Muller, D.W. Davis, S.E. Ullrich, D. McConkey, and H.N. Ananthaswamy. Temporal events in skin injury and the early adaptive responses in ultraviolet-irradiated mouse skin. *The American journal of pathology*, 156(1): 201, 2000. 141

T. Ozaki, R. Okoshi, M. Sang, N. Kubo, and A. Nakagawara. Acetylation status of e2f-1 has an important role in the regulation of e2f-1-mediated transactivation of tumor suppressor p73. *Biochemical and biophysical research communications*, 386(1):207–211, 2009. 29

S. Pal, R. Yun, A. Datta, L. Lacomis, H. Erdjument-Bromage, J. Kumar, P. Tempst, and S. Sif. msin3a/histone deacetylase 2-and prmt5-containing brg1 complex is involved in transcriptional repression of the myc target gene cad. *Molecular and cellular biology*, 23(21):7475–7487, 2003. 31

Y.P. Pang, G.A. Kumar, J.S. Zhang, and R. Urrutia. Differential binding of sin3 interacting repressor domains to the pah2 domain of sin3a. *FEBS letters*, 548 (1-3):108–112, 2003. 28

T Parija and B Das. Involvement of YY1 and its correlation with c-myc in NDEA induced hepatocarcinogenesis, its prevention by d-limonene. *Molecular Biology Reports*, 30(1):41–46, 2003. 162

J Patel, Y Du, P Ard, C Phillips, B Carella, C Chen, C Rakowski, C Chatterjee, P Lieberman, W Lane, and S McMahon. The c-MYC oncoprotein is a substrate of the acetyltransferases hGCN5/PCAF and TIP60. *Molecular and Cellular Biology*, 24(24):10826–10834, 2004. 29, 107, 110

R. Paus, G. Cotsarelis, et al. The biology of hair follicles. *N Engl J Med*, 341(7): 491–497, 1999. 9, 12

C Payne, S Gallagher, O Foreman, J Dannenberg, R DePinho, and Braun R. Sin3a is required by sertoli cells to establish a niche for undifferentiated spermatogonia, germ cell tumors, and spermatid elongation. *Stem Cells*, 28(8): 1424–1434, 2010. 31, 74, 160

G. Pellegrini, E. Dellambra, O. Golisano, E. Martinelli, I. Fantozzi, S. Bondanza, D. Ponzin, F. McKeon, and M. De Luca. p63 identifies keratinocyte stem cells. *Proceedings of the National Academy of Sciences*, 98(6):3156, 2001. 18

J. Pellegrino, D.H. Castrillon, and G. David. Chromatin associated sin3a is essential for male germ cell lineage in the mouse. *Developmental Biology*, 2012. 30, 31, 160, 161

C. Perez, J. Parker-Thornburg, C. Mikulec, D.F. Kusewitt, S.M. Fischer, J. Di-Giovanni, C.J. Conti, and F. Benavides. Skhin/sprd, a new genetically defined inbred hairless mouse strain for uv-induced skin carcinogenesis studies. *Experimental dermatology*, 21(3):217–220, 2012. 155

C Pincelli and A Marconi. Keratinocyte stem cells: friends and foes. *Journal of Cellular Physiology*, 225(2):310–315, 2010. 1

M.V. Plikus, D.L. Gay, E. Treffeisen, A. Wang, R.J. Supapannachart, and G. Cotsarelis. Epithelial stem cells and implications for wound repair. In *Seminars in Cell & Developmental Biology*. Elsevier, 2012. 157, 158

N. Popov, C. Schülein, L.A. Jaenicke, and M. Eilers. Ubiquitylation of the amino terminus of myc by scf [beta]-trcp antagonizes scffbw7-mediated turnover. *Nature cell biology*, 12(10):973–981, 2010. 162

A.E. Powell, Y. Wang, Y. Li, E.J. Poulin, A.L. Means, M.K. Washington, J.N. Higginbotham, A. Juchheim, N. Prasad, S.E. Levy, et al. The pan-erbb negative regulator lrig1 is an intestinal stem cell marker that functions as a tumor suppressor. *Cell*, 149(1):146–158, 2012. 159

S. Rampalli, L. Pavithra, A. Bhatt, T.K. Kundu, and S. Chattopadhyay. Tumor suppressor smar1 mediates cyclin d1 repression by recruitment of the sin3/histone deacetylase 1 complex. *Molecular and cellular biology*, 25(19): 8415–8429, 2005. 139

G. Rao, L. Alland, P. Guida, N. Schreiber-Agus, K. Chen, L. Chin, J.M. Rochelle, M.F. Seldin, A.I. Skoultchi, and R.A. DePinho. Mouse sin3a interacts with and can functionally substitute for the amino-terminal repression of the myc antagonist mxi1. *Oncogene*, 12(5):1165, 1996. 26

E. Raveh, S. Cohen, D. Levanon, V. Negreanu, Y. Groner, and U. Gat. Dynamic expression of runx1 in skin affects hair structure. *Mechanisms of development*, 123(11):842–850, 2006. 19

T. Reya and H. Clevers. Wnt signalling in stem cells and cancer. *Nature*, 434 (7035):843–850, 2005. 19, 20

H. Rhee, L. Polak, and E. Fuchs. Lhx2 maintains stem cell character in hair follicles. *Science*, 312(5782):1946–1949, 2006. 19

J Rheinwald and H Green. Serial cultivation of strains of human epidermal keratinocytes: the formation of keratinizing colonies from single cells. *Cell*, 6 (3):331–343, 1975. 48

S. Sano, K.S. Chan, S. Carbajal, J. Clifford, M. Peavey, K. Kiguchi, S. Itami, B.J. Nickoloff, and J. DiGiovanni. Stat3 links activated keratinocytes and immunocytes required for development of psoriasis in a novel transgenic mouse model. *Nature medicine*, 11(1):43–49, 2004. 165

A. Satou, T. Taira, S.M.M. Iguchi-Ariga, and H. Ariga. A novel transrepression pathway of c-myc. *Journal of Biological Chemistry*, 276(49):46562–46567, 2001. 31

M.R. Schneider and R. Paus. Sebocytes, multifaceted epithelial cells: lipid production and holocrine secretion. *The international journal of biochemistry & cell biology*, 42(2):181–185, 2010. 17

N Schreiber-Agus, L Chin, K Chen, R Torres, G Rao, P Guida, A Skoultchi, and R DePinho. An amino-terminal domain of Mxi1 mediates anti-Myc oncogenic activity and interacts with a homolog of the yeast transcriptional repressor SIN3. *Cell*, 80(5):777–786, 1995. 26

M. Schuler, E. Bossy-Wetzel, J.C. Goldstein, P. Fitzgerald, and D.R. Green. p53 induces apoptosis by caspase activation through mitochondrial cytochrome c release. *Journal of Biological Chemistry*, 275(10):7337–7342, 2000. 154

J Segre, C Bauer, and E Fuchs. Klf4 is a transcription factor required for establishing the barrier function of the skin. *Nature Genetics*, 22(4):356–360, 1999. 9

G.L. Sen, J.A. Reuter, D.E. Webster, L. Zhu, and P.A. Khavari. Dnmt1 maintains progenitor function in self-renewing somatic tissue. *Nature*, 463(7280):563–567, 2010. 21

S. Sengupta and C.C. Harris. p53: traffic cop at the crossroads of dna repair and recombination. *Nature Reviews Molecular Cell Biology*, 6(1):44–55, 2005. 153

M. Senoo, F. Pinto, C.P. Crum, and F. McKeon. p63 is essential for the proliferative potential of stem cells in stratified epithelia. *Cell*, 129(3):523–536, 2007. 18

X. Shi and D.J. Garry. Sin3 interacts with foxk1 and regulates myogenic progenitors. *Molecular and cellular biochemistry*, pages 1–8, 2012. 32

Y. Shimomura and A.M. Christiano. Biology and genetics of hair. *Annual review of genomics and human genetics*, 11:109–132, 2010. 11, 103

J.D. Siliciano, C.E. Canman, Y. Taya, K. Sakaguchi, E. Appella, and M.B. Kastan. Dna damage induces phosphorylation of the amino terminus of p53. *Genes & Development*, 11(24):3471–3481, 1997. 153

A. Smith. A glossary for stem-cell biology. *Nature*, 441(7097):1060–1060, 2006. 13

M.L. Smith, I.T. Chen, Q. Zhan, I. Bae, C.Y. Chen, T.M. Gilmer, M.B. Kastan, P.M. O'Connor, A.J. Fornace Jr, et al. Interaction of the p53-regulated protein gadd45 with proliferating cell nuclear antigen. *Science (New York, NY)*, 266 (5189):1376, 1994. 153

H Snippert, A Haegebarth, M Kasper, V Jaks, J Es, N Barker, M Wetering, M Born, H Begthel, R Vries, D Stange, and Clevers H Toftgrd R. Lgr6 marks stem cells in the hair follicle that generate all cell lineages of the skin. *Science*, 327(March):1385–1389, 2010. 16, 17, 159

P. Soriano. Generalized lacz expression with the rosa26 cre reporter strain. *Nature genetics*, 21(1):70–71, 1999. 34

P.A. Sotiropoulou and C. Blanpain. Development and homeostasis of the skin epidermis. *Cold Spring Harbor Perspectives in Biology*, 4(7), 2012. 16, 18, 19

M Stewart and D Downing. Chemistry and function of mammalian sebaceous lipids. *Advances In Lipid Research*, 24:263–301, 1991. 12

L.R. Strachan and R. Ghadially. Tiers of clonal organization in the epidermis: the epidermal proliferation unit revisited. *Stem Cell Reviews and Reports*, 4 (3):149–157, 2008. 13

H. Suzuki, M. Ouchida, H. Yamamoto, M. Yano, S. Toyooka, M. Aoe, N. Shimizu, H. Date, and K. Shimizu. Decreased expression of the sin3a gene, a candidate

tumor suppressor located at the prevalent allelic loss region 15q23 in non-small cell lung cancer. *Lung cancer*, 59(1):24–31, 2008. 139

K.A. Swanson, P.S. Knoepfler, K. Huang, R.S. Kang, S.M. Cowley, C.D. Laherty, R.N. Eisenman, and I. Radhakrishnan. Hbp1 and mad1 repressors bind the sin3 corepressor pah2 domain with opposite helical orientations. *Nature structural & molecular biology*, 11(8):738–746, 2004. 28

A. Tien, S. Senbanerjee, A. Kulkarni, R. Mudbhary, B. Goudreau, S. Ganesan, K. Sadler, and C. Ukomadu. Uhrf1 depletion causes a g2/m arrest, activation of dna damage response and apoptosis. *Biochem. J*, 435:175–185, 2011. 90

C Trempus, R Morris, C Bortner, G Cotsarelis, R Faircloth, J Reece, and R Tennant. Enrichment for living murine keratinocytes from the hair follicle bulge with the cell surface marker CD34. *The Journal of Investigative Dermatology*, 120(4):501–511, 2003. 15

A.B. Truong, M. Kretz, T.W. Ridky, R. Kimmel, and P.A. Khavari. p63 regulates proliferation and differentiation of developmentally mature keratinocytes. *Genes & development*, 20(22):3185–3197, 2006. 18

T Tumbar, G Guasch, V Greco, C Blanpain, W Lowry, M Rendl, and E Fuchs. Defining the epithelial stem cell niche in skin. *Science*, 303(5656):359–363, 2004. 15

C. van Genderen, R.M. Okamura, I. Farinas, R.G. Quo, T.G. Parslow, L. Bruhn, and R. Grosschedl. Development of several organs that require inductive epithelial-mesenchymal interactions is impaired in lef-1-deficient mice. *Genes & development*, 8(22):2691–2703, 1994. 20

C. van Oevelen, J. Wang, P. Asp, Q. Yan, W.G. Kaelin Jr, Y. Kluger, and B.D. Dynlacht. A role for mammalian sin3 in permanent gene silencing. *Molecular cell*, 32(3):359–370, 2008. 31

H. Vanbokhoven, G. Melino, E. Candi, and W. Declercq. p63, a story of mice and men. *Journal of Investigative Dermatology*, 131(6):1196–1207, 2011. 18

C VanOevelen, C Bowman, J Pellegrino, P Asp, J Cheng, F Parisi, M Micsinai, Y Kluger, A Chu, A Blais, G David, and B Dynlacht. The mammalian Sin3 proteins are required for muscle development and sarcomere specification. *Molecular and Cellular Biology*, 30(24):5686–5697, 2010. 31, 160, 161

J. Vervoorts, J.M. Lüscher-Firzlaff, S. Rottmann, R. Lilischkis, G. Walsemann, K. Dohmann, M. Austen, and B. Lüscher. Stimulation of c-myc transcriptional activity and acetylation by recruitment of the cofactor cbp. *EMBO reports*, 4 (5):484–490, 2003. 162

J.P. Viallet and J. Thelu. Skin field formation: morphogenetic events. *Int. J. Dev. Biol*, 48:85–91, 2004. 4

V Vidal, M Chaboissier, S Lützkendorf, G Cotsarelis, P Mill, C Hui, N Ortonne, J Ortonne, and A Schedl. Sox9 is essential for outer root sheath differentiation and the formation of the hair stem cell compartment. *Current Biology*, 15(15): 1340–1351, 2005. 19

K. Viiri, T. Heinonen, M. Mäki, and O. Lohi. Phylogenetic analysis of the sap30 family of transcriptional regulators reveals functional divergence in the domain that binds the nuclear matrix. *BMC evolutionary biology*, 9(1):149, 2009. 28

KM Viiri, H. Korkeamäki, MK Kukkonen, LK Nieminen, K. Lindfors, P. Peterson, M. Mäki, H. Kainulainen, and O. Lohi. Sap30l interacts with members of the sin3a corepressor complex and targets sin3a to the nucleolus. *Nucleic acids research*, 34(11):3288–3298, 2006. 28

R Waikel, X Wang, and D Roop. Targeted expression of c-Myc in the epidermis alters normal proliferation, differentiation and UV-B induced apoptosis. *Oncogene*, 18(34):4870–4878, 1999. 153

R Waikel, Y Kawachi, P Waikel, X Wang, and D Roop. Deregulated expression of c-Myc depletes epidermal stem cells. *Nature Genetics*, 28(2):165–168, 2001. 23, 24, 105, 164

X. Wang and X. Jiang. Mdm2 and mdmx partner to regulate p53. *FEBS letters*, 2012. 153

X. Wang, E.E. Tredget, and Y. Wu. Dynamic signals for hair follicle development and regeneration. *Stem Cells and Development*, (ja), 2012. 10

F Watt, M Frye, and S Benitah. MYC in mammalian epidermis: how can an oncogene stimulate differentiation? *Nature Reviews in Cancer*, 8(3):234–242, 2008a. 23, 25

F.M. Watt. Role of integrins in regulating epidermal adhesion, growth and differentiation. *The EMBO journal*, 21(15):3919–3926, 2002. 68

F.M. Watt, S. Estrach, and C.A. Ambler. Epidermal notch signalling: differentiation, cancer and adhesion. *Current opinion in cell biology*, 20(2):171–179, 2008b. 18

P. Workman, EO Aboagye, F. Balkwill, A. Balmain, G. Bruder, DJ Chaplin, JA Double, J. Everitt, DAH Farningham, MJ Glennie, et al. Guidelines for the welfare and use of animals in cancer research. *British journal of cancer*, 102 (11):1555–1577, 2010. 141, 154

L. Wu and A.J. Levine. Differential regulation of the p21/waf-1 and mdm2 genes after high-dose uv irradiation: p53-dependent and p53-independent regulation of the mdm2 gene. *Molecular Medicine*, 3(7):441, 1997. 153

S. Xiaozhong, C.S. David, and J.G. Daniel. Foxk1 recruits the sds3 complex and represses gene expression in myogenic progenitors. *Biochemical Journal*, 2012. 32

T. Xie, Y. He, H. Korkeamaki, Y. Zhang, R. Imhoff, O. Lohi, and I. Radhakrishnan. Structure of the 30-kda sin3-associated protein (sap30) in complex with the mammalian sin3a corepressor and its role in nucleic acid binding. *Journal of Biological Chemistry*, 286(31):27814–27824, 2011. 28

A. Yang, R. Schweitzer, D. Sun, M. Kaghad, N. Walker, R.T. Bronson, C. Tabin, A. Sharpe, D. Caput, C. Crum, et al. p63 is essential for regenerative proliferation in limb, craniofacial and epithelial development. *Nature*, 398(6729): 714–717, 1999. 4

X. Yang, F. Zhang, and J.E. Kudlow. Recruitment of o-glcnac transferase to promoters by corepressor msin3a: Coupling protein o-glcnacylation to transcriptional repression. *Cell*, 110(1):69–80, 2002. 30

XJ Yang and E. Seto. Hats and hdacs: from structure, function and regulation to novel strategies for therapy and prevention. *Oncogene*, 26(37):5310–5318, 2007. 29

K Youssef, A Keymeulen, G Lapouge, B Beck, C Michaux, Y Achouri, P Sotiropoulou, and C Blanpain. Identification of the cell lineage at the origin of basal cell carcinoma. *Nature Cell Biology*, 12(3):299–305, 2010. 15

J. Zhang, S. Chen, W. Zhang, J. Zhang, X. Liu, H. Shi, H. Che, W. Wang, F. Li, and L. Yao. Human differentiation-related gene ndrg1 is a myc downstream-regulated gene that is repressed by myc on the core promoter region. *Gene*, 417(1-2):5–12, 2008. 23

J. Zhang, E. Bardot, and E. Ezhkova. Epigenetic regulation of skin: focus on the polycomb complex. *Cellular and Molecular Life Sciences*, pages 1–12, 2012. 22

Y. Zhang, Z.W. Sun, R. Iratni, H. Erdjument-Bromage, P. Tempst, M. Hampsey, and D. Reinberg. Sap30, a novel protein conserved between human and yeast, is a component of a histone deacetylase complex. *Molecular cell*, 1(7):1021–1031, 1998. 28

P. Zhou, C. Byrne, J. Jacobs, and E. Fuchs. Lymphoid enhancer factor 1 directs hair follicle patterning and epithelial cell fate. *Genes & development*, 9(6):700, 1995. 20